Preparation and Spectroscopic Investigations of Mixed Octahedral Complexes and Clusters

Wilhelm Preetz,* Gerhard Peters, and Dirk Bublitz

Institut für Anorganische Chemie, Universität Kiel, D-24098 Kiel, Germany

Received July 25, 1995 (Revised Manuscript Received February 19, 1996)

Contents

I. Introduction

The different classes of compounds presented in this review have octahedral arrangements as a common structural feature as shown in Figure 1. The close interrelation between geometric structure, molecular symmetry, and spectroscopic properties can be demonstrated comprehensively and systematically by the properties of octahedral mixed-ligand complexes, such as the hexahalogeno metalates formed by two different halide ligands X and Y. Such complexes, given by the formula $[MX_nY_{6-n}]^{z-}$, where $n = 0-6$ (Figure 1a), define a series of two homoleptic and eight heteroleptic species: six of which belong to three pairs of stereoisomers for $n = 2, 3, 4$. These 10 complexes display a descent in symmetry from point group O_h to D_{4h}, C_{4v}, C_{3v} down to C_{2v} (Table 5). Through substitution and the subsequent mutual influences of different ligands, the chemical and physical properties of the complexes are altered incrementally, resulting in predictable changes in reactivity, electronic structure, and bonding properties. This alteration of molecular symmetry and the magnitude of the interactions causes specific splittings and shifts of bands or signals in the electronic, vibrational, and nuclear magnetic resonance spectra.

Of central importance to this phenomenon are the mutual interactions, described by the terms *cis* or *trans* effect, and *cis* or *trans* influence. These interactions have been the subject of numerous research and review articles, and are still a subject of controversy.[1−8] Here, the *trans* effect is reserved for a kinetic phenomenon, best described as the ability of a ligand to enhance the attachment of another ligand at the coordination site directly opposite the original one, while the *trans* influence refers to a thermodynamic phenomenon in which the mutual interactions of *trans* coordinated ligands cause redistributions in the molecular ground state electronic structures. These redistributions result in changes in electronic absorptions and emissions, redox potentials, bond strengths, bond lengths, molecular vibrations, force constants, NMR shifts, and couplings. In this context it should be noted that the terms *trans* effect and *trans* influence have been previously used in the limited sense of *trans* weakening of an opposite ligand, only. However, it should be emphasized that these interactions are mutual indeed, in that one metal to ligand bond is weakened while the opposite one is strengthened. The usage of *cis* with the terms effect and influence have corresponding meanings for mutual interactions of ligands *cis* coordinated to each other.

The formation and existence of such mixed-ligand complexes have been known for quite a long time, but the preparation, separation, and identification of individual species have been of more recent realization. In his pioneering work at the beginning of this century, A. Werner established the beauty, symmetry, and simplicity of octahedral coordination, and became the founder of the theoretical concept of coordination chemistry.[9] Without the aid of modern spectroscopy or X-ray diffraction techniques, which are so often taken for granted now, he proved his theory by observing the reactions of octahedral mixed-ligand complexes, in particular such stereoisomeric pairs as the green *trans* or the violet *cis* forms of $[Co(NH_3)_4Cl_2]Cl$. These compounds were

0009-2665/96/0796-0977$25.00/0

Wilhelm Preetz was born 1934 in Breitenfeld (Altmark, East Germany), studied in West Berlin and received his Diploma and Ph.D. degree (1963) from the Technical University of Berlin—Charlottenburg. His graduate study was performed under the supervision of Professor G. Jander and Professor E. Blasius. In 1969 he finished his habilitation at the University des Saarlandes, Saarbrücken, with a thesis on new ionophoretic separation methods applied to coordination compounds. In 1971 he became Full Professor of Inorganic Chemistry at the Christian-Albrechts-University of Kiel. His main fields of research are the preparation, separation, and spectroscopic investigation of octahedral mixed-ligand complexes, clusters of boron and transition metals and compounds with multiple metal–metal bonds.

Gerhard Peters was born in 1946 in Heinkenborstel (Schleswig-Holstein, Germany). He studied chemistry at the Christian-Albrechts-University of Kiel, joined the group of Professor W. Preetz in 1976 with a diploma thesis on thiocyanato linkage isomers of osmium, and received his doctoral degree on the synthesis of new Re and Tc complexes with multiple metal–metal bonds. Currently he is engaged in multinuclear high-resolution NMR spectroscopy on solutions and solids as a supervisor of a joint project of inorganic, organic, and pharmaceutical chemistry and mineralogy, and besides he is as an instructor of advanced students and adviser of graduate co-workers.

Dirk Bublitz was born in 1965 in Lübeck (Schleswig-Holstein, Germany). He studied chemistry at Christian-Albrechts-University of Kiel where he received his diploma for work on the preparation and characterization of molybdenum clusters. He is working in the research group of Professor W. Preetz and completed his Ph.D. thesis in 1995 on preparation and normal coordinate analysis of isotopically labeled cluster compounds. Currently he is engaged in X-ray structure determination and computational chemistry especially in force field calculations of coordination compounds and clusters.

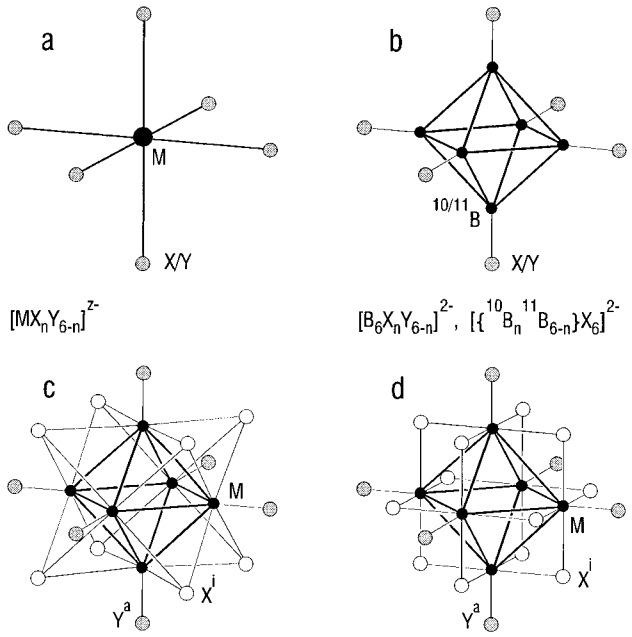

$[MX_nY_{6-n}]^{z-}$

$[B_6X_nY_{6-n}]^{2-}$, $[\{^{10}B_n\,^{11}B_{6-n}\}X_6]^{2-}$

$[(\{M_nM'_{6-n}\}\{X^i_mX'^i_{8-m}\})Y^a_pY'^a_{6-p}]^{2-}$

$M \neq M'$ = Mo, W; $X^i \neq X'^i$ = Cl, Br, I; $Y^a \neq Y'^a$ = F, Cl, Br, I

$[(\{M_nM'_{6-n}\}X^i_{12})Y^a_6]^{z-}$

$M \neq M'$ = Nb, Ta, Mo; X^i = Cl, Br; Y^a = F, Cl, Br, I

Figure 1. Archetypes of mixed complexes and clusters.

formerly designated by their colors as *praseo* and *violeo* salts by Fremy.[10]

Mixed-ligand octahedral cluster compounds also offer opportunities for studying the effects of mutual interactions of ligands. For example, the *closo*-hexahydrohexaborate anion, $[B_6H_6]^{2-}$, and its halogeno-substituted derivatives, create an octahedral cage around which an octahedral ligand sphere can be distributed (Figure 1b). Also, the two prototypes of octahedral metal clusters, $[(M_6X^i_8)Y^a_6]^{2-}$ and $[(M_6X^i_{12})Y^a_6]^{z-}$, where X and Y are halides (Figure 1c,d) can give rise to hundreds or thousands of distinct species, constructed from the three building units: the octahedral metal core M_6, the inner ligand sphere X^i, and the octahedral outer ligand sphere Y^a, if two different metals or ligands are used, respectively.

Although there is a vast number of mixed-ligand octahedral complexes and clusters with many different kinds of ligands other than the halide ions, which may be of importance to the applicability of theory and practical use, this review will focus on basic research of classical paradigms of mixed-halogeno systems and the special case of linkage isomerism. Special emphasis will be placed on the systematic behavior of complete series and the unique and detailed understanding of the physical properties that these provide. It is hoped that this will lead to

an improved understanding of the mutual interactions in these compounds in a chemical as well as in a physical sense.

II. Mixed-Hexahalogeno Complexes

A. Synthesis Routes

1. General Comments

Although hexahalogeno transition metal complexes provide an excellent medium for synthesizing compounds of systematic chemical variation while maintaining the primary octahedral environment, it is not possible to synthesize pure species by straightforward chemical reactions. Instead, mixtures are inevitably produced, the compositions of which depend upon the rate constants. However, these difficulties can be overcome either by detection techniques allowing the unambiguous *in situ* identification, characterization, and quantification of individual species within such mixtures, or by separation and isolation of individual species, followed by physical characterization.

Unfortunately, with regard to direct analysis of mixed-component systems, most bulk analysis methods are unable to distinguish pure substances from mixtures of such closely related compounds. For example, the very similar mixed-hexahalogeno complexes form continuous series of mixed crystals, which obey Vegard's rule[11] sufficiently, and therefore behave like homogeneous phases which cannot be differentiated by powder X-ray diffraction. Even single-crystal X-ray structure analysis fails for alkali salts of stereoisomers because they form crystals of high, mostly cubic symmetry. The resulting statistical orientation of the complex anions in such lattices makes them indistinguishable.[12,13]

Similarly, electronic and vibrational spectroscopy, which respond to molecular properties or building groups, are of rather limited value for the identification or elucidation of multicomponent mixtures. Often, the ranges of vibrational frequencies or maxima in electronic spectra are too close, and the band widths are too broad; thus, resolution and assignment of distinct transitions from individual species is not possible. Even simple problems, such as the unambiguous assignment of a mixture of a pair of stereoisomers like *cis*- and *trans*-$[OsCl_4I_2]^{2-}$ by means of UV−vis and IR spectroscopy is possible only if the spectra of the pure isomers are previously known.[14] This severely limiting factor has also been found for the IR and Raman spectra of the pairs of stereoisomers in the chlorobromoosmate(IV) series.[15] A prime example of this can be found in the literature, where what had been reported as the pure *cis* complexes have actually been shown to be statistical mixtures. Therefore, it seems risky to deduce the existence of *cis*-$[MX_4Y_2]^{2-}$, M = Sn, Ti, X ≠ Y = Cl, Br, I, from the vibrational spectra,[16] because the more numerous bands of the *cis* isomer obscure the few observable vibrations from the *trans* isomer, especially if it is present in only small amounts (see section II.B.2). Thus, the wish of Sillen[17] to have a method which allows the distinct *in situ* detection of different species coexisting in complex equilibria has not yet been fulfilled, even with the availability of modern high-resolution spectrometers. Also, the potential of laser Raman spectroscopy, once anticipated by Schläfer[18] to be able to solve this problem, is of rather limited use. Nevertheless, Sillen's intention has been realized by multinuclear NMR spectroscopy in the case of suitable nuclei (see section II.D.1).

The other approach to the problems presented by the case of mixed-hexahalogeno metalates, the direct preparation of pure species, is burdened with difficulties, and any reports of such must be considered with severe scepticism.[19] Not only in early publications,[20−24] but even recently,[25] there have been many reports of direct synthesis of unique mixed complexes that are actually mixtures of several components, regardless of a correct gross analytic composition, which implies the presence of only the desired species. The fundamental error is the supposition that by the reaction of educts in distinct molar ratios, distinct substances of defined composition are obtainable. This is especially true for Nb(V), Ta(V), Ti(IV), and Sn(IV) which form kinetically labile complexes which interconvert by a fast exchange in dynamic equilibria.[16,26−30]

Mixed compounds with ionic and neutral ligands like $[MCl_n(NH_3)_{6-n}]^{z-n}$, $n = 0-6$, where the charges of the complexes alter within the series, and enable chemical separation by different counter ions and solubilities, stand in marked contrast to mixed-hexahalogeno series, where this opportunity is ruled out by the very similar solubilities of the components and their already mentioned tendency to form mixed crystals. Therefore, powerful and efficient separation techniques are indispensable for studies on systems defying *in situ* investigations. Fortunately, diverse forms of ionophoresis and particularly ion exchange chromatography have been successfully utilized during the past three decades (see section II.A.5). By allowing the separation of octahedral mixed-ligand complexes and the isolation of appreciable amounts of the individual species in high purity, these techniques have paved the way for systematic investigations of complete series of the mixed-halogeno metalates. Furthermore, optimized syntheses utilizing the *trans* effect, in stereospecific or stereoselective reactions, are of crucial importance. However, the limiting factor in the separation and isolation of pure individual heteroleptic complexes is their kinetic stability, i.e. the rates of ligand exchange reactions and interconversion processes must be slow. This so-called inert behavior is common with electronic configurations from d^3 to d^6, especially for Cr(III), Co(III), and the platinum group metals.[8]

2. Complex Equilibria

As stated, an understanding of the equilibria responsible for the formation of individual mixed-halogeno compounds is crucial in any attempt at systematic syntheses and investigations. Therefore, with reference to Bjerrum[31,32] six interdependent equilibria must be considered for the successive formation of mixed octahedral complexes. The resulting six stepwise stability constants k_i ($i = 1-6$) define the molar ratios of the seven species in a

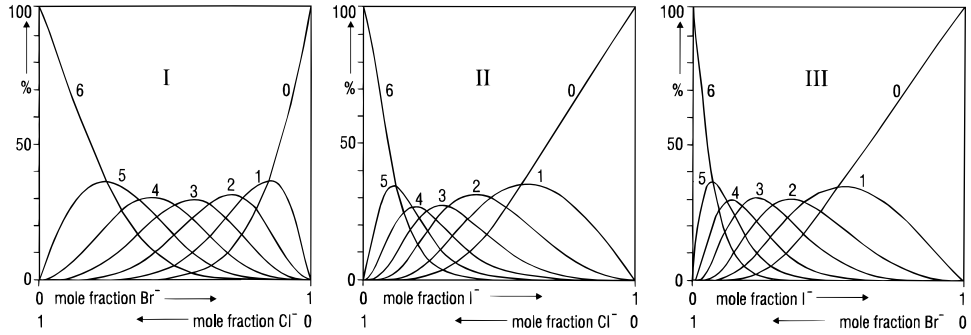

Figure 2. Equilibrium diagrams for the series $[OsCl_nBr_{6-n}]^{2-}$ (I), $[OsCl_nI_{6-n}]^{2-}$ (II), and $[OsBr_nI_{6-n}]^{2-}$ (III), $n = 0-6$.

Table 1. Stepwise Stability Constants k_i and Overall Stability Constants K_s for the Mixed-Ligand Complex Ions, $[OsX_nY_{6-n}]^{2-}$, $X \neq Y = Cl, Br, I$, $n = 0-6$

	$[OsCl_nBr_{6-n}]^{2-}$	$[OsI_nCl_{6-n}]^{2-}$	$[OsI_nBr_{6-n}]^{2-}$
k_1	5.56	7.75	13.22
k_2	3.03	4.72	7.03
k_3	1.67	3.41	4.48
k_4	1.00	2.26	2.37
k_5	0.58	1.15	1.43
k_6	0.32	0.71[a]	0.87[a]
$K_{s(X/Y)}$	5.2	230	1225

[a] Extrapolated.

system MX_nY_{6-n}, $n = 0-6$ (eq 1a−1f). The product

$$MX_6 + Y \rightleftharpoons MX_5Y + X \qquad \frac{[MX_5Y][X]}{[MX_6][Y]} = k_1 \quad (1a)$$

$$MX_5Y + Y \rightleftharpoons MX_4Y_2 + X \qquad \frac{[MX_4Y_2][X]}{[MX_5Y][Y]} = k_2 \quad \ldots (1b)$$

$$MXY_5 + Y \rightleftharpoons MY_6 + X \qquad \frac{[MY_6][X]}{[MXY_5][Y]} = k_6 \quad (1f)$$

of the six k_i is the overall stability constant K_s, which describes the equilibrium of the two homoleptic complexes (eq 2). The calculation of k_i requires four cor-

$$MX_6 + 6Y \rightleftharpoons MY_6 + 6X \qquad \frac{[MY_6][X]^6}{[MX_6][Y]^6} = K_s \quad (2)$$

responding concentrations from the respective equilibria, *viz*. two of the free ligands X and Y and two of the successive mixed-ligand complexes. In every case, several components coexist in equilibria, as will be shown later in detailed quantitative studies.

Equilibration in series of kinetically inert complexes, $[OsX_nY_{6-n}]^{2-}$, ($X \neq Y = Cl, Br, I$, $n = 0-6$), has been accomplished in HX/HY mixtures at 80 °C within a few days. Below 20 °C the exchange reactions cease, enabling ionophoretic separation and quantitative determination of the individual species by γ-radiometry of the ^{185}Os nuclide.[33] From these data and the given X and Y concentrations the k_i and K_s have been calculated, as shown in Table 1. The fraction of the two successive k_i corresponds approximately to those expected for statistical occupation of equivalent coordination sites.[34] The ratios of

Table 2. Stepwise Stability Constants k_i and Overall Stability Constant K_s for $[RhBr_nCl_{6-n}]^{3-}$, $n = 0-6$

k_1	142.8
k_2	11.1
k_3	7.1
k_4	4.0
k_5	1.92
k_6	0.42
$K_{s(Br/Cl)}$	36 500

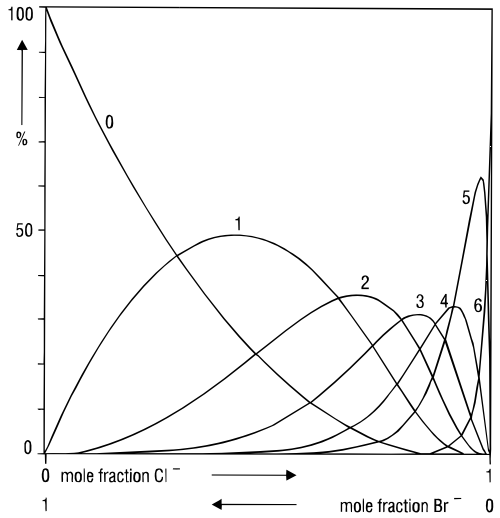

Figure 3. Equilibrium diagram for the series $[RhCl_nBr_{6-n}]^{3-}$, $n = 0-6$.

the stereoisomers are close to statistical expectations, being *cis*:*trans* = 4:1 and *fac*:*mer* = 2:3.

Differences between these series can be visualized by equilibrium diagrams computed from the k_i, as shown in Figure 2. Accordingly, the mixed complexes in the three series are present at 25−35% maximum. In wide ranges of the free ligand mole fractions, all components coexist in appreciable amounts, proving impressively the inaccessibility of a defined individual species by adjustment of fixed stoichiometric ratios.

Quantitative ^{103}Rh NMR *in situ* measurements are also very useful for the elucidation of complex equilibria and stereoisomeric ratios. Individual stability constants have been obtained for the $[RhCl_nBr_{6-n}]^{3-}$ series (Table 2) with k_i differences of successive complexes exceeding those of the Os(IV) series. The overall stability constant $K_s = 36\,000$ indicates the greater stability of $[RhBr_6]^{3-}$ in comparison to $[RhCl_6]^{3-}$.[35] Correspondingly, the equilibrium diagram is more asymmetric (Figure 3). Again, it is

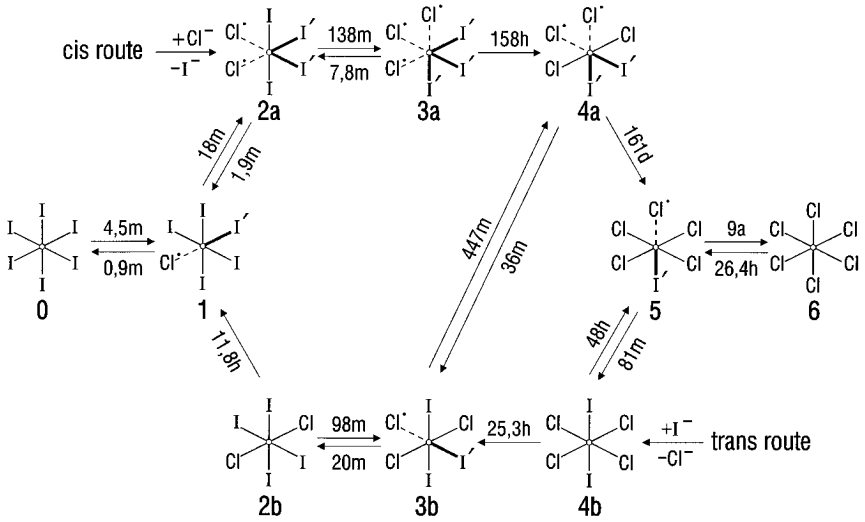

Figure 4. Stereospecific ligand exchange reactions in the system, $[OsCl_nI_{6-n}]^{2-}$, $n = 0-6$ (a corresponds to *cis/fac*, b corresponds to *trans/mer*) half-lives at 20 °C, dotted lines for weakened bonds, fat lines for strengthened bonds due to *trans* influence.

shown that individual complexes may be enriched to some extent, in this case up to a 65% maximum for $[RhCl_5Br]^{3-}$. The stereoisomeric ratios of *cis:trans* = 3:1 and *fac:mer* = 1:5 deviate from statistical expectation.

3. Substitutive Ligand Exchange

In 1926 Chernyaev[1] discovered the *trans* effect, which had been exclusively applied to quadratic planar complexes for a long time. However, over the past 25 years this effect has been transferred to octahedral complexes and their substitution reactions, as has been demonstrated for many mixed-ligand series of the heavier transition metals, especially for the platinum metals. With regard to the halides considered here, *trans* effects increase within the series, F < Cl < Br < I. A complete reaction scheme with 18 possible substitution steps is presented for the $[OsCl_nI_{6-n}]^{2-}$ series in Figure 4.

The kinetics, including all consecutive reactions, have been investigated at several temperatures in the range from −10 to +90 °C, revealing reaction rate constants and activation energies. The half-lives depicted in Figure 4 refer to 20 °C. Through the use of ^{185}Os and ^{191}Os radiometry, all reaction pathways have been studied quantitatively by monitoring the decrease of the individual species, which had been obtained as pure substances by preceding high-voltage paper ionophoresis.[36] With regard to the Cl and I mixed Os complexes, due to the much stronger *trans* effect of I in comparison with Cl, and the resulting weakening of the Os−Cl• and strengthening of the Os−I′ bonds of the asymmetric Cl•−Os−I′ axes, two stereospecific routes of substitution are possible with respect to the stereoisomers. By starting with $[OsI_6]^{2-}$, and reacting it via the *cis* route with HCl, only the *cis/fac* isomers are formed. Because the Os−I′ bonds *trans* positioned to Cl• are strengthened, the progress of substitution reaches a kinetic barrier at *fac*-$[OsCl_3I_3]^{2-}$ (3a). On the other hand, by following the *trans* route, $[OsCl_6]^{2-}$ initially reacts with HI to the *trans/mer* isomers in alternatingly slow and fast steps. These processes are governed by the ease of substitution of Cl• along the Cl•−Os−I′ axis (the

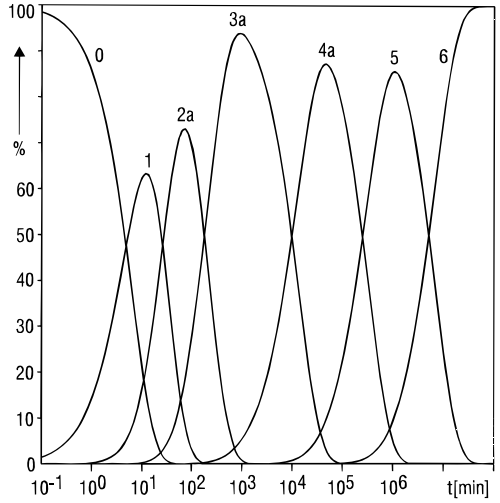

Figure 5. Percent−time diagram for the reaction of $[OsI_6]^{2-}$ with 5 N HCl (*cis* route) at 20 °C to give $[OsCl_nI_{6-n}]^{2-}$, $n = 0-6$ (a corresponds to *cis/fac*).

fast steps), and the more difficult attack on the stable symmetric Cl−Os−Cl and I−Os−I axes (the slow steps). With the exception of *cis*-$[OsCl_4I_2]^{2-}$ (4a) and *trans*-$[OsCl_2I_4]^{2-}$ (4b), which react strictly in only one direction, all neighboring complexes are reversibly interconvertible by reaction with HCl or HI, respectively. Additionally, the isomeric series are reversibly cross connected by *cis*-$[OsCl_4I_2]^{2-}$ (4a) and *mer*-$[OsCl_3I_3]^{2-}$ (3b) (Figure 4).

Once the reaction rate constants for all consecutive steps are known, the percent−time diagrams can be computed, revealing the optimal conditions for the enrichment of special mixed-ligand complexes, as presented for the *cis* and *trans* route at 20 °C in Figures 5 and 6.[37] Table 3 gives a compilation of reaction times and achievable maximum amounts at three different reaction temperatures. Clearly, it is easy to obtain 60−95% yields of the *cis/fac* species, while the *trans* isomers are more difficult to prepare, such as *mer*-$[OsCl_3I_3]^{2-}$, whose 1% yield is worst. This yield can be improved, however, if *cis*-$[OsCl_4I_2]^{2-}$ instead of $[OsCl_6]^{2-}$ as starting material is treated with HI resulting in enrichments of 26% for *mer*-

Table 3. Reaction Times *t* and Maximum Percentage of the Mixed-Ligand Complex Ions, $[OsCl_nBr_{6-n}]^{2-}$, $n = 1-5$, at 20, 40, and 60 °C

	20 °C		40 °C		60 °C	
n[a]	*t* (min)	max (%)	*t* (min)	max (%)	*t* (min)	max (%)
			cis-series: $[OsI_6]^{2-}$ + 5 N HCl (Figure 5)			
1	12	63.3	0.9	64.2	9.0×10^{-2}	64.9
2a	69	73.3	5.2	72.3	5.2×10^{-1}	71.7
3a	900	93.8	60	88.8	5.2	88.8
4a	4.6×10^4	87.2	2100	86.4	142	87.6
5	1.1×10^6	85.7	4.95×10^4	85.9	3300	84.1
			trans-series: $[OsCl_6]^{2-}$ + 5 N HI (Figure 6)			
5	370	4.3	30.5	7.0	4	12.5
4b	2400	35.8	147	37.2	13	38.4
3b	2400	0.46	150	0.8	13	1.3
2b	3600	15.0	220	14.8	18	16.0
1	–	<0.01	–	<0.01	–	<0.01

[a] a corresponds to *cis*/*fac*; b corresponds to *trans*/*mer*.

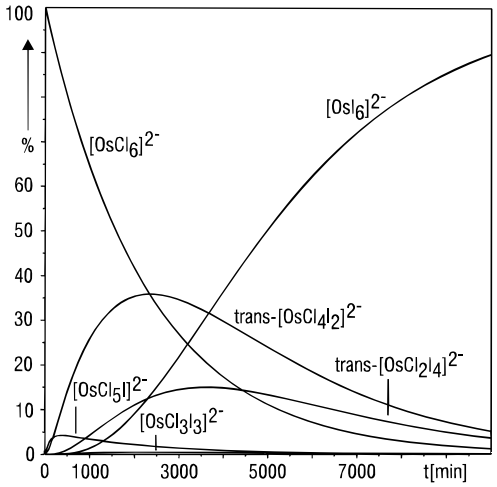

Figure 6. Percent−time diagram for the reaction of $[OsCl_6]^{2-}$ with 5 N HI (*trans* route) at 20 °C to give $[OsCl_nI_{6-n}]^{2-}$, $n = 0-6$.

$[OsCl_3I_3]^{2-}$ and 84% for *trans*-$[OsCl_2I_4]^{2-}$; the latter of which reacts with HCl yielding 65% of *mer*-$[OsCl_3I_3]^{2-}$.[37]

However, because of the significantly smaller difference between the *trans* effects of Cl and Br, the corresponding reactions in the $[OsCl_nBr_{6-n}]^{2-}$ system are no longer stereospecific but only stereoselective. Regarding both the *cis* and *trans* routes, there are 24 single steps shown in Figure 7, 12 of which are unambiguous, while the others, depicted as a and b, result in mixtures of isomers.[38]

In comparison with symmetrically occupied axes, the mutual interactions of strengthened Br′ and weakened Cl• in the Cl•−Os−Br′ axis are insufficient for stereospecific control, and a statistical substitution results. The reaction rate constants have been determined for all consecutive and parallel reactions,[38] from which parameters have been deduced indicating the predominance of the *trans* effect with regard to the minor *cis* effect.[39] Inspection of the percent−time diagrams computed for the *cis* route (Figure 8) and the *trans* route (Figure 9) show strong overlap of the individual species and unavoidable mixtures of the respective stereoisomers within the two series. This clearly demonstrates the necessity of separation techniques for the preparation of pure species. Nevertheless, the diagrams do show the optimal reaction conditions for a specific species.

The strategies of optimal syntheses using the kinetic data and *trans* effects have been applied successfully to the very complicated family of 3-fold mixed-ligand complexes, $[OsCl_nBr_mI_{6-n-m}]^{2-}$, $n + m = 2-5$, which comprises 29 individual complexes, including a pair of optical isomers for *all-cis*-$[OsCl_2Br_2I_2]^{2-}$.[40] Reaction rate constants have been calculated, and from them the percent−time diagrams have been computed for the consecutive and parallel routes. These have been shown to be in good agree-

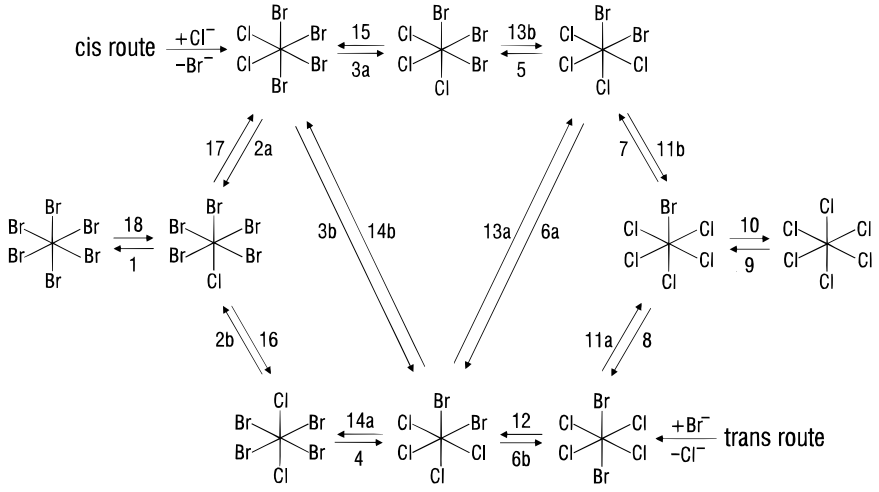

Figure 7. Stereoselective ligand exchange reactions in the system $[OsCl_nBr_{6-n}]^{2-}$, $n = 0-6$.

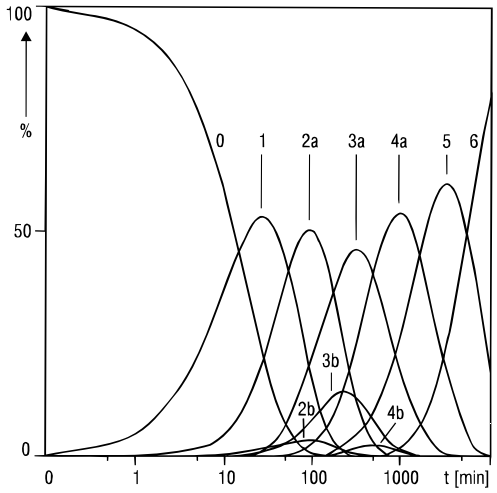

Figure 8. Percent−time diagram for the reaction of $[OsBr_6]^{2-}$ with 5 N HCl at 20 °C (*cis* route) to give $[OsCl_nBr_{6-n}]^{2-}$, $n = 0-6$ (a corresponds to *cis*/*fac*; b corresponds to *trans*/*mer*).

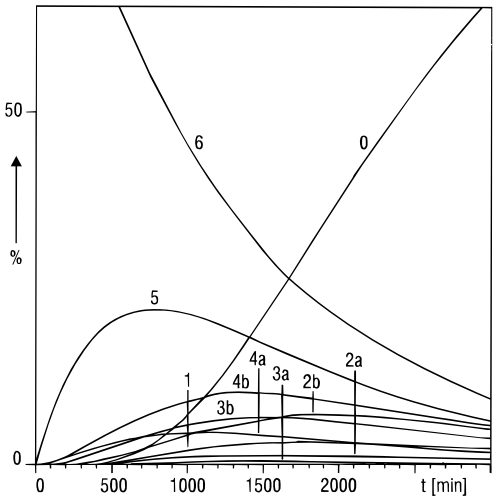

Figure 9. Percent−time diagram for the reaction of $[OsCl_6]^{2-}$ with 5 N HBr at 20 °C (*trans* route) to give $[OsCl_nBr_{6-n}]^{2-}$, $n = 0-6$ (a corresponds to *cis*/*fac*, b corresponds to *trans*/*mer*).

ment with experimentally determined concentrations of the individual species.[40] An illustrative example

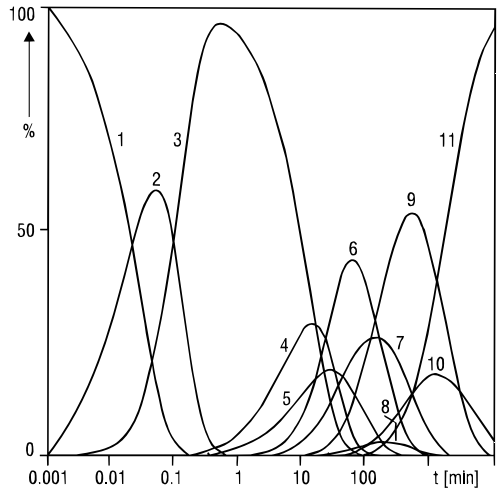

Figure 10. Percent−time diagram for the reaction of *cis*-$[OsBr_4I_2]^{2-}$ with Cl^- (see Figure 11).

of deliberate syntheses with predictable maximum yields is given in Figures 10 and 11 for the reaction sequence initiated by HCl treatment of *cis*-$[OsBr_4I_2]^{2-}$.[41]

Obviously, under similar conditions, the reaction of *cis*-$[OsCl_4I_2]^{2-}$ with HBr results in other products.[41] This is shown in Figures 12 and 13.

The preparation of mixed-fluoro complexes by substitution of the heavier halides with F^- has been a special challenge. Because of its considerable hydration energy, F^- is too inert in aqueous solution with respect to metal coordination. Fortunately, this problem has been overcome by phase transfer of F^- and complex anions by means of long-chain alkylammonium cations in solvents of low or no polarity like chloroform, toluene, or benzene. The resulting intimate ion pairs are marginally solvated and thus very reactive.[42−44] For instance, in toluene, fast intramolecular isomerizations of pure *cis*- and *trans*-chlorobromoosmates(IV) as tridodecylammonium(TDDA) ion pairs occur even at room temperature. Under such strictly nonaqueous conditions, the mixed series, $[OsCl_nBr_{6-n}]^{2-}$, has been obtained not only by reaction of $(TDDA)_2[OsCl_6]$ with gaseous HBr(g) or (TDDA)-Br, but also by reaction of $(TDDA)_2[OsBr_6]$ with HCl-

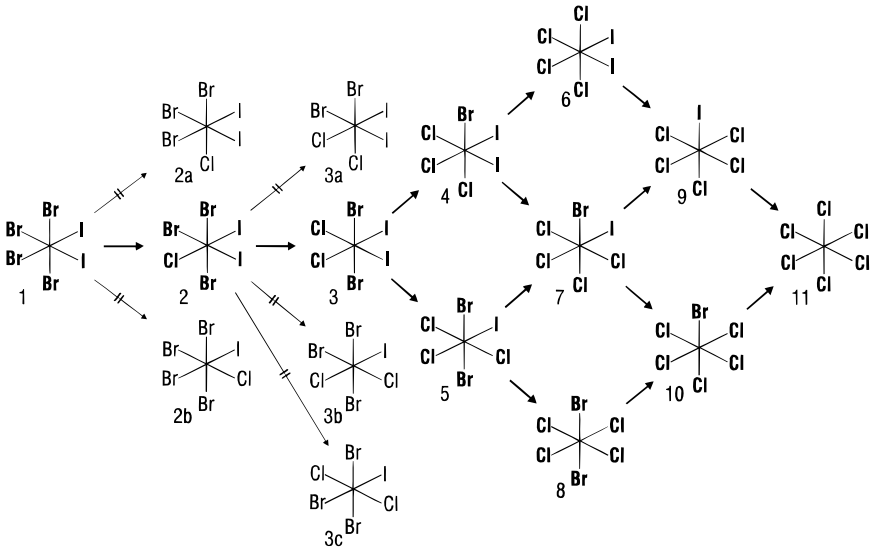

Figure 11. Reaction sequence of *cis*-$[OsBr_4I_2]^{2-}$ with Cl^-.

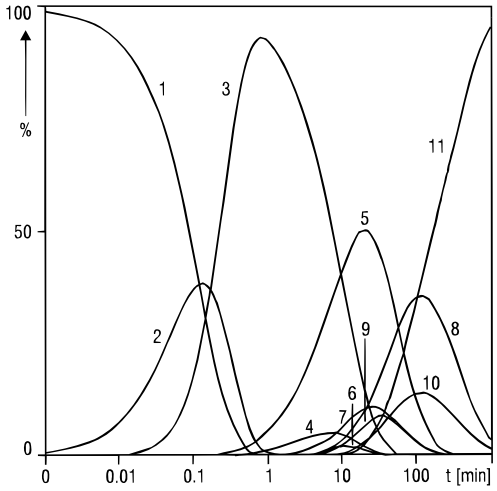

Figure 12. Percent−time diagram for the reaction of *cis*-$[OsCl_4I_2]^{2-}$ with Br^- (see Figure 13).

(g) or (TDDA)Cl. However, all of these pathways yield the different members of the $[OsCl_nBr_{6-n}]^{2-}$ series in various concentrations. Another success of this nonaqueous approach is the elusive series $[OsF_nBr_{6-n}]^{2-}$, which has been obtained by the reactions of $(TDDA)_2[OsF_6]$ with HBr(g).[44,45] By planned sequences of concerted substitution reactions in aqueous and nonaqueous media, nearly every mixed-hexahalogeno complex with an unambiguous geometric arrangement of ligands can be synthesized. This is illustrated in Figure 14 by the 4-fold mixed species $[OsFCl_3BrI]^{2-}$.

It is important to note that these mixed species are not only obtained by solution syntheses, but also by reactions in the solid state. For instance, through the use of n,γ -processes of radioactive recoil atoms, it has been possible to form mixed-hexahalogeno complexes of crystalline systems such as $K_2[ReCl_6]$/$K_2[ReBr_6]$ or $K_2[OsCl_6]$/$K_2[OsBr_6]$. These n,γ-reactions utilized $^{35}Cl \rightarrow {}^{36}Cl$, $^{37}Cl \rightarrow {}^{38}Cl$, $^{81}Br \rightarrow {}^{82}Br$, $^{185}Re \rightarrow {}^{186}Re$, and $^{190}Os \rightarrow {}^{191}Os$, and the subsequent replacement schemes have been interpreted in terms of billiard ball processes.[46] However, at energies tremendously lower, it is possible to thermally initiate such *intramolecular* isomerizations. These isomerizations have been observed by tempering pure stereoisomers of the series, $K_2[OsCl_nY_{6-n}]$, $n = 2, 3, 4$, Y = Br, I, at temperatures in the range of 115−135 °C, with half-lives between 0.5 and 6 h.[47] Elevated temperatures of 170−190 °C initiate *intermolecular* solid-state exchange reactions, resulting in the formation of all of the complexes with $n = 0-6$ and statistical distribution of the ligands to all of the species at equilibrium. However, for complexes containing many I ligands, the exchange rates are low, with half-lives on the order of a few hours, but increase as the number of Cl increases, and reach maximum values for complexes with many Br ligands. Crucial to the exchange mechanism are the octahedral vacancies in the antifluorite lattice.[48]

For the *intramolecular* exchange rates, the series, $K_2[OsCl_6] < K_2[OsBr_6] < K_2[OsI_6]$, is observed, while for *intermolecular* exchange the series, $K_2[OsI_6] < K_2[OsCl_6] < K_2[OsBr_6]$, is found.[49] Also, heterogeneous solid-state reactions have been observed on tempering alkali halide pellets of $K_2[OsX_6]$/KY, $X \neq Y = Cl$, Br, I.[50] Finally, such solid-state isomerizations can also be photochemically induced. For example, the tetra-*n*-butylammonium(TBA) salts of *cis*- and *trans*-$[OsCl_2I_4]^{2-}$ are completely isomerized at −50 °C after a few hours of irradiation by a mercury lamp.[51]

Clearly, the most noticeable and important aspect of all of these items is that the preparation and handling of pure species are in no way trivial. Even during apparently routine operations, such as dissolving or grinding and pressing pellets for spectroscopic investigations, the special circumstances previously discussed must be considered, and appropriate precautions in sample preparation and measuring techniques must be taken.

4. Oxidative Ligand Exchange

Another synthetic route to mixed-ligand complexes is the removal of ligands by oxidation with subsequent occupation of the free coordination sites by other donor atoms. In some special cases, the reduced form of the oxidizing agent can itself act as

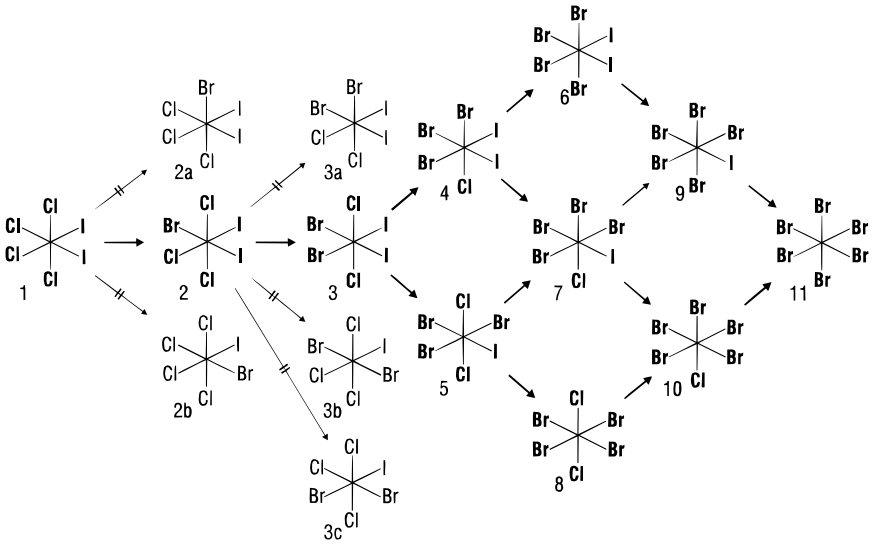

Figure 13. Reaction sequence of *cis*-$[OsCl_4I_2]^{2-}$ with Br^-.

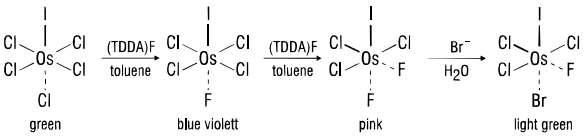

Figure 14. A route to a 4-fold mixed hexahalogeno complex.

the donor atom, such as in the hexahalogenoosmates(IV). Corresponding to the increasing normal potentials 0.53 (I_2), 1.09 (Br_2), 1.36 (Cl_2), 1.80 (F_2) V, the respective lighter halogens oxidize the heavier halide ligands and serve in their reduced forms as new ligands. Thus, mixed complexes are formed by oxidation of $[OsI_6]^{2-}$ with aliquot amounts of Cl_2 in aqueous HCl or Br_2 in HBr. To prevent substitution reactions, the oxidations must be carried out at −30 °C. In concentrated solutions, mainly two respective neighboring species have been stepwise obtained. The desired product distribution may be controlled by limiting the reaction time. It is important to note that in dilute solutions and at elevated temperatures, hydrolysis occurs.[52] The observed exclusive formation of the *cis/fac* isomers is surprising from a mechanistic point of view, because a statistic attack of the oxidizing agent is expected. A possible explanation is the participation of a 5-fold coordinated transition state after oxidation. This molecule rapidly rearranges in a Berry rotation manner via trigonal-bipyramidal configurations to a tetragonal-pyramidal arrangement. Characteristic of this arrangement is that the most *trans*-active ligand, in this case I, occupies the *trans* position to the vacant coordination site. This vacancy then behaves like a ligand with a very weak *trans* effect, while the *trans* Os−I bond is considered to be very stable.[52] Therefore, at low temperatures, the octahedral coordination is restored by nucleophilic attack of that halide ion originating from the oxidizing halogen, because it is inevitably in close vicinity to the vacant site.

From a preparative point of view, oxidative ligand exchange is of great interest, especially for the *trans/mer* isomers of the series, $[OsCl_nBr_{6-n}]^{2-}$, $n = 2, 3, 4$, which are elusive by substitutive ligand exchange. However, these complexes have been obtained stereospecifically and quantitatively by oxidation with Br_2 in HCl solution at −20 °C from the respective $[OsCl_nI_{6-n}]^{2-}$ species, which can be obtained as pure stereoisomers (vide supra). In the same manner $[OsClBr_5]^{2-}$ and $[OsCl_5Br]^{2-}$ are formed from the respective chloroiodoosmates(IV).[52]

Oxidative ligand exchange is not only restricted to solutions, but is also possible in solids. Finely powdered $K_2[OsI_6]$ reacts with Cl_2 or Br_2 via a total exchange mechanism, and forms $K_2[OsCl_6]$ or $K_2[OsBr_6]$, while $K_2[OsBr_6]$ does not react with Cl_2. By controlled exposure to the oxidizing agents reactions may be interrupted and the intermediately present mixed complexes can be observed. These principles can be clearly seen in the case of $K_2[OsCl_nI_{6-n}]$, such as for the *trans* and *mer* isomers and *cis*-$K_2[OsCl_4I_2]$. In these compounds, oxidation by Br_2 results in the exclusive replacement of I, and the corresponding chlorobromo homologues can be obtained quantitatively and stereospecifically. However, from *fac*-$K_2[OsCl_3I_3]$ a 70:30 mixture of *fac/mer*-$K_2[OsCl_3Br_3]$ is obtained, while in the case of *cis*-$K_2[OsCl_2I_4]$ the massive interchange of four I results in the intermixing of the entire coordination sphere, and all of the possible $K_2[OsCl_nBr_{6-n}]$ species are formed.[52]

A more common type of oxidative ligand exchange is the preparation of fluoro-mixed complexes utilizing BrF_3. The postulated stereospecific formation of *fac*-$K_2[PtF_3Cl_3]$[53] as the sole oxidation product of $K_2[PtCl_6]$ with BrF_3 has never been verified.[19,54] Depending on the reaction conditions, other mixed species $[PtF_nCl_{6-n}]^{2-}$ have been detected; however, for $n = 2, 3, 4$, only the *cis/fac* isomers have been present.[55] Corresponding fluorochloro complexes are known for Re(IV,V), Os(IV,V), and Ir(IV,V).[56−60] Octahedral complexes containing the heavier halides, Br or I, together with F are rare, but are known for Pt(IV) and Os(IV),[13,42,45] and most notably Re(IV), for which there are many examples of 3-fold mixed species.[61]

At first glance, the oxidative addition to quadratic planar systems seems a promising route to octahedral species with *trans* configuration, but caution should prevail. As has been demonstrated on the oxidation of $[PtCl_4]^{2-}$ by Br_2, only under strict obedience of distinct reaction conditions is it possible to synthesize *trans*-$[PtCl_4Br_2]^{2-}$ stereospecifically.[62−64]

5. Separation Methods

Apart from a very few exceptions, the preparation of mixed-ligand complexes results in mixtures of several or even all of the conceivable components. This is true especially for equilibrium reactions, but also for substitution sequences under kinetic control and for oxidative ligand exchange. As the series under discussion contains closely related compounds with respect to their physical and chemical properties, the preparation of distinct pure species inevitably demands powerful and specific separation techniques. Good introductions to the various separation techniques and basic principles are given in refs 65−67.

Ionophoresis. Initially, high-voltage paper ionophoresis was applied to the separation of mixed-hexahalogeno complexes. Here, migration in the electric field is based on different ionophoretic mobilities supported by specific interactions with the paper and depends mainly on the mass, size, degree of hydration, and effective charge. In this way, the series, $[MCl_nBr_{6-n}]^{2-}$, M = Re, Os, Ir, Pt, $n = 0-6$, have been separated for the first time.[68,69] By paper ionophoresis, seven equidistant zones appear, with the hexachloro complex being the fastest and the 20% slower hexabromo complex being last. The stereoisomers have not been separable and are only available as pure substances if their preparation can be carried out along a stereospecific route (see sections II.A.3 and 4). From the separated zones, the individual complexes have been obtainable on a low milligram scale thus requiring multiple runs for the isolation of sufficient quantities for characterization. Attempts to improve yields by carrier-free continuous flow ionophoresis have failed because of insufficient differences in the mobilities. This difficulty has proven unsurmountable even by counterflow ionophoresis.[67,70−72]

Some physical effects and chemical requirements oppose each other in ionophoretic methods, resulting in general drawbacks with respect to mixed transition metal complexes. On one hand, high voltages are required for acceptable and rapid separation, as well as a high electrolyte concentration to suppress hydrolysis. However, on the other hand, the inevitably produced Joule heat is proportional to the square of the electrical current, which rises with the electrolyte concentration.[67] With respect to the electrolyte a compromise between suppression of hydrolysis and specific mobility of the complex ions must be found, with dilution being the favored variable. In every case, efficient cooling is necessary to dissipate the heat produced. In summary, ionophoresis is a quick, inexpensive method for qualitative investigations of the aforementioned problems, but unsuitable for the separation of pairs of stereoisomers.

Ion Exchange Chromatography. Ion exchange resins, composed of synthetic polymers with large numbers of ionic functional groups, are unsuitable for the separation of the mixed-hexahalogeno metalates because the strength of the interactions between the complex ions and the stationary phase renders the ions completely immobile. The most useful compromise of possible stationary phases is [(diethylamino)-ethyl] cellulose (DEAE cellulose), because of its weakly basic anchor groups. As mobile phases, ~2 M acids or salt solutions are sufficiently appropriate to suppress hydrolysis even of sensitive compounds, especially when combined with cooling. Due to the interactions of the stationary phase with the complex anions, which is mainly dependent on their effective charge and size, very subtle differences in mobility result, and render possible the separation of stereoisomers.[73] The technique of column chromatography[74] is favorable, because the separation is very suitable for gram scale preparation. In the majority of cases, colored zones are observed as the result of separation. For pale colored or colorless compounds, such as the multiple F-substituted species, spray agents or UV light allow the different zones to be located. To avoid large elution volumes and excess dilution of species by break-through elution, a more convenient technique has been used. After complete separation of the zones the aqueous eluent is removed, the wet cellulose material is ejected from the column, the complex containing zones are cut out, and the complexes are gathered from the DEAE cellulose by displacement elution. Appropriate eluents for this purpose are tetraalkylammonium salts in organic solvents such as acetone or dichloromethane.[74]

The velocities of $[OsCl_6]^{2-}$, $[OsBr_6]^{2-}$, and $[OsI_6]^{2-}$ on DEAE cellulose are 8:4:1; and thus decrease with increasing ionic size and mass. Because the mixed species are arranged between the respective homoleptic complexes, the problem of separation is easiest for the $[OsCl_nI_{6-n}]^{2-}$ series, enabling the clean separation of even the stereoisomeric pairs, with the *trans/mer* isomers being faster than their corresponding *cis/fac* congeners. All 10 species migrate as totally independent zones of characteristic colors, which contrast strongly with the white stationary phase. An example of the typical data found for this series is given in Table 4.[73]

Table 4. Ion Exchange Chromatography[a] of Mixed Chloroiodoosmates(IV) on DEAE Cellulose

complex ion	V_D[b]	V_E[b]	color
$[OsCl_6]^{2-}$	266	112	yellow
$[OsCl_5I]^{2-}$	412	122	green
cis-$[OsCl_4I_2]^{2-}$	674	110	blue-grey
trans-$[OsCl_4I_2]^{2-}$	834	124	blue
fac-$[OsCl_3I_3]^{2-}$	1085	61	russet
mer-$[OsCl_3I_3]^{2-}$	1277	150	light-blue
cis-$[OsCl_2I_4]^{2-}$	1869	205	pale-green
trans-$[OsCl_2I_4]^{2-}$	2180	400	blue-green
$[OsClI_5]^{2-}$	2703	440	grass-green
$[OsI_6]^{2-}$	–	–	violet

[a] Diameter of column, 20 mm; packing height, 150 mm; eluent, 2 N HCl; temperature, −5 °C; pressure, 1 bar; flow velocity, 3 mL/min. [b] Total break-through volumina V_D and volumina V_E (mL) necessary for complete elution of a special complex ion.

Thin-layer chromatography[75] and high-performance liquid chromatography(HPLC) are other techniques,[76,77] although much smaller quantities are separable than those isolated by low-pressure column liquid chromatography on DEAE cellulose. Additionally, it should be mentioned that for the separation of cationic complexes, carboxymethyl cellulose with weakly acid anchor groups is a suitable stationary phase.[78]

B. Vibrational Spectroscopy

The interpretation and complete assignment of vibrational spectra of molecules in accordance with given or anticipated structures and symmetries is based on group theory and selection rules. The two techniques for the experimental investigation of molecular vibrations, IR and Raman spectroscopy, are complementary, and should be jointly applied. General introductions with respect to basic theory, instrumentation, sampling techniques, and special applications are given by Rossiter and Hamilton[79] and by Ebsworth et al.[80] Special texts on Raman spectroscopy and Fourier transform techniques are to be found in refs 81−84. A valuable data base, as well as an excellent introduction to theory of normal vibrations, is Nakamoto's textbook.[85] A comprehensive treatise of quantum mechanical and group theoretical fundamentals and formalisms is presented in ref 86 while Herzberg's *Infrared and Raman Spectroscopy*[87] and Cotton's *Chemical Applications of Group Theory*[88] may serve as the standard references on the fundamentals of these subjects. The GF matrix method as the common basis of normal coordinate analysis has been dealt with in detail by Wilson, Decius, and Cross.[89] Computer calculation programs for the solution of the vibrational secular equation often originate from an algorithm developed by Shimanouchi;[90] however, modifications and other programs are frequently used.[91−93]

1. Vibrational Spectra

Complete series of octahedral mixed hexahalogeno complexes $[MX_nY_{6-n}]^{z-}$ are well-suited for IR and Raman spectroscopic studies. In combination with

normal coordinate analyses, total assignments of observed frequencies to normal modes of vibration, their numerical calculation, the determination of force constants, and the elucidation of the inherent problems of vibrational coupling is achieved in most cases, because (1) the monoatomic ligands are in stereochemical arrangements with well-known symmetries; (2) the number of normal modes is limited to 15; (3) the number of force constants remains tractable; (4) each series consists of 10 individual species with graduated chemical and physical properties and point groups descending from O_h to D_{4h}, C_{4v}, C_{3v}, or C_{2v} symmetry; (5) in the case of chloro complexes additional data for normal coordinate analyses are provided by isotopic labeling with ^{35}Cl and ^{37}Cl; and (6) empirical parameters quantifying the mutual interactions of the ligands, in particular the *trans* influence, are revealed.

It is important to emphasize that all components of a series must be isolated as salts containing the same cation for the sake of comparable frequencies. For isotopic shift experiments a precise internal referencing, best done by laser plasma lines, as well as high resolution by low-temperature measurements are necessary (Figure 15). In the case of Raman spectroscopy, enhanced resolution is achieved at 80 K on rotating samples.[94−96] Further improvement is attained by a moving Raman cell at 10 K.[97] Another advantage of these devices is that deeply colored compounds can be measured without decomposition even by irradiation of absorption maxima, which enables the observation of resonance Raman effects.

The reducible representations of vibrations and depictions of IR and Raman activity for the individual species of the general series $[MX_nY_{6-n}]$, $n = 0-6$, are compiled for the respective point groups in Table 5.

With the exception of the modes T_{2u} in O_h, A_2 in C_{3v}, and B_{2u} in D_{4h}, which are inactive, all vibrations are allowed. In centrosymmetric molecules, the rule of mutual exclusion states that all vibrations with even (g = gerade) parity are Raman active, and that those with odd (u = ungerade) parity are IR active, exclusively. In absence of a center of inversion, certain vibrations are allowed in both the IR and the Raman spectrum. Unfortunately, in spectra of these compounds, fewer bands than theoretically expected may be observed, or more bands may appear due to hot bands, overtones, combination or difference bands, Fermi resonances, resonance Raman effects, band splittings by solid-state effects, and lattice vibrations. Thus, complete and accurate assignment is difficult and may be improperly done if only a single compound from a series is studied. On the whole, these difficulties can be overcome by considering an entire series and the provided systematics therein. Also useful to this problem of assignment is the comparison of spectra measured at various temperatures in both the solution and the solid state. Furthermore, a comparison of homologous series with the same central atom, but in different oxidation states, or with different central atoms, can be insightful, as has been proven by mixed-hexahalogeno complexes of the platinum metals.

An impressive example for the combination of IR and Raman spectroscopy with normal coordinate analysis is the series, $[PtF_nCl_{6-n}]^{2-}$, $n = 0-6$, which has been synthesized with $^{n.a.}Cl$ (natural abundance)[55] and in isotopic labeling with ^{35}Cl and ^{37}Cl.[98] The vibrational spectra of the $^{n.a.}Cl$ series are presented in Figure 15. The notation of the vibrations is adopted from ref 56, where the involved point groups, the irreducible representations, IR and Raman activities, degrees of depolarization, and illustrations of all normal modes are given.

The corresponding spectra of the isotopically labeled compounds are to be found in ref 98. The Raman spectra and normal coordinate analyses data of the complete series of the stereospecifically synthesized pure individual isotopomers, $[Pt^{35}Cl_n{}^{37}Cl_{6-n}]^{2-}$, $n = 0-6$, are given in ref 97.

In comparison with the other platinum metals, the fluorochloroplatinates(IV) possess by far the sharpest and most intense lines. Thus, splitting of certain bands according to the chlorine isotopes has been observable, e.g. of ν_3 in the complexes *mer*-$[PtF_3Cl_3]^{2-}$ (3b) and $[PtFCl_5]^{2-}$ (5), with intensities being in agreement with the natural abundance ratio of ^{35}Cl: $^{37}Cl = 3:1$. This can be seen even in the IR spectrum of $[PtFCl_5]^{2-}$ (5) in the case of ν_3, although the IR bands naturally have larger half-widths. The three possible chlorine isotopomers of *trans*-$[PtF_4Cl_2]^{2-}$ (4b), with the axes $^{35}Cl-Pt-^{35}Cl$, $^{35}Cl-Pt-^{37}Cl$, and $^{37}Cl-Pt-^{37}Cl$, are resolved by the Raman active Pt−Cl stretching mode ν_2 into three lines with intensities in agreement with the statistical ratio of 9:6:1 for $^{n.a.}Cl$ (see inset in Figure 15). It is noteworthy, that even without detailed normal coordinate analysis,[99] the sole application of the Teller−Redlich product rule provides excellent agreement between the observed and the calculated isotopic shifts, allowing unambiguous assignment of all stretching modes and most of the bending modes.[55]

Another advantage of the fluorochloroplatinates-(IV), with respect to complete assignment and dependable frequency data for normal coordinate analyses, is that the F^- ligand has low mass and short bonds to the central ion in comparison to the heavier halides. Therefore, the stretching vibrations of Pt−F, found in the region between 590 and 500 cm^{-1}, are clearly separable from those of Pt−Cl, found in the region between 380 to 310 cm^{-1}. The bending modes of F−Pt−F fall in the range between 270 and 215 cm^{-1}, which are seperable from the Cl−Pt−Cl modes, found in the region between 190 and 160 cm^{-1}, although they do overlap with the modes of F•−Pt−Cl′ which are between 280 and 180 cm^{-1}. The lattice vibrations are below 100 cm^{-1} and of low intensity in the Raman spectra.

Of special interest in mixed-ligand complexes are the mutual interactions of the different ligands acting along the octahedral axes as either a *trans* influence or between ligands in vicinity as a *cis* influence. This can be seen clearly in the spectra of these compounds (Figure 15). The stretching vibrations originating from symmetric F−Pt−F or Cl−Pt−Cl axes remain relatively unaffected, whereas the mutuality of the *trans* influences on F•−Pt−Cl′ axes causes shifts of the Pt−F• vibrations 40−55 cm^{-1} toward lower frequencies, and shifts of the Pt−Cl′ vibrations toward higher frequencies by 25−40 cm^{-1}. *mer*-

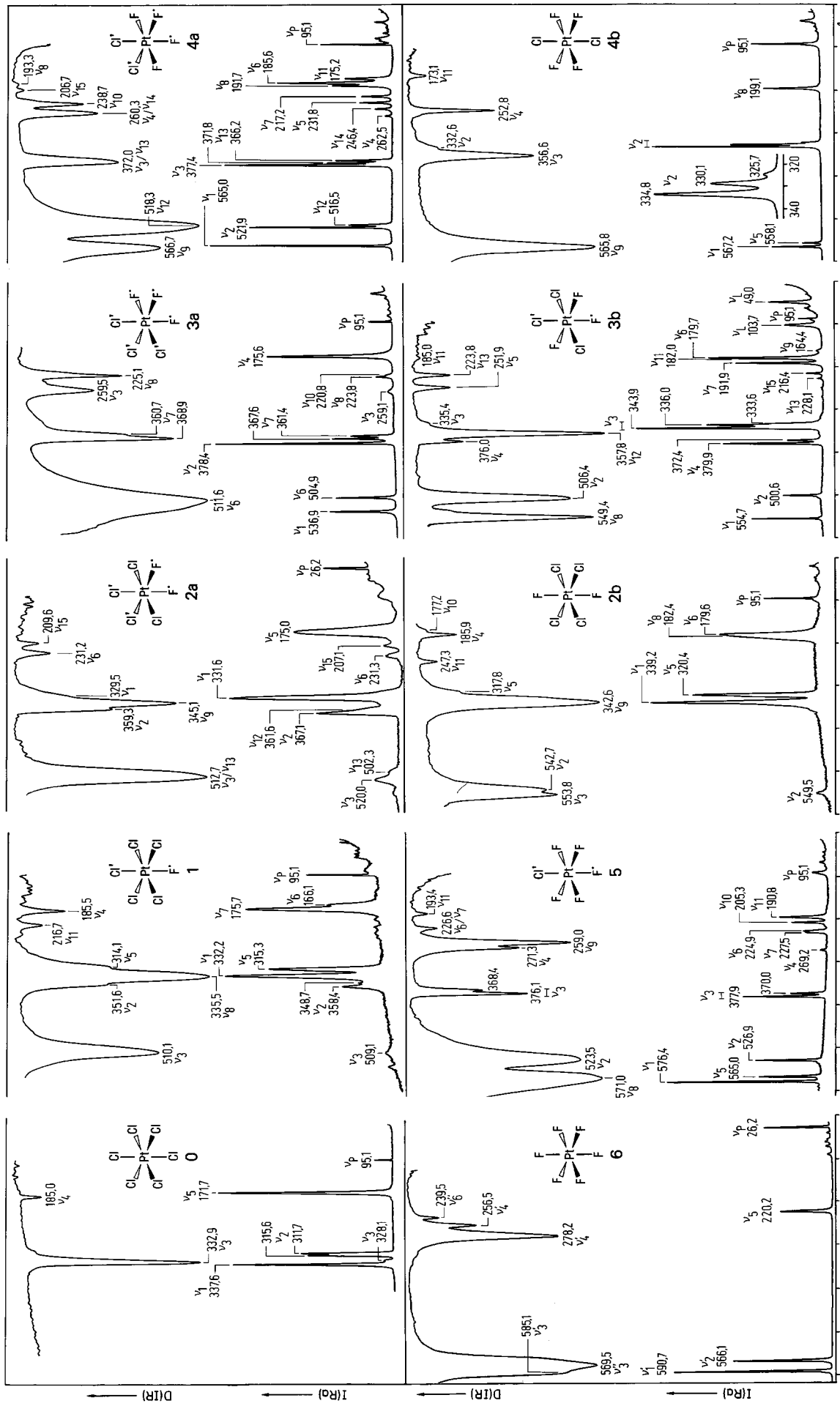

Figure 15. IR and Raman spectra (80 K) of $Cs_2[PtF_nCl_{6-n}]$, $n = 0-6$ (a corresponds to *cis*/*fac*; b corresponds to *trans*/*mer*); $\lambda_0 = 647.1$ nm ($\nu_p = 95.1$ cm^{-1}); $\lambda_0 = 568.2$ nm ($\nu_p = 26.2$ cm^{-1}).

Table 5. Point Symmetry and Characters of Normal Vibrations for $[MX_nY_{6-n}]$, $n = 0-6$

n[a]	symmetry	characters[b]
6, 0	O_h	$A_{1g} + E_g + \mathbf{2T_{1u}} + T_{2g} + T_{2u}$
5, 1	C_{4v}	$\boldsymbol{4A_1} + 2B_1 + B_2 + \boldsymbol{4E}$
4a, 2a	C_{2v}	$\boldsymbol{6A_1} + \mathbf{2A_2} + \boldsymbol{3B_1} + \boldsymbol{4B_2}$
4b, 2b	D_{4h}	$2A_{1g} + \mathbf{2A_{2u}} + B_{1g} + B_{2g} + B_{2u} + E_g + \mathbf{3E_u}$
3a	C_{3v}	$\boldsymbol{4A_1} + A_2 + \boldsymbol{5E}$
3b	C_{2v}	$\boldsymbol{6A_1} + A_2 + \boldsymbol{4B_1} + \boldsymbol{4B_2}$

[a] a corresponds to *cis*/*fac*; b corresponds to *trans*/*mer*. [b] IR activity, bold; Raman activity, italics.

$Cs_2[PtF_3Cl_3]$ (3b) because it contains the aforementioned three different axes, is an excellent example of this. For this compound, the streching vibration ν_2 of the *trans* weakened Pt−F• bond is found at 500.6 cm^{-1}, while the corresponding mode ν_1 of the symmetric F−Pt−F axis is located at 554.7 cm^{-1}. Similarly, ν_4 of the *trans*-strengthened Pt−Cl′ bond, found at 379.9 and 372.4 cm^{-1}, is shifted higher by about 40 cm^{-1} in comparison to ν_3 of the Cl−Pt−Cl axis, which lie at 343.9, 336.0, and 333.6 cm^{-1}. The observed splittings are in accordance with the $^{n.a.}$Cl isotopomers. A detailed discussion of all spectra in Figure 15 would be too time consuming, therefore we refer to refs 55 and 99. For $[PtF_6]^{2-}$ it must be considered that its alkaline salts crystallize in the $K_2[GeF_6]$ type (D_{3d}),[100,101] and as a result of the lowered symmetry, splittings of degenerate vibrations are observed. Furthermore, the observed frequencies are very dependent on the cation present.[99]

Similar investigations, sometimes supported by crystal structure determinations, have been performed on many series of the fluorochloro metalates $[MF_nCl_{6-n}]^{z-}$ of Ta(V),[102] Os(IV),[56] Os(V),[57] Ir(IV),[58] Ir(V),[59,60] and Pt(IV),[103] fluorobromoosmates(IV),[44,45] chlorobromometalates $[MCl_nBr_{6-n}]^{z-}$ of Nb(V),[102] Ta(V),[102] Tc(IV),[104] Ru(IV),[105] Rh(III),[106] Os(IV),[15,107] Ir(III),[108] Ir(IV),[108] and Pt(IV),[62,109−111] bromoiodometalates $[MBr_nI_{6-n}]^{2-}$ of Re(IV),[112] and Os(IV)[113,114] and the unique chloroiodo series $[OsCl_nI_{6-n}]^{2-}$.[107,115]

Besides these mixed-hexahalogeno metalates, there are several series of molecular compounds of the heavier transition metals and actinides, $[MF_nCl_{6-n}]$ (M = Mo, W, Re, U, and Th),[116−120] some of which are volatile and stable in the gas phase. These properties allow supplementary information on the molecular structure to be gathered by other techniques, such as by microwave spectroscopy as in case of $[MF_5Cl]$, M = Te, W.[119] It has also been reported that mixed hexahalogeno complexes of main group elements, Sn,[16] Sb,[121] S,[122−126] Se,[122,123,127] and Te[124,128−130] have been studied by vibrational spectroscopy.

2. Normal Coordinate Analysis

Due to the availability of very efficient and inexpensive personal computers, and the development of diverse programs,[90−93] normal coordinate analysis has become more and more popular. The general course of force field calculations, along with the necessary requirements and common results is presented in Scheme 1.

A practicable approach to this problem is based on the GF matrix method introduced by Wilson, Decius, and Cross.[89] Different kinds of force fields are used to treat intramolecular and, in more advanced calculations, intermolecular forces. Most common are the generalized valence force field (GVFF), the Urey−Bradley force field (UBFF), the orbital valence force field (OVFF), and their respective modifications (MVFF, MUBFF, and MOVFF).[131] The GVFF and MVFF are the most straightforward ways to deal with force fields and utilize a simple potential function of valence and angle sustaining forces and their interactions, neglecting anharmonicity. While in the GVFF, the F matrix must consider all of the force constants, in the MVFF interaction force constants are either partially or totally neglected. The UBFF and MUBFF use another approach, based on a different potential function, which takes into consideration stretching and bending force constants, as well as repulsive force constants between nonbonded atoms. In close resemblance to the UBFF, the OVFF and MOVFF also account for distortions of bonding orbitals. Evidently, the values of force constants depend on the force field initially chosen, and thus deviate from one another. A comparative study of the three aforementioned force fields applied to homoleptic halogenometalates is presented in refs 132 and 133.

Normal coordinate analyses are performed either to determine force constants by fitting calculated and observed frequencies or to calculate frequencies from a set of force constants. The fitting can be done via a Jacobi matrix by interactive adjustment of force constants or by iteration with appropriate algorithms. By calculation of the potential energy distribution, the type of coupling, and especially the degree of coupling can be found.

In application to mixed octahedral complexes, the Cartesian coordinates of the seven-atom molecules

Scheme 1

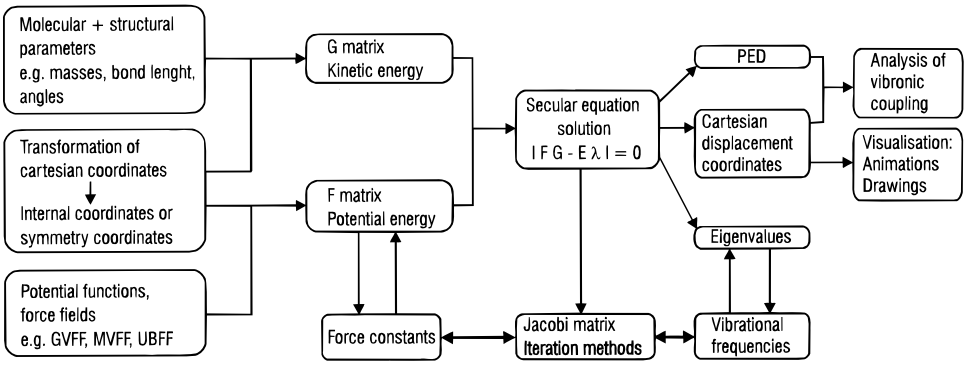

Table 6. Number and Types of Force Constants *f* for $[MX_nY_{6-n}]$, $n = 0-6$[135]

n[a]	symmetry	f_d	f_α	$f_{dd'}$	f_{dd}	$f_{d\alpha}$	$f_{d\alpha'}$	$f_{d\alpha''}$	$f_{\alpha\alpha}$	$f_{\alpha\alpha'}$	$f_{\alpha\alpha''}$	$f_{\alpha\alpha'''}$	Σf
0, 6	O_h	1	1	1	1	1	1	1	1	1	1	1	11
2b, 4b	D_{4h}	2	2	2	2	3	2	3	2	3	2	2	25
1, 5	C_{4v}	3	3	2	3	5	4	5	4	4	2	3	38
3a	C_{3v}	2	3	1	3	4	6	4	2	5	2	4	36
2a, 4a	C_{2v}	3	5	2	5	8	7	8	5	7	3	7	60
3b	C_{2v}	4	5	3	5	10	6	10	7	6	3	6	65

[a] a corresponds to *cis*/*fac*; b corresponds to *trans*/*mer*.

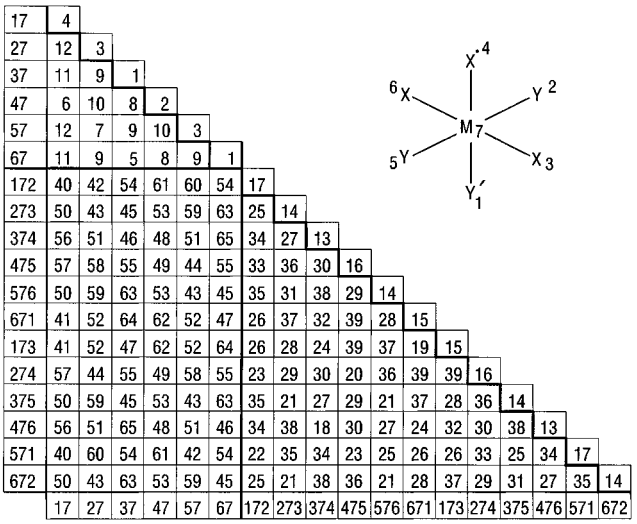

Figure 16. F matrix for a *mer*-$[MX_3Y_3]$ complex (C_{2v}).

are transformed into a matrix of internal coordinates, containing the six bonds and 12 angles of the system. The G matrix is then defined as the inverse matrix of the kinetic energies. The corresponding F matrix of the potential energies is partitioned into five areas, two of which are reserved for the valence and deformation force constants, while the remaining three are assigned to the force constants of valence−valence, valence−angle, and angle−angle interactions. In total there are 171 elements in the triangular matrix. Depending on the symmetry of the species, a maximum of 65 different elements is obtained, as in the case of a *mer*-$[MX_3Y_3]$ species, with point group C_{2v} (see Figure 16). This F matrix has been chosen, because it demonstrates the most complicated case within the mixed $[MX_nY_{6-n}]$ series. For species with higher symmetries, the number of different force constants decreases and reaches a minimum of 11 different elements for O_h symmetry (see Table 6).

Furthermore, the meridional species are noteworthy, in that they represent the only example of a molecule containing three different axes X−M−X, X′−M−Y′, and Y−M−Y. Thus, they are especially well-suited for studies of the different mutual influences, particularly the *trans* influence and its effect on the force constants.

The intrinsic problem of underdetermination due to a deficient number of experimentally available frequencies makes it impossible to set up a meaningful general valence force field without further information. This problem can be moderated either by simplification of the GVFF or by providing supplementary experimental data, although a combination of both approaches is the most beneficial. The first path is to establish a modified valence force field by deliberate neglect of some force constants. For this approximation, the interaction force constants are either partially or totally omitted. As there is no generally valid algorithm to deal with this problem of restricting the number of force constants to a MVFF, personal decisions which seem most plausible must be made. Here, the greatest advantage of complete and closely related series becomes evident. By comparison of the data from different species within a given series, as well as from isostructural species of different series, insight into systematic behavior can be found. At this point, the Jacobi matrix is a very useful tool for a meaningful selection of force constants, because the effect of changes in the various constants becomes immediately evident by the calculated frequency shifts.

The second approach, especially required for the determination of interaction terms, is to acquire supplementary spectroscopic data from the measurement of isotopically labeled systems, which have identical force fields to a first approximation. The resulting two different G matrices contain the reciprocal masses of the isotopes and additional sets of *eigenvalues* are obtained. This, together with the increased number of experimental frequencies, extends the number of determinants for the force constants. One unavoidable condition is that the mass differences between the isotopes must be sufficient to cause an observable shift of valence vibrations and, whenever possible, of deformation bands. With respect to stable isotopes, there are only a few examples within the transition metals, e.g. ^{92}Mo and ^{100}Mo, ^{96}Ru and ^{104}Ru, ^{102}Pd and ^{110}Pd. In the case of molybdenum, this has been evidenced by distinct isotopic shifts on labeled MoF_6 and confirmed by normal coordinate analyses.[120,134] Within mixed-hexahalogeno metalates, only isotopic labeling with ^{35}Cl and ^{37}Cl results in sufficient frequency shifts of up to 9 cm^{-1} (Figure 15), as has already been discussed for the $^{n.a.}$Cl spectra of the fluorochloro platinates(IV). Of special notice, the spectra of the corresponding isotopically pure compounds $[PtF_n{}^{35}Cl_{6-n}]^{2-}$ and $[PtF_n{}^{37}Cl_{6-n}]^{2-}$ are much more informative and serve as an extended data basis for dependable normal coordinate analysis.[99] The valence force constants are compiled in Table 7 and reveal a systematic dependence on the degree of substitution.

A remarkable example of a mixed series is presented by $[Pt^{35}Cl_n{}^{37}Cl_{6-n}]^{2-}$, $n = 0-6$, for which all individual species have been prepared as pure compounds[97] (Figure 17).

The most striking feature of these data is the splitting of the "E_g" mode ν_2 in the spectrum of

Table 7. Valence Force Constants f_d (mdyne/Å) for Fluorochloroplatinates(IV)

compound	f_d(Pt−F)	f_d(Pt−F′)	f_d(Pt−Cl)	f_d(Pt−Cl′)
$Cs_2[PtCl_6]$	–	–	1.87	–
$Cs_2[PtCl_5F]$	–	2.66	1.90	2.18
cis-$Cs_2[PtCl_4F_2]$	–	2.67	2.00	2.31
trans-$Cs_2[PtCl_4F_2]$	3.13	–	2.03	–
mer-$Cs_2[PtCl_3F_3]$	3.12	2.50	2.08	2.56
fac-$Cs_2[PtCl_3F_3]$	–	2.65	–	2.43
cis-$Cs_2[PtCl_2F_4]$	3.27	2.68	–	2.45
trans-$Cs_2[PtCl_2F_4]$	3.25	–	2.00	–
$Cs_2[PtClF_5]$	3.33	2.86	–	2.43
$Cs_2[PtF_6]$	3.40	–	–	–

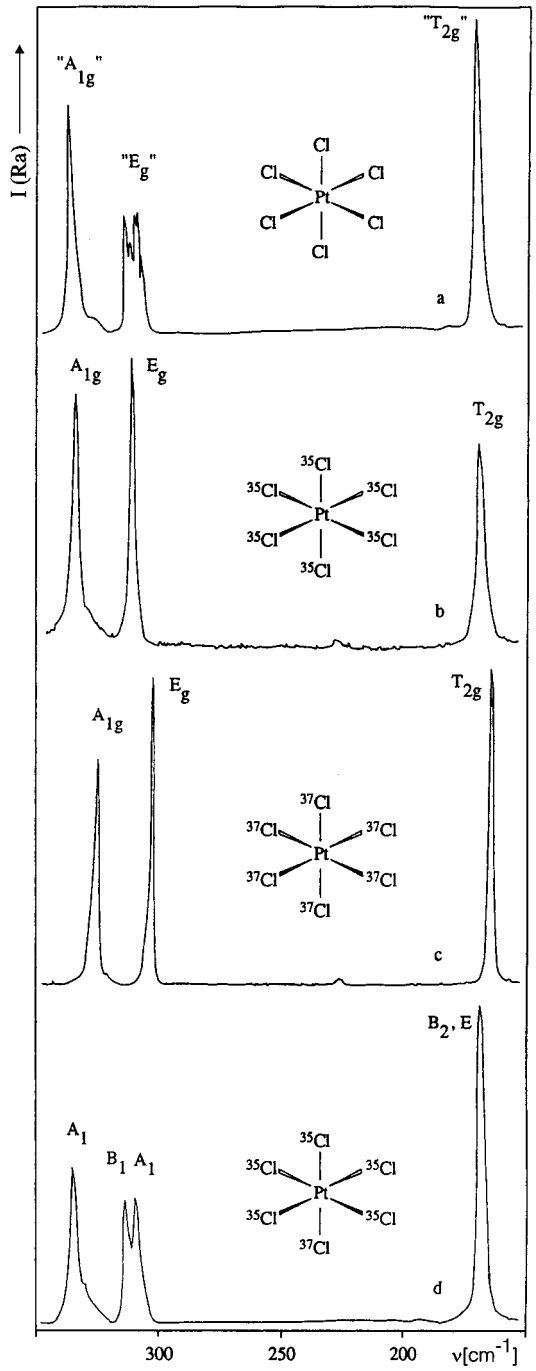

Figure 17. Raman spectra (10 K) of $Cs_2[Pt^{35}Cl_n{}^{37}Cl_{6-n}]$: $^{n.a.}Cl$ (a), $n = 6$ (b), 0 (c), 5 (d).

$Cs_2[Pt^{n.a.}Cl_6]$. The limits of this band are clearly defined by $Cs_2[Pt^{35}Cl_6]$ and $Cs_2[Pt^{37}Cl_6]$, with a shift difference of 8.6 cm^{-1}, while $Cs_2[Pt^{35}Cl_5{}^{37}Cl]$ reveals

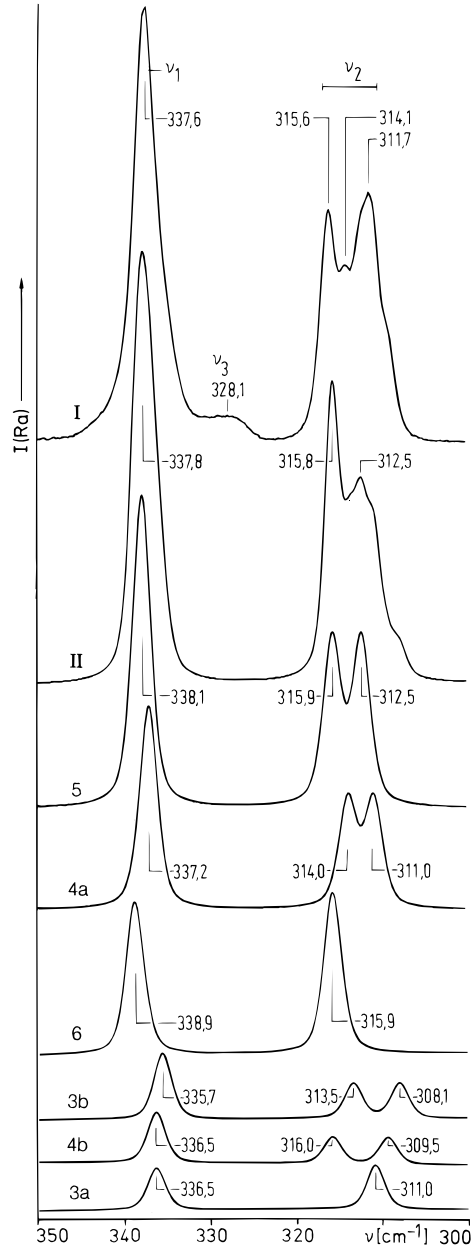

Figure 18. Comparison of the measured spectrum of $[Pt^{n.a.}Cl_6]^{2-}$ (I) and the superposition (II) of calculated spectra of $[Pt^{35}Cl_n{}^{37}Cl_{6-n}]^{2-}$, $n = 3-6$ (a corresponds to *cis*/*fac*; b corresponds to *trans*/*mer*) according to statistic probabilities.[99]

instead of "E_g", the A_1 and B_1 modes, as derived by group theory. On the basis of the precise frequencies available from the individual species of this series, the spectrum of $Cs_2[Pt^{n.a.}Cl_6]$ has been simulated by superposition of the spectra of the most frequent isotopomers according to their statistical probabilities for $^{n.a.}Cl$. This is shown to correspond excellently with the observed spectrum in Figure 18.

A survey of MVFF-based normal coordinate analyses on mixed-hexahalogeno complexes is given by the force constants in Table 8, which have been averaged within the respective series for a rough elucidation of general trends.

Not yet thoroughly considered is the dependence of the *trans* influence on the valence-shell electron configuration of the central atom, which exhibits some new systematic trends. A comparison of the

Table 8. Averaged Valence Force Constants f_d(M−X) (mdyne/Å) for Complete Series of Hexahalogenometalates, $[MX_nY_{6-n}]^{z-}$

series[a]	F•	F	Cl•	Cl	Cl′	Br•	Br	Br′	I	I′	ref
$[TcCl_nBr_{6-n}]^{2-}$			1.32	1.47			1.06	1.12			104
$[ReBr_nI_{6-n}]^{2-}$						1.24	1.33		0.82	0.89	112
$[ReCl_nI_{6-n}]^{2-}$			1.52	1.67					0.80	0.90	142
$[ReF_nCl_{6-n}]^{2-}$	2.98	3.23		1.67	1.80						142
$[ReF_nBr_{6-n}]^{2-}$	2.92	3.23					1.33	1.38			142
$[RuCl_nBr_{6-n}]^{2-}$			1.36	1.45			1.00	1.08			135
$[RhCl_nBr_{6-n}]^{3-}$			1.29	1.44			1.17	1.33			135
$[OsCl_nBr_{6-n}]^{2-}$			1.60	1.70			1.31	1.39			135
$[OsCl_nI_{6-n}]^{2-}$			1.55	1.66					0.88	0.96	115
$[OsBr_nI_{6-n}]^{2-}$						1.27	1.31		0.88	0.93	113
$[OsF_nCl_{6-n}]^{2-}$	2.80	3.07		1.69	1.93						135
$[OsF_nCl_{6-n}]^{-}$	3.50	3.90		1.94	2.35						135
$[IrCl_nBr_{6-n}]^{3-}$			1.55	1.61			1.25	1.44			135
$[IrCl_nBr_{6-n}]^{2-}$			1.66	1.75			1.37	1.43			135
$[IrF_nCl_{6-n}]^{2-}$	2.74	3.12		1.80	2.14						135
$[IrF_nCl_{6-n}]^{-}$	3.42	3.85			2.31						135
$[PtCl_nBr_{6-n}]^{2-}$			1.79	1.91			1.54	1.63			135
$[PtF_nCl_{6-n}]^{2-}$	2.67	3.25		1.98	2.39						135

[a] X· corresponds to weakened ligand; X′ corresponds to strengthened ligand.

Table 9. Influence of Oxidation State on Valence Force Constants f_d (mdyne/Å) of $[OsF_nCl_{6-n}]^{z-}$, $z = 1, 2$

	Os(IV)	Os(V)	Δ (%)
f_d(OsF)	3.07	3.90	27
f_d(OsF•)	2.80	3.50	25
f_d(OsCl)	1.69	1.94	16
f_d(OsCl′)	1.93	2.35	22

$5d^3$, $5d^4$, $5d^5$, and $5d^6$ series, $[MF_nCl_{6-n}]^{2-}$ of Re, Os, Ir, and Pt, respectively, reveals in that order an increase in f_d(Cl) from 1.67 to 1.98 mdyne/Å and in f_d(Cl′) from 1.80 to 2.39 mdyne/Å, while f_d(F•) for the *trans* weakened Os−F• bond decreases from 2.98 to 2.67 mdyne/Å. However, the changes of f_d(F) are small and not systematic. Thus, the mutual influences along the F•−M−Cl′ axes referred to the F−M−F or Cl−M−Cl axes, respectively, are strongest for d^6 Pt(IV) by ∼21% and lowest for d^3 Re(IV) on the order of 8% (Table 8). These conspicuous effects are greatly reduced and disarrayed in the comparable chlorobromo series, $[MCl_nBr_{6-n}]^{z-}$, with $4d^3$ Tc(IV), $4d^4$ Ru(IV), and $4d^6$ Rh(III) or with $5d^4$ Os(IV), $5d^5$ Ir(IV), and $5d^6$ Pt(IV). However, they become more pronounced again in the $[MCl_nI_{6-n}]^{2-}$ and the $[MBr_nI_{6-n}]^{2-}$ series {M = $5d^3$ Re(IV) and $5d^4$ Os(IV)}. The massive effect of the central ions's oxidation state is clearly demonstrated by the series, $[OsF_nCl_{6-n}]^{2-}$ and $[OsF_nCl_{6-n}]^{-}$. As expected, the higher oxidation state causes bond strengthening, as well as shortened bond distances and increased valence force constants (Table 9). Interestingly, the mutual *trans* influence in the Os(IV) series is of nearly the same magnitude, weakening the Os−F• bond by 9% and strengthening the Os−Cl′ bond by 14%, taking the respective symmetric axes as a reference. However, in the Os(V) system Os−F• is weakened by 10%, while Os−Cl′ is strengthened by 21%.

Normal coordinate analyses, which have been performed previously on single compounds or only a few members of a series, lack the certainty that can be found by studying the systematic trends of a complete series. Such examples are given by some mixed-hexahalogeno osmates(IV)[107] and platinates(IV).[110,111,136,137] The reported force constants of the osmates(IV) deviate slightly from the values in Table 8,[115,135] but the *trans* influence is of comparable order. The Os−Cl force constants of symmetric axes are approximately 1.45 mdyne/Å, while the Os−Cl• force constants of asymmetric axes are 1.25 for I′−Os−Cl• and 1.40 mdyne/Å for Br′−Os−Cl•. However, the reported force constants for the platinates(IV) vary greatly, and deviate considerably from those in Table 8. For example a GVFF calculation on *trans*-$[PtCl_4Br_2]^{2-}$ resulted in dubious force constants of 1.25 mdyne/Å for Pt−Cl and 3.53 mdyne/Å for Pt−Br.[136]

In the case of molecular compounds, besides normal coordinate analysis for $[UF_5Cl]$,[120] different calculations on $[WF_5Cl]$ have led to contradictory statements on the *trans* influence. Specifically, *trans* weakened F has been reported,[138] while other authors postulate just the opposite with *trans* strengthened F.[118,139] A similarly confusing situation is found for analogous S, Se, and Te compounds. While for $[SF_5Cl]$ *trans* weakened F is stated,[138] *trans* strengthened F is reported for $[SeF_5Cl]$ and $[TeF_5Cl]$.[125] Additional data for *trans*-$[TeF_4Cl_2]$ and *trans*-$[TeF_2Cl_4]$ have been reported.[124] However, in contrast to transition metals, it must be conceded that for main group central atoms the *cis* influence might play a greater role, and may even become more important than the *trans* influence (section II.D.2). Taken together, these latter examples clearly indicate the ambiguity of calculations based on insufficient experimental data and the uncertainty of any interpretation based on them.

Certain problems in normal coordinate analyses on heteroleptic complexes also arise from the lack of single-crystal X-ray structures and molecular parameters such as bond lengths and bond angles. In practice, however, these problems are not very severe if the structural parameters of the homoleptic terminal members of a series are available. Indeed, recent X-ray work on AB-type salts of the fluorochloroplatinates(IV) with divalent dipyridiniomethane cations, which promote an ordered arrangement of the complex anions in the lattices, reveals rather small mutual *trans* influences on the bond lengths.[140] As an example, it has been found for *fac*-$[PtF_3Cl_3]^{2-}$,

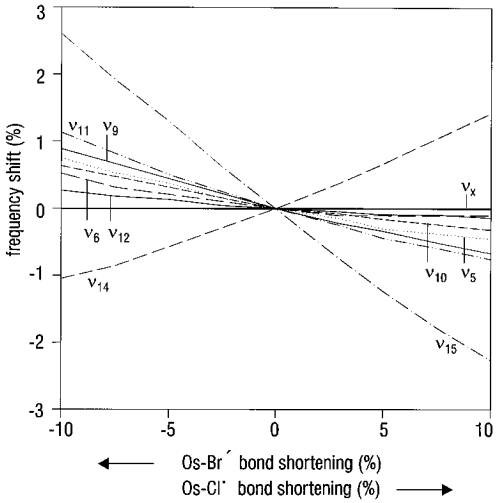

Figure 19. Shift of vibrational frequencies (%) resulting from bond length changes (%) in the Cl•−Os−Br′ axis of *mer*-$[OsCl_3Br_3]^{2-}$; ν_x: unaffected modes.

that *trans* weakening of the Pt−F• bond results in an elongation of 1.8%, while the Pt−Cl′ bond is shortened due to the *trans* strengthening by only 1.2%. Detailed calculations with a constant force field have clearly shown that such alterations of the respective bond distances result in only small changes in the observed frequencies. This is also generally true for the mixed-hexahalogeno complex series under discussion. For example, the Cl•−Os−Br′ axis in *mer*-$[OsCl_3Br_3]^{2-}$ (Figure 19) exhibits, at most, a maximum frequency shift of 2.5% for a bond length increase of + 10% for *trans* weakened Os−Cl• and a 10% decrease for *trans* strengthened Os−Br′.

The stretching vibrations, ν_1, of the Os−Cl• bond and the ν_4 of the Os−Br′ bond are unaffected by changes of bond length, while the bending modes ν_{11}, ν_{14}, and ν_{15} show shifts of varying degree. Altogether, the effects are so small that calculations on the basis of approximated bond lengths and their changes by mutual *trans* influences of <2% with respect to the homoleptic compounds seem to be justified. Generally, it has been found that the *trans* influence changes the bond lengths by about 1%, the frequencies by up to 10% and the force constants by up to 20%.[103] This clearly demonstrates the advantage of combined vibrational spectroscopic and normal coordinate analytic investigations on this phenomenon, with respect to the rather minimal changes revealed by X-ray structure analysis. In a similar manner, it has been proven that changes in bond angles caused by distortions of the octahedral arrangement as a consequence of substitution result in negligible frequency shifts. Also the splittings of the primary degenerate modes by lowered symmetry are calculated to be <2 cm^{-1}, which in most cases are barely resolvable in the vibrational spectra.[141] Therefore, the assumption of idealized symmetries for the heteroleptic species seems to be justified.

One of the great benefits of normal coordinate analysis, besides the advantage of having fitted frequencies or force constants, is the possibility of visualizing the vibrations by using the Cartesian displacement vectors. As an example, the 15 normal modes of vibration for *mer*-$[PtF_3Cl_3]^{2-}$ are presented in Figure 20. The calculated atomic motions are

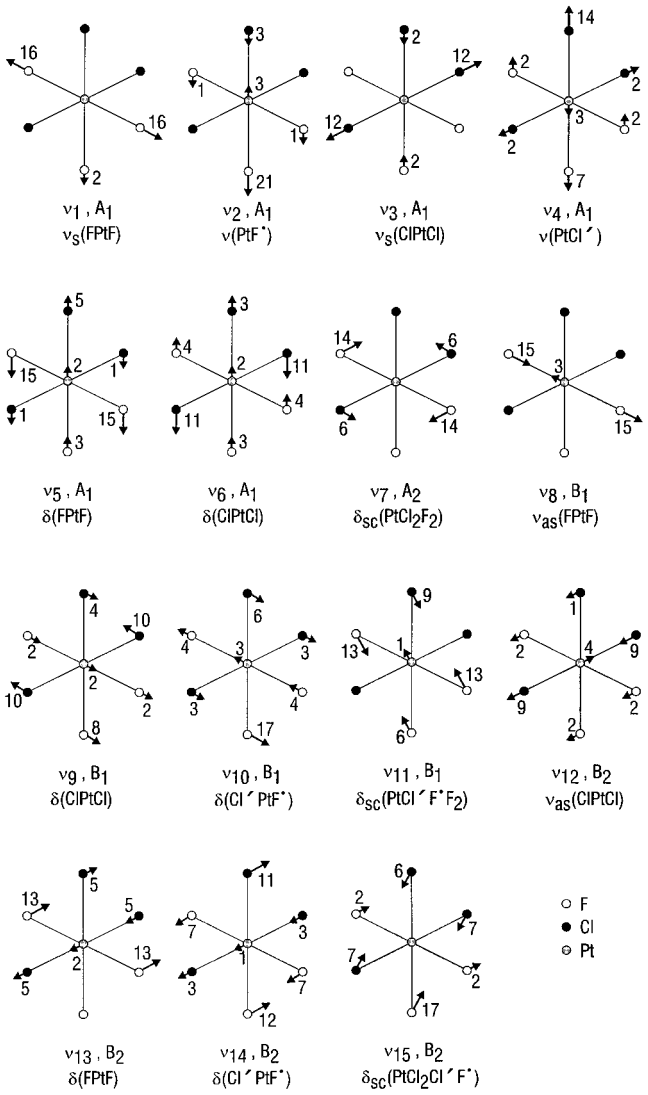

Figure 20. Normal vibrations of *mer*-$[PtCl_3F_3]^{2-}$; atomic displacements in picometers.

visualized by arrows and the amplitudes are given in picometers. It should be mentioned, however, that the applied force fields are based on a harmonic approximation, and certain inaccuracies must be considered, especially in cases of light atoms with large amplitudes.

A valuable tool is the PED matrix, which reveals the distribution of potential energy on the normal modes with respect to the force constants or internal coordinates, and allows the clear identification of the stretching and bending modes. However, the elucidation and quantification of couplings is even more important. This can be seen clearly for *mer*-$[PtF_3Cl_3]^{2-}$ by the PED in Table 10.

Obviously, there are only two genuine modes, namely ν_1 and ν_7, while the remaining vibrations are more or less coupled. Thus, the ν_2 mode is composed of 93% Pt−F• and 5% Pt−Cl′ stretching as well as 2% F−Pt−F• bending (Figure 20). The participation of the respective *trans* positioned F• appears in ν_4, of course, with 88% Pt−Cl′ and 6% Pt−F• stretching.

From thorough analyses of the vibrational spectra of the available complete systems of hexahalogeno metalates, which have been confirmed by normal coordinate analyses, generally valid sequences of

Table 10. Potential Energy Distribution (PED) for *mer*-$[PtCl_3F_3]^{2-}$ with Respect to Internal Coordinates (contributions < 3% neglected) (See Figure 20)

ν_1	Pt−F	100%				
ν_2	Pt−F•	93%	Pt−Cl′	5%		
ν_3	Pt−Cl	97%				
ν_4	Pt−Cl′	88%	Pt−F•	6%		
ν_5	Cl′−Pt−F	57%	F−Pt−F•	34%	Pt−Cl′	6%
ν_6	Cl−Pt−Cl′	62%	Cl−Pt−F•	35%		
ν_7	Cl−Pt−F	100%				
ν_8	Pt−F	99%				
ν_9	Cl−Pt−F	84%	F−Pt−F•	12%	Cl′−Pt−F	3%
ν_{10}	F−Pt−F•	81%	Cl′−Pt−F	11%	Cl−Pt−F	8%
ν_{11}	Cl′−Pt−F	72%	F−Pt−F•	28%		
ν_{12}	Pt−Cl	92%	Cl−Pt−F	4%		
ν_{13}	Cl−Pt−F	76%	Cl−Pt−Cl′	16%	Pt−Cl	8%
ν_{14}	Cl−Pt−Cl′	64%	Cl−Pt−F•	22%	Cl−Pt−F	13%
ν_{15}	Cl−Pt−F•	71%	Cl−Pt−Cl′	26%		

vibrations are derived and compiled in Table 11 for fluorochloro metalates and in Table 12 for chlorobromo metalates. The numeration is outlined in ref 56 and Figure 20.

Finally, the efficiency of normal coordinate analysis, based on dependable sets of force constants obtained in the described manner, has been demonstrated for 3-fold mixed complexes of the type $[ReX^{\bullet}Y_4Z']^{2-}$ with point group C_{4v}.[142] These complexes are built up from a ReY_4 plane and an asymmetrical X•−Re−Z′ axis with *trans* weakened X• = F, Cl, Br, and *trans* strengthened Z′ ≠ X• = Cl, Br, I. By means of the well-known force constants from the homoleptic compounds $[ReY_6]^{2-}$ and the 2-fold mixed species, MVFFs have been set up, which already describe the threefold systems fairly well and need only little modifications. In a first approach to a generally valid incremental system of force constants, the observed stretching vibrations for the 2- and 3-fold mixed hexahalogeno rhenates(IV) have

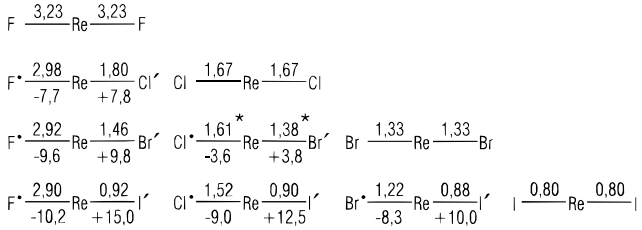

Figure 21. Valence force constants (mdyne/Å) and their changes (%) due to *trans* influence for heteroleptic 3-fold mixed rhenates(IV); asterisk indicate estimated values.

been reproduced within a few reciprocal centimeters by the force constants in Figure 21.

Generally, it has been shown that in the case of the hexahalogeno complexes of the heavier transition metals, the *cis* influence is negligibly small in comparison to the *trans* influence. If main group elements are the central atoms, and the ligands are the chalcogens, pseudohalogens and especially hydride, a more differentiated consideration is necessary since the *cis* influence may become increasingly important or even predominant.

In principle, a generally valid quantification and incrementation of force constants, aimed at the calculation of expectation spectra of previously unmeasured or even unknown compounds must take into account the mutual influences of the diverse ligands, as well as the dependence on the oxidation state of the different central atoms. Ultimately this requires the separation of two distinct effects on the observed or calculated frequencies, namely the electronic effect and the mass effect.[118] Such very extensive calculations are not yet possible, because more experimental data are required. However, in combination with new data and theoretical models, these calculations should be accessible in the future.

Table 11. Sequences of Observed and Calculated Frequencies ν_i of $[MF_nCl_{6-n}]^{z-}$, $n = 0-6$, M = Os(IV), Os(V), Ir(IV), Ir(V), Pt(IV), $z = 1, 2$

	n[a]	
O_h	6	$\nu_1 > \nu_3 > \nu_2 > \nu_4 > \nu_5 > \nu_6$
	0	$\nu_1 > \nu_3 > \nu_2 > \nu_4 > \nu_5 > \nu_6$
D_{4h}	4b	$\nu_1 > \nu_9 > \nu_5 > \nu_3 > \nu_2 > \nu_4 > \nu_7 > \nu_6 \approx \nu_{10} > \nu_8 > \nu_{11}$
	2b	$\nu_3 > \nu_2 > \nu_1 > \nu_9 > \nu_5 > \nu_{11} > \nu_8 > \nu_6 > \nu_4 \approx \nu_{10} > \nu_7$
C_{4v}	5	$\nu_1 > \nu_8 > \nu_2 > \nu_5 > \nu_3 > \nu_4 > \nu_9 > \nu_6 > \nu_7 > \nu_{10} > \nu_{11}$
	1	$\nu_3 > \nu_2 > \nu_1 > \nu_8 > \nu_5 > \nu_{11} > \nu_{10} > \nu_4 \approx \nu_7 > \nu_9 > \nu_6$
C_{3v}	3a	$\nu_1 > \nu_6 > \nu_2 > \nu_7 > \nu_3 > \nu_8 > \nu_{10} > \nu_5 > \nu_4 > \nu_9$
C_{2v}	3b	$\nu_1 > \nu_8 > \nu_2 > \nu_4 > \nu_{12} > \nu_3 > \nu_5 > \nu_{13} > \nu_{15} > \nu_{14} > \nu_7 > \nu_{10} > \nu_{11} > \nu_6 > \nu_9$
	4a	$\nu_1 > \nu_9 > \nu_2 > \nu_{12} > \nu_3 > \nu_{13} > \nu_4 > \nu_{14} > \nu_5 \approx \nu_{10} > \nu_7 > \nu_{15} > \nu_{11} > \nu_8 > \nu_6$
	2a	$\nu_3 > \nu_{13} > \nu_2 > \nu_{12} > \nu_9 > \nu_1 > \nu_6 > \nu_{11} > \nu_8 > \nu_{15} > \nu_5 \approx \nu_{10} > \nu_7 > \nu_4 \approx \nu_{14}$

[a] a corresponds to *cis*/*fac*; b corresponds to *trans*/*mer*.

Table 12. Sequences of Observed and Calculated Frequencies ν_i of $[MCl_nBr_{6-n}]^{z-}$, $n = 0-6$, M = Re(IV), Os(IV), Ir(III), Pt(IV), Ru(IV), $z = 2, 3$

	n[a]	
O_h	6	$\nu_1 > \nu_3 > \nu_2 > \nu_4 > \nu_5 > \nu_6$
	0	$\nu_3 > \nu_1 > \nu_2 > \nu_4 > \nu_5 > \nu_6$
D_{4h}	4b	$\nu_1 > \nu_9 > \nu_5 > \nu_3 > \nu_2 > \nu_6 > \nu_{10} > \nu_4 \approx \nu_7 \approx \nu_8 > \nu_{11}$
	2b	$\nu_3 \approx \nu_2 > \nu_9 > \nu_1 > \nu_5 > \nu_{11} \approx \nu_8 > \nu_4 > \nu_6 > \nu_{10} > \nu_7$
C_{4v}	5	$\nu_1 > \nu_8 > \nu_2 \approx \nu_5 > \nu_3 > \nu_7 > \nu_{10} > \nu_9 \approx \nu_4 > \nu_6 > \nu_{11}$
	1	$\nu_3 > \nu_8 > \nu_2 > \nu_1 > \nu_5 > \nu_{11} > \nu_7 > \nu_4 \approx \nu_{10} > \nu_9 > \nu_6$
C_{3v}	3a	$\nu_1 > \nu_6 > \nu_2 > \nu_7 > \nu_3 \approx \nu_8 > \nu_{10} > \nu_5 > \nu_4 > \nu_9$
C_{2v}	3b	$\nu_1 > \nu_8 > \nu_2 > \nu_{12} > \nu_4 > \nu_3 > \nu_{11} > \nu_7 > \nu_{15} > \nu_5 > \nu_{13} > \nu_{10} > \nu_{14} > \nu_6 > \nu_9$
	4a	$\nu_1 > \nu_9 > \nu_2 > \nu_{12} > \nu_3 > \nu_{13} > \nu_7 \approx \nu_{10} > \nu_5 > \nu_4 \approx \nu_{14} > \nu_{11} > \nu_{15} > \nu_8 > \nu_6$
	2a	$\nu_3 > \nu_{13} > \nu_9 > \nu_2 > \nu_{12} > \nu_1 > \nu_6 > \nu_8 \approx \nu_{11} > \nu_{15} > \nu_5 \approx \nu_{10} > \nu_7 > \nu_4 \approx \nu_{14}$

[a] a corresponds to *cis*/*fac*; b corresponds to *trans*/*mer*.

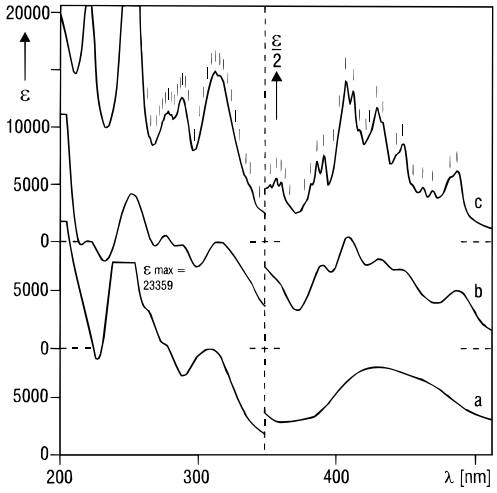

Figure 22. Absorption spectra of *trans*-$(TEA)_2[ReCl_4I_2]$ in 2 N H_2SO_4 (a), as a KBr pellet at 293 K (b), and at 10 K (c).

C. Electronic Spectroscopy

The most obvious feature of the mixed hexahalogeno complexes of the heavier transition metals are the characteristic, beautiful colors of the individual species, which are observed impressively during ion exchange chromatography on DEAE columns (see Table 4). The markedly different colors of the stereoisomers underline the decisive influence of molecular structure and symmetry on the electronic transitions. Thus, electronic spectroscopy is clearly the tool of choice for the investigation of these excited states. For an introduction to the fundamentals, comprehensive textbooks on inorganic electronic spectroscopy,[143] on ligand-field theory,[144−147] and on group theory[88] are available.

The spectral range is roughly divided into two distinct regions. The first range, from the higher energy UV range down to the visible region, is dominated by the very intense ligand to metal charge-transfer (LMCT) bands. The second range, from the visible region down to the lower energy of the near infrared region are dominated by the markedly weaker d−d transitions. Generally, strong enhancement of spectral resolution is gained by measuring the compounds in environments of as low polarity as possible and at low temperatures. This is exemplified by Figure 22 on the tetraethylammonium (TEA) salt *trans*-$(TEA)_2[ReCl_4I_2]$.[148]

The spectrum of *trans*-$(TEA)_2[ReCl_4I_2]$ in 2 N H_2SO_4 solution shows broad, marginally structured bands. However, when the solid compound, embedded in a KBr pellet, is measured, some absorption maxima are observed. These maxima become even more pronounced upon cooling to 10 K, where even the vibronic fine structure is revealed. The vibronic progressions of ∼290 cm^{-1} are consistent with overtones of the totally symmetric Re−Cl stretching vibration (A_{1g}) at 333 cm^{-1} in the electronic ground state, and decrease by ∼13% in the electronic excited state. Well suited for low temperature spectroscopy are complex salts formed with long-chain alkylammonium cations,[149] because optically isotropic samples can be obtained either by dissolving the compounds in appropriate organic solvents and preparing thin layers on quartz disks by solvent evaporation or by squeezing these solids to transparent films between two sapphires. With respect to the very intense LMCT bands, in most cases optical dilution is necessary, which is accomplished by mixing the samples with materials like KBr or, if cation or ligand exchange is suspected, other appropriate alkali halides.

1. Ligand-to-Metal Charge-Transfer Transitions

LMCT transitions of hexahalogeno complexes are observable in the visible and near-UV range of the absorption spectra as metal reduction bands, because electronic transitions occur from ligand π (t_{1g},t_{2g},t_{1u},t_{2u}) and σ (t_{1u},e_g,a_{1g}) orbitals into partially occupied d (t_{2g},e_g) levels of the central ion. As an example the low-temperature absorption spectra of $(TBA)_2$-$[OsF_nCl_{6-n}]$, $n = 0-6$, are presented in Figure 23.

Here, the u → g transitions are parity allowed, and thus the absorption bands are very intense. From analysis of the electronic spectra, along with theoretical calculations on the homoleptic octahedral species, $[MX_6]^{z-}$, X = Cl, Br, I, the following series of molecular orbitals with increasing energies has been deduced:[147,150]

$$d_{eg} < d_{t2g} \ll \pi_{t1g} < (\pi + \sigma)_{t1u} < \pi_{t2u} < (\sigma + \pi)_{t1u} < \pi_{t2g} \ll \sigma_{eg} < \sigma_{a1g}$$

In principle, the same order can be used to interpret the LMCT spectra of mixed hexahalogeno complexes, $[MX_nY_{6-n}]^{z-}$. However, degenerate states are split according to the respective lowered point symmetry of the heteroleptic species. By virtue of the different optical electronegativities of Cl = 3.0 and F = 3.9 a partitioning of the six σ and 12 π ligand orbitals into those belonging to F and others belonging to Cl is possible in the $[OsF_nCl_{6-n}]^{2-}$series.[151] The energy levels of F are so low that corresponding transitions from these orbitals are below the limits of normal UV equipment at 200 nm ≡ 50 000 cm^{-1}. Consequently, the LMCT bands are clearly assigned to transitions from Cl orbitals. With increasing number of F ligands, the number of involved Cl orbitals decreases, resulting in simplified spectra, as can be seen in the short wave regions of Figure 23. Furthermore, a systematic hypsochromic shift of corresponding bands with increasing number of F ligands within the series is observed due to progressively impeded charge transfer because the averaged optical electronegativities of all ligands increase. An interesting feature is the analogous band pattern of $[OsCl_6]^{2-}$ (0) and *fac*-$[OsF_3Cl_3]^{2-}$ (3a), which suggests that holohedrized symmetry (pseudo-O_h) should be applied to the latter, as was already done on *fac*-$[OsCl_3Br_3]^{2-}$.[152] This implies that the absorption spectrum of *fac*-$[OsF_3Cl_3]^{2-}$ corresponds to an octahedral complex with six hypothetical ligands (F + Cl)/2 of optical electronegativity 3.45.

Vibrational spectroscopy has proven, by virtue of the *trans* influence, that the bond to Cl in an asymmetric F•−M−Cl′ axis is stronger than in the symmetric Cl−M−Cl axis (see section II.B). This can bee seen qualitatively by the splitting and broadening of respective bands in the LMCT spectra of the

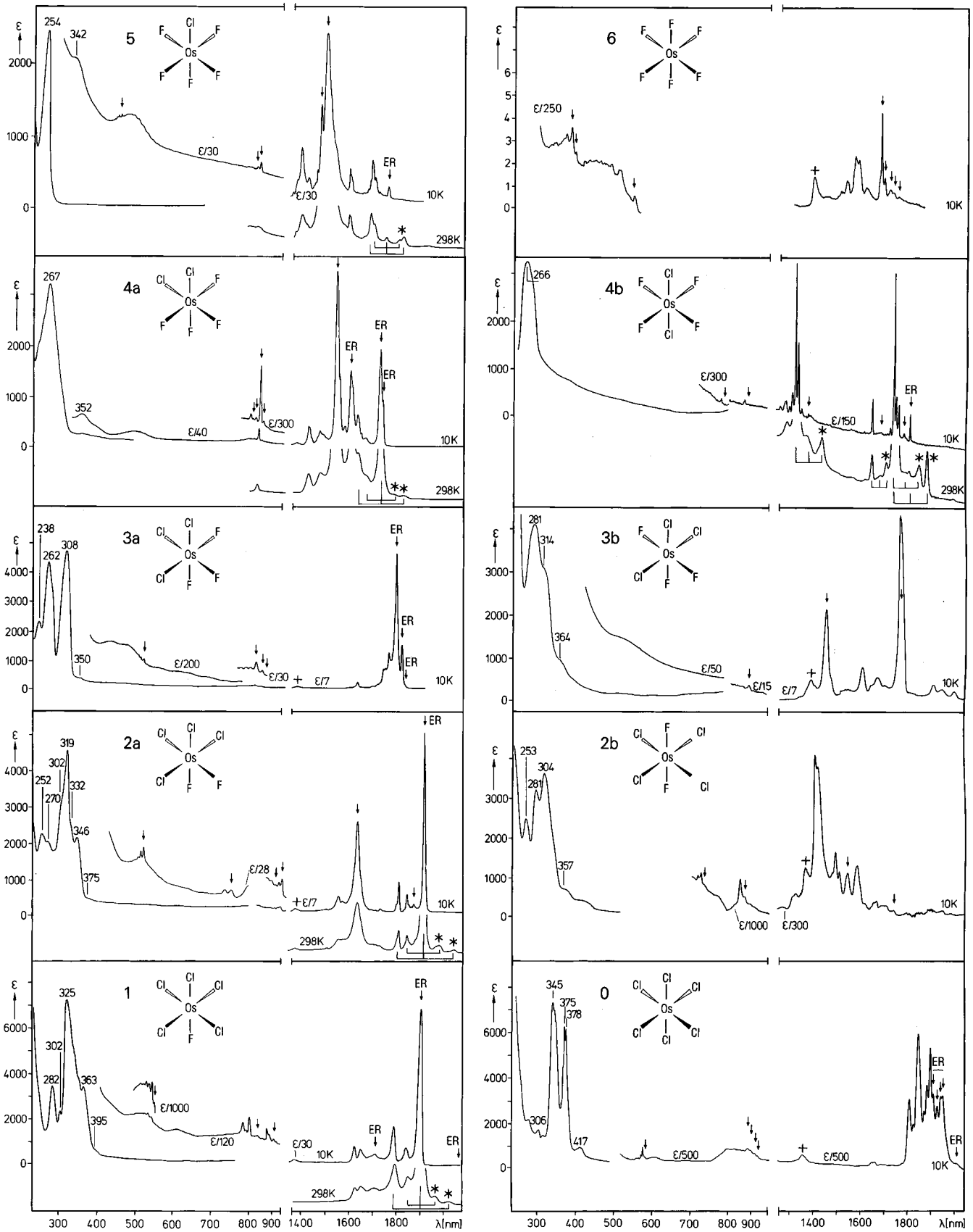

Figure 23. Absorption spectra (10 K) of $[OsF_nCl_{6-n}]^{2-}$, $n = 0-6$ (a corresponds to *cis*/*fac*; b corresponds to *trans*/*mer*). LMCT transitions of the (TBA) salts in the UV−vis range (nm); intraconfigurational transitions of the (TEA) salts in the NIR range; + = quartz absorption; * = hot bands; ER = electronic Raman bands.

complexes $[OsFCl_5]^{2-}$ (1), *cis*-$[OsF_2Cl_4]^{2-}$ (2a), and *mer*-$[OsF_3Cl_3]^{2-}$ (3b), which have F•−Os−Cl′ axes as well as Cl−Os−Cl axes. Logically, the bathochromic shift within a respective split band is assigned to *trans* strengthened Os−Cl′, which has a shortened bond distance and thereby easier transitions, while

the hypsochromic shift is due to transitions from the Cl in normal Cl−Os−Cl bonds. Correspondingly, the complexes *trans*-$[OsF_2Cl_4]^{2-}$ (2b) and *trans*-$[OsF_4Cl_2]^{2-}$ (4b), which possess D_{4h} symmetry and exclusively symmetric axes, exhibit simpler spectra than the other stereoisomers. Thus their LMCT transitions are observed at relatively high energies with respect to the low-energy transitions of *fac*-$[OsF_3Cl_3]^{2-}$ (3a), *cis*-$[OsF_4Cl_2]^{2-}$ (4a), and *mer*-$[OsF_5Cl]^{2-}$ (5), all of which exclusively contain *trans* strengthened Os−Cl′ bonds.

In addition to the complete series, $[OsF_nCl_{6-n}]^{2-}$, $n = 0-6$, with the central metal ion in the d^4 configuration, LMCT spectra from the corresponding d^3 complexes of Os(V)[153] and d^5 complexes of Ir(IV),[154] and even some species from the d^4 Ir(V) system have been recorded.[60] Spectra of analogous complexes from the different series are essentially similar, although resolution is of a different quality, and there are no vibronic fine structures in the spectra within the Os(IV) and Os(V) series. However, distinctly long progressions of overtones on two LMCT bands of the tetramethylammonium (TMA) salt *trans*-$(TMA)_2[IrF_2Cl_4]$ are present,[154] which have been assigned by taking account of spin orbit coupling.[155] Similar fine structures have been observed on the Ir(V) complexes, (TEA)$[IrF_5Cl]$ and *cis*-(TEA)$[IrF_4Cl_2]$, diluted as mixed crystals with nonreducing (TEA)$[OsF_6]$, which has been chosen because it is transparent in the LMCT region.[60]

In spite of the different occupation of the highest occupied molecular orbital (HOMO) of Ir(IV):t_{2g}^5; Ir(V),Os(IV):t_{2g}^4; and Os(V):t_{2g}^3 arising from the respective d^5, d^4, and d^3 configurations for the low-spin case, the order of LMCT bands is quite similar for different central ions with identical coordination spheres. Due to the lowered symmetry in the heteroleptic complexes, the octahedral 3-fold degenerate t_{2g} state is split into two levels for D_{4h}, C_{4v}, C_{3v}, and into three levels for C_{2v} symmetry. A distinct assignment of the broadened or split LMCT bands to definite molecular orbitals demands supplementary information on their respective symmetry from polarized electronic absorption spectra. Unfortunately, these spectra are not easily obtainable because of the need for large single crystals. However, an illustrative example has been presented for trigonally distorted $[ReCl_6]^{2-}$.[156]

By comparison of LMCT bands of the isostructural species from the d^3, d^4, and d^5 systems characteristic shifts have been correlated to the optical electronegativity and the oxidation state of the central ions. According to the strongly oxidizing power of the pentavalent metals, which facilitates charge transfer from the ligands, bathochromic shifts of $\sim$8000 cm^{-1} between Ir(V) and Ir(IV), 7000 cm^{-1} between Os(V) and Os(IV) and 15 000 cm^{-1} between corresponding d^4 species of the fluorochloroiridates(V) and -osmates(IV) have been observed.[60,151,153,154]

The minor differences of the electronegativities between the heavier halides, Cl, Br, and I, make the assignments of LMCT transitions to the respective ligands in mixed coordination spheres impossible. Nevertheless, for the sake of an overall spectroscopic characterization, the spectra have been measured in solution and at low temperature in solid state for the following series: $[ReCl_nBr_{6-n}]^{2-}$,[157] $[ReCl_nI_{6-n}]^{2-}$,[148] $[OsCl_nBr_{6-n}]^{2-}$,[158] $[IrCl_nBr_{6-n}]^{2-}$,[158] $[OsCl_nI_{6-n}]^{2-}$,[159] and $[RuCl_nBr_{6-n}]^{2-}$.[160] In every case, substitution of a halide by a heavier one is accompanied by a bathochromic shift. Generally, spectra of *trans* species with point symmetry D_{4h} are simpler than those of the corresponding *cis* complexes with C_{2v} symmetry. Some chlorobromo complexes of Ir(IV) and Os(IV) have been interpreted on the basis of MO theory.[152,155,159] A detailed assignment of LMCT bands has been achieved by investigation of the magnetic circular dichroism on chlorobromo and chloroiodo complexes of Ir(IV) and Os(IV).[161]

2. Intraconfigurational Transitions

The series, $(TEA)_2[OsF_nCl_{6-n}]$, may serve as an example of the fundamentals required for an interpretation of d−d spectra in the long wave range of Figure 23. For the low spin t_{2g}^4 configuration of Os(IV) in point group O_h a triplet ground state, $^3T_{1g}$, has been derived from magnetic data.[162,163] Therefore, transitions occur into the singlet states, $^1T_{2g}$, ^1E_g, and $^1A_{1g}$. By virtue of spin−orbit coupling, with a coupling constant $\xi_{Os(IV)} \sim 3200$ cm^{-1}, the $^3T_{1g}$ is split, according to the octahedral double group O_h* and Bethe's nomenclature, into the terms, Γ_1, Γ_3, Γ_4, and Γ_5, with Γ_1 as the ground state, while the singlet states belong to the irreducible representations Γ_5, Γ_3, and Γ_1 (see Figure 24). As a consequence of selection rules for electric dipole radiation, intraconfigurational transitions are orbital forbidden as d−d transitions between states with the same orbital momentum quantum number and are parity forbidden as g−g transitions. All in all, they are Laporte forbidden and thus have small oscillator strengths. A further selection rule, regarding the spin multiplicity, demands that transitions between states of equal spin multiplicity are allowed, but are spin forbidden between those of different multiplicity, and therefore also affect spectral intensities. Thus, in the d^4 configuration transitions between levels of the spin−orbit split ground state are spin allowed, while the triplet to singlet transitions are spin forbidden. However, these become formally spin allowed by spin−orbit coupling, although, in general, they are 10 times less intense. Because of the descent in symmetry from O_h* to the respective double subgroups, D_{4h}*, D_{2h}*, C_{4v}*, C_{3v}*, and C_{2v}*, within a complex series like $[OsF_nCl_{6-n}]^{2-}$, the orbital-degenerate levels are split additionally as given in Figure 24.

The D_{2h}* group has been included into the series in order to account for the Jahn−Teller distortion of the homoleptic members. As a consequence of the lowered symmetry, transitions of noncentrosymmetric complexes become formally parity allowed.[151] The approximate positions and intensities of the d−d absorptions of the fluorochloroosmates(IV) correlate well with the comprehensively investigated spectra of $[OsCl_6]^{2-}$ [164−166] and complexes of lower symmetry such as the $[OsX_4ox]^{2-}$, $[OsX_nY_{4-n}ox]^{2-}$, X ≠ Y = Cl, Br, I; ox = chelating oxalate,[167−169] and linkage isomeric mixed halogenothiocyanatoosmates(IV).[170,171] The transitions within the series, $[OsF_nCl_{6-n}]^{2-}$, derived from O_h* for the corresponding subgroups,

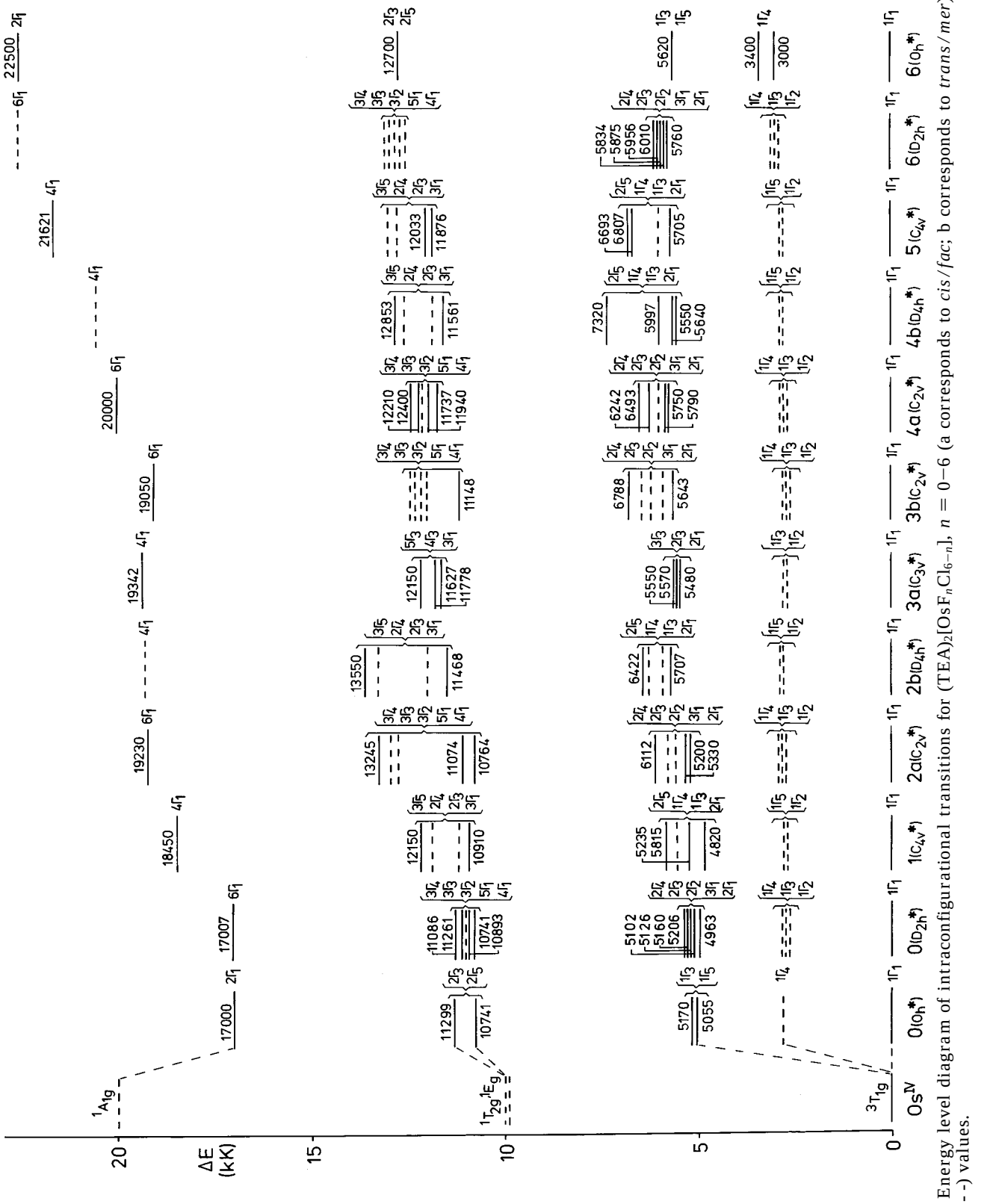

Figure 24. Energy level diagram of intraconfigurational transitions for $(TEA)_2[OsF_nCl_{6-n}]$, $n = 0-6$ (a corresponds to *cis*/*fac*; b corresponds to *trans*/*mer*); observed (—), estimated (- - -) values.

appear in four clearly separated ranges. They are observed for the excitations from $1\Gamma_5$, $1\Gamma_3$ between 4700 and 7300 cm^{-1}, from $2\Gamma_5$, $2\Gamma_3$ between 10 700 and 13 500 cm^{-1} and from $2\Gamma_1$ between 17 000 and 22 500 cm^{-1}. The lowest energy transition, $1\Gamma_1 \rightarrow 1\Gamma_4$, calculated to occur near 3000 cm^{-1}, has not been observed. Corresponding to the respective point symmetries, the heteroleptic species reveal the group theoretically demanded splittings of electronic states. They are located in relatively narrow ranges between the terminal members of a series with expected nephelauxetic shifts for the different ligands. In the energy level diagram (Figure 24) the transitions both predicted by group theory and those experimentally observed are compiled. A distinct assignment of the split terms is not possible without polarized electronic absorption spectra from single crystals, which unfortunately have not been available. Nevertheless, a systematic hypsochromic shift on increasing substitution of Cl by F within the $[OsF_nCl_{6-n}]^{2-}$ series is observed, according to the nephelauxetic series and the decreasing covalent nature of the metal to ligand bonds.[147]

A striking feature of these d−d absorptions is the vibrational fine structure, which arises from a coupling with appropriate normal modes and relaxes the parity selection rule. In centrosymmetric molecules, these are vibrations of odd parity. To address this subject, many different experimental and fundamental theoretical investigations have been performed.[172] As a point of prime importance, in some cases the electronic origins, or in other words the 0−0 transitions, can be deduced reliably and assigned correctly only if vibrational fine structure is present. For instance, the centrosymmetric complexes *trans*-$[OsF_2Cl_4]^{2-}$ (2b) and *trans*-$[OsF_4Cl_2]^{2-}$ (4b) have Laporte-forbidden 0−0 transitions of extremely low intensities ($\epsilon < 1$ cm^2/mmol), which result in fairly intense bands by coupling with "promoting modes" like stretching and bending vibrations of odd parity. The origin of these vibrational bands have been falsely assigned as the virtual 0−0 transitions, and thus are so-called false origins.[173] Upon strong vibrational coupling, with vibrations of even parity, serving as "progressing modes", long series of overtones are built up from appropriate electronic transitions, as observed for *trans*-$[OsO_2(CN)_4]^{2-}$ [174] and *trans*-$[OsFCl_4(NCS)]^{2-}$.[171]

An unambiguous assignment of 0−0 transitions can also be accomplished if the electronic Raman (ER) spectra are known, because d−d transitions are allowed as Raman scattering process. However, the detection with a photomultiplier and excitation with visible light limits the shift range to <7000 cm^{-1}. Verified 0−0 transitions are marked by arrows amended by ER in Figure 23. Corresponding to the observed absorption bands, solid $(TEA)_2[OsCl_6]$ exhibits five sharp ER signals, while in a CH_2Cl_2 solution only two lines are observed, as is expected for the octahedral case, O_h*. Therefore, in the solid state an orthorhombic distortion, resulting in D_{2h}* symmetry, has been deduced,[151] because the degeneracy is completely suspended. Analogous to this, a similar change from solution to solid state has been presumed for $(TEA)_2[OsF_6]$.[175] Coupling of normal modes with ER transitions has been demonstrated for the pair of linkage isomers, $(TBA)_2[OsCl_5(NCS)]$/$(TBA)_2[OsCl_5(SCN)]$.[170] Another special effect in ER spectra has been explained for $(TBA)_2[OsBr_5(SCN)]$, which belongs to the double group C_{4v}*. Group theory demands different polarization behavior, and this has been proven experimentally by a clear distinction between inverse polarization of the $1\Gamma_1 \rightarrow 1\Gamma_2$ transition at 2390 cm^{-1} and depolarization of the $1\Gamma_1 \rightarrow 1\Gamma_5$ transition at 2190 cm^{-1}.[171]

In some cases hot bands occur, which are very useful in the assignment of 0−0 transitions. Noticeably, a comparison of the 298 and 10 K absorption spectra of $[OsFCl_5]^{2-}$ (1), *cis*-$[OsF_2Cl_4]^{2-}$ (2a), *cis*-$[OsF_4Cl_2]^{2-}$ (4a), and $[OsF_5Cl]^{2-}$ (5) shows a loss of the hot bands, which vanish completely at 10 K and thus are clearly identified (see Figure 23). This allows the assignment of the very weak 0−0 transitions by the symmetrical appearance of vibrational bands at higher and lower frequencies. In the same manner, the intraconfigurational transitions of the individual species within the series, $[OsF_nCl_{6-n}]^-$,[153] $[OsCl_nBr_{6-n}]^{2-}$,[176] $[IrF_nCl_{6-n}]^{2-}$,[154] $[IrF_nCl_{6-n}]^-$,[60] and $[RuCl_nBr_{6-n}]^{2-}$,[160] have been measured and assigned.

3. Luminescence Spectra

While luminescence spectra of homoleptic transition metal complexes have been studied exhaustively,[177−179] there are only a few investigations of mixed-ligand complexes. In order to avoid fluorescence quenching, which takes place when pure compounds are measured, these samples must be prepared in a highly diluted form (<1%). This can be achieved by formation of mixed crystals in host lattices such as $Cs_2[SnX_6]$ or $Cs_2[TeX_6]$, X = Cl, Br. For high resolution, it is necessary to record the spectra at low temperatures (10 K or lower). As an example, the 10 K luminescence spectra of the heteroleptic complexes, $[OsCl_nBr_{6-n}]^{2-}$, $n = 1-5$, in $Cs_2[TeCl_6]$, are presented in Figure 25.[180]

With the use of a laser source, $\lambda_0 = 488$ nm, the $\Gamma_1(^1A_{1g}) \rightarrow \Gamma_1(^3T_{1g})$ or the respective subgroup transition (compare Figure 24) is excited, serving as the starting point of luminescence. The compilation of the 0−0 transitions in Table 13 reveals nephelauxetic shifts to higher wave numbers as the number of Cl ligands increases. Apart from a small luminescence shift due to the host lattice these observations are in good agreement with the corresponding data from the electronic absorption spectra.[176] All species exhibit typical fine structures by vibrational coupling, which have been assigned in Table 14.

The electronic origins, which are very strong for the noncentrosymmetric species, have been unobservable for the two centrosymmetric complexes, *trans*-$[OsCl_2Br_4]^{2-}$ (2b) and *trans*-$[OsCl_4Br_2]^{2-}$ (4b), and therefore have been deduced from analyses of the vibronic couplings. If the spectra of pure compounds are known, even small impurities may be detected, as is demonstrated in Figure 25 by *trans*-$[OsCl_2Br_4]^{2-}$ (2b) containing small amounts of *mer*-$[OsCl_3Br_3]^{2-}$ (3b) and by $[OsClBr_5]^{2-}$ (1) containing small amounts of *cis*-$[OsCl_2Br_4]^{2-}$ (2a). Very weak emissions with distances of 30−70 cm^{-1} to the electronic as well as to the vibronic origins correlate well with the lattice vibrations, ν_L, and vibron−

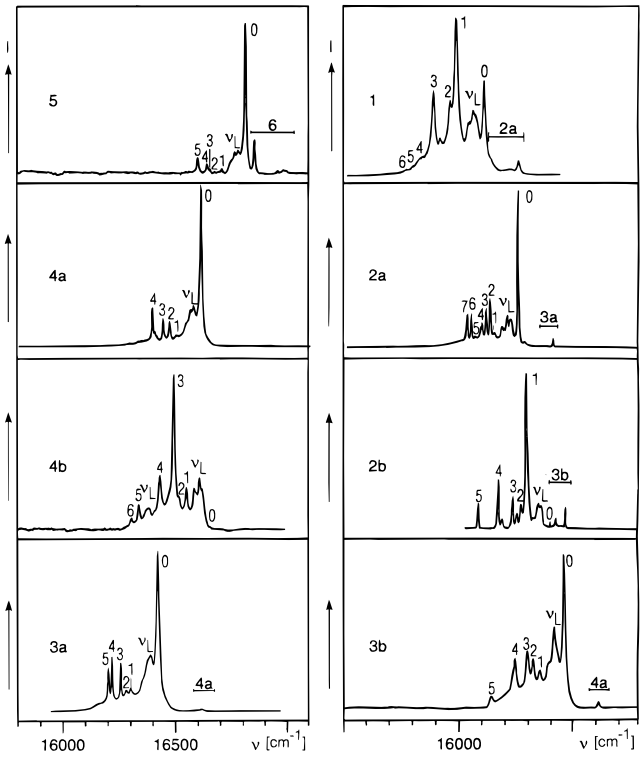

Figure 25. Luminescence transitions $\Gamma_1(^1A_{1g}) \rightarrow \Gamma_1(^3T_{1g})$ of $Cs_2[OsCl_nBr_{6-n}]$, $n = 1-5$ (a corresponds to *cis*/*fac*; b corresponds to *trans*/*mer*) in the host lattice $Cs_2[TeCl_6]$ at 10 K, $\lambda_0 = 488$ nm.

Table 13. Point Symmetry and Electronic Origins of the Luminescence Transitions $\Gamma_1(^1A_{1g}) \rightarrow \Gamma_1(^3T_{1g})$ of $Cs_2[OsCl_nBr_{6-n}]$, $n = 0-6$

n[a]	symmetry	$\Gamma_1(^1A_{1g}) \rightarrow \Gamma_1(^3T_{1g})$[b]
6	O_h	16955 (17030)
5	C_{4v}	16816 (16860)
4a	C_{2v}	16608 (16695)
4b	D_{4h}	16653 (16750)
3a	C_{3v}	16412 (16445)
3b	C_{2v}	16445 (16585)
2a	C_{2v}	16263 (16340)
2b	D_{4h}	16382 (16400)
1	C_{4v}	16116 (16210)
0	O_h	16018 (16000)

[a] a corresponds to *cis*/*fac*, b corresponds to *trans*/*mer*, doped in $Cs_2[TeCl_6]$. [b] In parentheses, assignments from electronic absorption spectra (cm^{-1}).[176]

phonon modes.[180] The emission spectra of some selected hexahalogeno complexes like $[OsCl_5X]^{2-}$ and *cis*-$[OsCl_4X_2]^{2-}$, X = Br, I,[181] *trans*-$[OsCl_4I_2]^{2-}$,[181] and *mer*-$[OsCl_3I_3]^{2-}$ [182] have been analyzed in detail. The energy differences, determined for transitions from the $^1A_{1g}$ level (t_{2g}^4) to the ground state and to some lower lying multiplets, as well as from the latter to the ground state, fit very well to the energy level diagrams derived from the absorption spectra. Thus, an independent confirmation of the spectroscopic results has been given by these two complementary methods.

From the weak β-emitter ^{99}Tc all species of the series, $[^{99}TcCl_nBr_{6-n}]^{2-}$, have been prepared in a pure form by anion exchange on DEAE cellulose. In host lattices of $Cs_2[SnCl_6]$ and $Cs_2[SnBr_6]$, the luminescence transition, $\Gamma_7(^2T_{2g}) \rightarrow \Gamma_8(^4A_{2g})$, of Tc(IV) exhibits distinct vibrational fine structures. The promoting

Table 14. Assignment of the Luminescence Bands in Figure 24

no.	ν (cm^{-1})	Δ (cm^{-1})	assignment
		C_{4v}, 5, $Cs_2[OsCl_5Br]$	
0	16816	0	Origin
1	16708	108 (106)	$+\nu_{11}$, E
2	16678	138 (138)	$+\nu_9$, E
3	16656	160 (160)	$+\nu_{10}$, E
4	16645	171 (166)	$+\nu_7$, B_2
5	16603	213 (205)	$+\nu_3$, A_1
		C_{4v}, 1, $Cs_2[OsClBr_5]$	
0	16116	0	Origin
1	15994	122 (117)	$+\nu_7$, B_2
2	15967	149 (144)	$+\nu_{11}$, E
3	15924	192 (188)	$+\nu_1$, A_1
4	15897	219 (217)	$+\nu_2$, $A_1/+\nu_8$, E
5	15812	304 (307)	$+\nu_3$, A_1
6	15786	330 (217+106)	$+\nu_2+\nu_4$, $A_1/+\nu_8+\nu_4$
		C_{2v}, 4a, *cis*-$Cs_2[OsCl_4Br_2]$	
0	16608	0	Origin
1	16501	107 (99)	$+\nu_6$, $A_1/+\nu_{15}$, B_2
2	16469	139 (139)	$+\nu_5$ (host), T_{2g}
3	16440	168 (160)	$+\nu_7$, A_2
4	16392	216 (210)	$+\nu_3$, A_1
		C_{2v}, 2a, *cis*-$Cs_2[OsCl_2Br_4]$	
0	16263	0	Origin
1	16161	102 (94)	$+\nu_7$, A_2
2	16141	122 (119)	$+\nu_{15}$, B_2
3	16124	139 (138)	$+\nu_{11}$, B_1
4	16107	156 (159)	$+\nu_6$, A_1
5	16076	187 (180)	$+\nu_1$, A_1
6	16060	203 (196)	$+\nu_{12}$, B_2
7	16043	220 (217)	$+\nu_9$, B_1
		D_{4h}, 4b, *trans*-$Cs_2[OsCl_4Br_2]$	
0	16653	0	Origin (not obs.)
1	16547	106 (97)	$+\nu_{11}$, E_u
2	16511	142 (134)	$+\nu_4$, A_{2u}
3	16493	160 (157)	$+\nu_{10}$, E_u
4	16430	223 (217)	$+\nu_3$, A_{2u}
5	16336	317 (307)	$+\nu_9$, E_u
6	16303	350 (157+186)	$+\nu_{10}+\nu_2$, A_{1g}
		D_{4h}, 2b, *trans*-$Cs_2[OsCl_2Br_4]$	
0	16382	0	Origin (not obs.)
1	16282	100 (98)	$+\nu_{10}$, E_u
2	16261	121 (125)	$+\nu_6$ (host), T_{2u}
3	16224	158 (141)	$+\nu_{11}$, E_u
4	16161	221 (216)	$+\nu_9$, E_u
5	16074	308 (306)	$+\nu_3$, A_{2u}
		C_{3v}, 3a, *fac*-$Cs_2[OsCl_3Br_3]$	
0	16412	0	Origin
1	16291	121 (118)	$+\nu_5$, A_2
2	16271	141 (133)	$+\nu_{10}$, E
3	16248	164 (163)	$+\nu_3$, $A_1/+\nu_8$, E
4	16207	205 (198)	$+\nu_7$, E
5	16190	222 (219)	$+\nu_2$, A_1
		C_{2v}, 3b, *mer*-$Cs_2[OsCl_3Br_3]$	
0	16455	0	Origin
1	16347	108 (105)	$+\nu_{14}$, B_2
2	16321	134 (132)	$+\nu_{13}$, B_2
3	16297	158 (156)	$+\nu_{11}$, B_1
4	16243	212 (210)	$+\nu_4$, A_1
5	16138	317 (210+105)	$+\nu_4+\nu_{14}$

[a] In parentheses, vibrational frequencies of pure $(TBA)_2[OsCl_nBr_{6-n}]$, $n = 1-5$,[15] or of the host lattice $Cs_2[TeCl_6]$.

modes are determined to be normal vibrations, combination tones and overtones of the respective complexes.[183] By comparison with previous luminescence spectra measured on mixtures of the chlorobromotechnetates(IV), some misassignments have been revealed, which may easily arise from superpositioned bands of such similar compounds.[184] For

the same reason the interpretation of the spectra taken from mixtures of the related series, $[ReCl_nBr_{6-n}]^{2-}$, is doubtful.[185]

D. NMR Spectroscopy

1. General Considerations

In the early 1960s NMR spectrometers, operating in the continous wave mode at 1.4 T = 60 MHz for ^1H and 56.4 MHz for ^{19}F, became commercially available. Consequently, the first investigations on mixed-ligand compounds focused on ^{19}F NMR spectroscopy taking into account the central importance of fluorine in the field of coordination chemistry.[186−188] Because of this low magnetic field, only the most sensitive and 100% abundant spin $^1/_2$ nuclei ^1H and ^{31}P beside ^{19}F were initially investigated. However, in pioneering studies the indirect observation of low sensivity spin $^1/_2$ nuclei like ^{57}Fe, ^{103}Rh, $^{107,109}Ag$, and ^{183}W subsequently became possible by means of the internuclear double resonance (INDOR) technique[189a−c] via the aforementioned highly abundant and sensitive nuclei. An extension to direct measurement of other, especially quadrupolar nuclei became possible with the introduction of the first truly multinuclear spectrometers in 1967 and the pulse Fourier transform technique in 1969. Recommended textbooks with emphasis on inorganic and multinuclear aspects are Mason *Multinuclear NMR*,[190] Harris and Mann *NMR and the Periodic Table*,[191] Pregosin *Transition Metal Nuclear Magnetic Resonance*,[192] Lambert and Riddel *The Multinuclear Approach to NMR Spectroscopy*,[193] and as a practical guide, Brevard and Granger *Handbook of High Resolution Multinuclear NMR*.[194]

Since NMR spectroscopy responds to the magnetic properties of individual isotopes in a local electronic environment, the observed nucleus is an atomic probe of the molecule. Because of this, NMR spectroscopy has become one of the most important methods for structural analysis of pure substances, for the qualitative and quantitative determination of individual species within multicomponent mixtures, and for the elucidation of intra- and intermolecular dynamics of exchange processes and chemical equilibria. If separation is impossible, often NMR spectroscopy is the only reliable method, because UV−vis, IR, and Raman spectroscopy are unable to determine individual species in mixtures due to broad line widths and band overlaps along with insufficient resolution.

As with the other experimental techniques already discussed, the unique properties of the 10 closely related species of octahedral mixed series are of primary interest to NMR spectroscopy. Some of the best advantages of NMR spectroscopy applied to these mixed- ligand species are as follows:

(i) The number of signals due to NMR-active ligands or central atoms is indicative for the presence and completeness of an octahedral series. The most favorable situations occur if the central atom, as well as one or several ligand atoms, are NMR active.

(ii) The individual species are readily characterized and distinguished from byproducts utilizing the systematics of the chemical shift. Further support arises from analyses of multiplicities, coupling constants, or line forms in combination with signal intensities.

(iii) The ratios of the individual species and the pairs of stereoisomers give evidence for reaction schemes or the preference of distinct reaction paths.

(iv) Time- and temperature-dependent measurements reveal kinetic and thermodynamic data, thus complex stability constants and enthalpies of formation become accessible.

(v) By temperature-variant measurement, transitions between rigidity and fluxionality can be verified and inter- and intramolecular exchange processes can be identified and elucidated.

(vi) Empirical correlations of chemical shifts with ligand parameters like electronegativity or polarizability provide practical hints for measurements of unknown substances, and reveal interesting phenomena, like the normal or inverse halogen dependence (NHD or IHD), the normal or inverse electronegativity dependence (NED or IED), and the normal or inverse polarizability dependence (NPD or IPD). Normal behavior is characterized by a central atom shift to high field in the series, F < Cl < Br < I, or in the order of high electronegativity < low electronegativity, and poor polarizability < good polarizability, respectively.

(vii) Important results are obtained by correlating the systematics of the chemical shift with the systematics from other spectroscopic methods, such as those observed for the spectrochemical and nephelauxetic series or for the *trans* influence.

(viii) The evaluation of the influences of the molecular properties, their systematic variation and the mutual interactions on observed central atom NMR shifts lead to the electronic origin and the mechanics of the chemical shift. Thus, the paramagnetic and diamagnetic contribution to the chemical shift can be quantified, and a better understanding of the theory with respect to the Ramsey equation[190a] or derived approaches is possible. Finally, a verification of experimental data and assumed models by *ab initio* calculations have become tractable.[195]

(ix) Valuable support in the assignment of NMR spectra of mixtures is provided by empirical relations, which have been confirmed for many series of octahedral mixed-ligand complexes. For ligand atoms the Dean−Evans relation,[196] and for central atoms the pairwise additivity method[197] and the *trans* or axis method[198] have to be mentioned, which will be explored in detail in the following section.

2. Main Group Elements

The first systematic investigation on ∼100 mixed-fluoro stannates(IV) with ligands like OH^-, H_2O, Cl^-, Br^-, I^-, NCS^-, $NCSe^-$, NCO^-, N_3^-, $C_2O_4^{2-}$, and $RCOO^-$ by ^{19}F NMR spectroscopy has already demonstrated the power of this method and the need for data from a complete series for accurate assignments and a full understanding.[196] After suitable reaction conditions for fluorine-containing mixed complexes had been found by NMR spectroscopy, analysis of the reaction mixtures revealed the following general trends that are valid for ligands like the halogens and pseudohalogens.

(1) Increasing substitution of F ligands results in an increasing downfield shift of the ^{19}F resonances.

Table 15. Observed and Calculated by the Dean−Evans Relation (eq 4) ^{19}F Chemical Shifts (ppm) for the Series $[SnF_nCl_{6-n}]^{2-}$, $n = 0-6$, in Methanol[a]

			$\delta(^{19}F)$	
n[b]	p	q	calcd	obsd
6	0	0	−161.9	−161.9
5	1	0	−136.8	−136.5
5	0	1	−153.5	−154.9
4b	2	0	−111.7	−109.8
4a	2	0	−111.7	−113.1
4a	1	1	−128.4	−
3b	3	0	−86.6	−88.5
3b	2	1	−103.3	−100.5
3a	2	1	−103.3	−104.5
2b	4	0	−61.5	−
2a	3	1	−78.2	−
1	4	1	−53.1	−

[a] $\delta(^{19}F)_{ref} = -161.9$ ppm; $C = 25.1$ ppm; $T = 8.4$ ppm. [b] a corresponds to *cis/fac*; b corresponds to *trans/mer*.

(2) ^{19}F resonances of F−Sn−F axes are at lower field than those of F−Sn−X axes.

(3) $^1J(^{119}Sn,^{19}F)$ coupling constants, obtainable from the Sn satellites, are considerably greater for F−Sn−F axes than for F−Sn−X axes.

(4) Signals of F atoms are shifted more downfield the more polarizable the *cis* positioned Sn−X bond is.

(5) Ions of the types, $[SnF_5X]^{2-}$, *cis*-$[SnF_4X_2]^{2-}$, and *mer*-$[SnF_3X_3]^{2-}$, with two sets of inequivalent F atoms can be identified if the signal intensities and the multiplicity analysis by calculation of the spin systems are taken into account.

The generally valid Dean−Evans relation (eqs 3 and 4, respectively) is particularly important for the identification of species with only one ^{19}F signal like *trans*-$[SnF_4X_2]^{2-}$, *fac*-$[SnF_3X_3]^{2-}$, *cis*- and *trans*-$[SnF_2X_4]^{2-}$, and $[SnFX_5]^{2-}$.

$$\delta(^{19}F) = pC + qT \quad (3)$$

$$\delta(^{19}F) = \delta(^{19}F)_{ref} + pC + qT \quad (4)$$

where $\delta(^{19}F)$ is the chemical shift of the F atom under consideration referred to $[SnF_6]^{2-}$, $\delta(^{19}F)_{ref}$ is the chemical shift of $[SnF_6]^{2-}$ referred to a primary ^{19}F standard like $CFCl_3$, p is the number of ligands X in *cis* position to F (0−4), q is the number of ligands X in *trans* position to F (0 or 1). C and T are solvent-dependent empirical increments of the chemical shift and are characteristic for a substituent X. For systems containing more than one substituent extended relations are available.[196] Within each series, good agreement between calculated and observed shifts has been found, on the basis of these relations. Therefore, the implied additivity of the *cis* and the *trans* influences of the other ligands on the ^{19}F chemical shift has been proven. An example is given in Table 15 by the series, $[SnF_nCl_{6-n}]^{2-}$, $n = 0-6$. It is especially important to note that the relative positions within the pairs of stereoisomers, with the *cis/fac* isomers found at a higher field than the corresponding *trans/mer* isomers, are derived accurately.

From quantitative evaluations the *cis/trans* and the *fac/mer* ratios have been determined for various series. In general, they are nearly constant for different solvents but do deviate from the statistical values in most cases. Furthermore, equilibrium constants and relative kinetic stabilities have been deduced. The increasing ^{19}F downfield shift with increasing polarizability of the ligand in the *cis* position has been rationalized by its intramolecular van der Waals interaction with the resonating F atom. For that reason, the responsible electric field effects caused by time-dependent dipole moments have been calculated approximately.[196]

Table 16. Observed and Calculated Chemical Shifts $\delta(^{119}Sn)$ (ppm) of the Series $[SnCl_nBr_{6-n}]^{2-}$, $n = 0-6$, Pairwise Additivity Method (pa), and Axis Method (am)

		$\delta(^{119}Sn)$		
n[a]	pairs	calcd (pa)[b]	obsd	calcd (am)[c] (axes)
6	12u	−729.3	−729.3	−729 (3x)
5	8u+4v	−917.4	−916.1	−924 ($2x + y$)
4b	4u+8v	−1105.4	−1106.6	−1177 ($2x + z$)
4a	5u+6v+w	−1123.4	−1120.5	−1119 ($x + 2y$)
3b	2u+8v+2w	−1329.5	−1330.1	−1372 ($x + y + z$)
3a	3u+6v+3w	−1347.6	−1344.0	−1314 (3y)
2b	8v+4w	−1553.6	−1560.6	−1625 ($x + 2z$)
2a	u+6v+5w	−1571.7	−1571.0	−1567 ($2y + z$)
1	4v+8w	−1813.8	−1815.5	−1820 ($y + 2z$)
0	12w	−2074.0	−2074.0	−2073 (3z)

[a] a corresponds to *cis/fac*; b corresponds to *trans/mer*. [b] $u = -60.78$; $v = -107.79$; $w = -172.83$ ppm. [c] $x = -234$; $y = -438$; $z = -691$ ppm.

Additionally, the series, $[SnCl_nBr_{6-n}]^{2-}$,[199,200] $[SnF_nCl_{6-n}]^{2-}$,[199] and $[SnX_nY_{6-n}]^{2-}$, X = Cl, Br, Y = CN, NCS,[201] have been characterized by ^{119}Sn NMR. A complete system is offered by $[SnCl_nBr_{6-n}]^{2-}$, $n = 0-6$, with the stereoisomers in statistical ratio and the *cis/fac* isomers resonating about 11−14 ppm higher than the respective *trans/mer* complexes. The assignment was strongly supported by the pairwise additivity method, which is based on the summation of the contributions of the 12 pairs of substituents residing on the edges of the octahedron. Thus, this approach takes into account the mutual influences of *cis*-positioned ligands with respect to the electron distribution in the ligand wave functions and their effect on the chemical shift of the central atom. As an example, the ^{119}Sn NMR shifts for the series, $[SnCl_nBr_{6-n}]^{2-}$, $n = 0-6$, have been calculated by a fitted set of additivity parameters, u, v, and w, for the Cl−Cl, Cl−Br and Br−Br pair, respectively. The *trans* or axis method is based on the contributions of the three possible axes in an octahedron built up by two different ligands, thus it mainly reflects the mutual *trans* influence. In order to perform this calculation, a set of fitted axis parameters, x, y, and z, for the Cl−Sn−Cl, Cl−Sn−Br, and Br−Sn−Br axis has been used, respectively. The results of both methods are comparatively compiled with the observed shifts in Table 16.

Evidently the succession of signals, especially those of the stereoisomers with the *cis/fac* isomers resonating at higher field than the corresponding *trans/mer* isomers, is described very well by the pairwise additivity method, while the *trans* or axis method fails. This can be explained in terms of *cis* and *trans* influences, in that the *cis* influence is of primary importance in main group element complexes, while

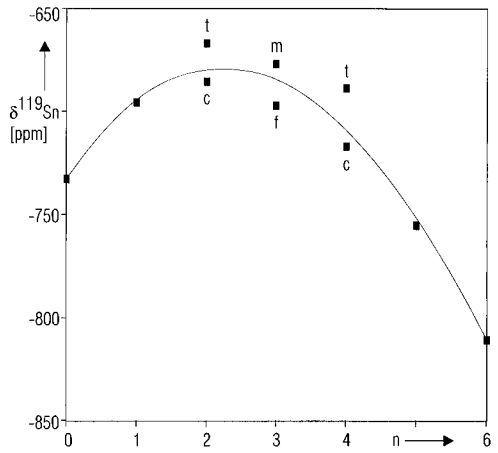

Figure 26. Plot of $\delta(^{119}Sn)$ vs n in the series $[SnF_nCl_{6-n}]^{2-}$, $n = 0-6$ (c = *cis*, f = *fac*, m = *mer*, t = *trans*).

the *trans* influence is of minor relevance. Although *mer*-$[SnF_3Cl_3]^{2-}$ is missing in the ^{119}Sn spectra of the flourochloro series,[199] it has been identified in the ^{19}F spectrum. The assignment of the partially overlapping signals has been achieved by multiplicity analysis with the known $^1J(^{19}F,^{119}Sn)$ couplings from the ^{19}F spectra[196] and was strongly supported by the pairwise additivity method, which again results in an upfield ^{119}Sn shift of the *cis* isomers in comparison to the *trans* isomers. A remarkable result, which is always observed for mixed-fluoro complexes, is the deviation of observed shifts from the calculated for both the ^{19}F and the central atoms. Thus, the Cl−F pairwise additivity term, derived from experimental shifts of individual species, increases systematically with increasing number of F atoms. This may be ascribed to a nonlinear additional mutual influence of the F ligands, for which the three-parameter model of the pairwise additivity method is not sophisticated enough. Therefore, the validity of the pairwise additivity method is not indicative of a linear correlation of the degree of substitution with the chemical shift (Figure 26).

In the case of $[SnF_5Cl]^{2-}$ and *cis*- and *trans*-$[SnF_4Cl_2]^{2-}$, the $^1J(^{19}F,^{119}Sn)$ coupling constants could be determined from the ^{119}Sn spectra, although this was not possible by ^{19}F spectroscopy. With respect to the halogen dependence of the ^{119}Sn shift, special attention must be drawn to the fact that $[SnF_6]^{2-}$ resonates at higher field than $[SnCl_6]^{2-}$, which resonates downfield from $[SnBr_6]^{2-}$. Therefore, the halogen dependence of ^{119}Sn in the order, Cl < F < Br, is unusual. Although mixed fluoroiodostannates(IV) have been identified by ^{19}F NMR, attempted ^{119}Sn measurements of mixed iodostannates(IV) remained unsuccessful, and even for $[SnI_6]^{2-}$ no ^{119}Sn signal has been observable. This was attributed to the large quadrupole moment of iodine, which causes rapid relaxation of the ^{119}Sn nucleus by quadrupolar coupling.[200]

Some mixed octahedral halogeno stannates with presumed *cis* configuration, like $[SnCl_2Br_4]^{2-}$, $[SnCl_2I_4]^{2-}$, $[SnCl_4Br_2]^{2-}$, and $[SnBr_2I_4]^{2-}$, have been characterized by ^{119}Sn Mössbauer spectroscopy, and *cis* configuration has been presumed.[40] As another result, the observed line broadening in the spectra of $[SnF_2Cl_4]^{2-}$ and $[SnF_2Br_4]^{2-}$ has led to the conclusion that these compounds are to be found in the *trans* configurations.[202,203] The Mössbauer isomer shift correlates linearly with the sum of the Pauling electronegativities of the ligands.

The application of the Dean−Evans relation for the assignment of ^{19}F shifts and the pairwise additivity method for the central atom shifts has become a common procedure in NMR assignment of mixed series and much of the following discussion is based upon these principles. For the following main group elements, Si, Ge, P, As, Sb, S, Te, octahedral mixed-fluoro complexes have been characterized by ^{19}F NMR spectroscopy, and a comprehensive discussion is given by Berger et al.[204]

In group 14, only a few monosubstituted products of $[SiF_6]^{2-}$ like $[SiF_5(C_6H_5)]^{2-}$,[205] $[SiF_5(NH_3)]^-$, $[SiF_5(NH(C_2H_5)_2)]^-$,[206] *cis*-$[SiF_4(bipy)]$, *cis*-$[SiF_4(ox)]^{2-}$, *cis*-$[SiF_4(mal)]^{2-}$, and *cis*-$[SiF_2(ox)_2]^{2-}$,[207,208] have been identified as octahedral species by ^{19}F NMR spectroscopy. For Ge only a few single fluoro complexes and the incomplete series, $[GeF_nX_{6-n}]^{2-}$, $n = 3-6$, X = NCS^-, and $n = 4-6$, X = CN^-, N_3^-, including the pairs of stereoisomers for $n = 3$ and 4, are known.[209] The mode of bonding of the thiocyanate has not been discussed explicitly, but was assumed to be the N coordination. The ^{19}F chemical shifts obey the Dean−Evans relation, in that the direction and magnitude of the effects of the substituents correlate to the corresponding Sn complexes.

As stated previously, one of the ideal situations for NMR spectroscopic examination would be if two NMR active nuclei can be found within one series. This, fortunately is the case for the group 15 elements, E = P, As, Sb, with several complete series of the type, $[EF_nX_{6-n}]^-$, which have been studied by ^{19}F and by ^{31}P, ^{75}As, and ^{121}Sb NMR spectroscopy. Series of the type $[EX_nY_{6-n}]^-$, X,Y ≠ F, have been characterized by ^{31}P and ^{121}Sb NMR. ^{31}P, which is an easily observable nucleus, has been extensively utilized, and many single octahedral mixed complexes have been identified by ^{31}P NMR spectroscopy.[210−214] The mixed series, $[PF_nCl_{6-n}]^-$,[215,216] $[PF_n(NCS)_{6-n}]^-$,[216] and $[PF_n(N_3)_{6-n}]^-$,[216] have been studied by ^{19}F NMR and confirmed by the Dean−Evans relation.[216] A subsequent ^{31}P study revealed complementary results, and, additionally, the identification of the homoleptic species, $[P(NCS)_6]^-$ and $[P(N_3)_6]^-$, has been achieved.[217] Non-first-order ^{19}F spectra of some $[PF_5(N\text{-base})]$ compounds have been analyzed and theoretically fit.[218] The following 3-fold mixed species, $[PF_3Cl_{3-n}X_n]^-$, $n = 1-3$; $[PF_2Cl_{4-n}X_n]^-$, $n = 1-4$, X = N_3^-, NCS^-; and $[PFCl_{5-n}(N_3)_n]^-$, $n = 1-5$, had been of special interest, because several of the species exhibit fluxional behavior.[219] The ^{31}P signals have been assigned utilizing the multiplicities and the pairwise additivity method. Generally, it has been found that the highly fluorine-substituted NCS-mixed species are fluxional at 307.2 K, while the species, $[PF_3Cl_{3-n}X_n]^-$ with $n = 0-2$, and those with two or one F atom are rigid. Also, the structures and fluxionality in the series, $[PF_n(CN)_{6-n}]^-$, have been investigated by ^{19}F and ^{31}P NMR, revealing fluxional behavior by a ^{31}P sextet for $[PF_5(CN)]^-$ and a ^{31}P quintet for *cis*-$[PF_4(CN)_2]^-$ at 307 K. These compounds become rigid at 178 K, as indicated by a doublet and a quintet for $[PF_5(CN)]^-$ and two triplets for *cis*-$[PF_4(CN)_2]^-$. Ad-

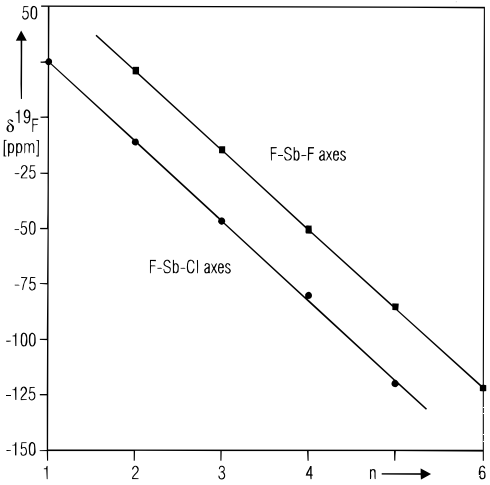

Figure 27. Plot of $\delta(^{19}F)$ vs n in the series $[SbF_nCl_{6-n}]^-$, $n = 1-6$.

ditionally, some mixed species of the type, $[PF_3Cl_{3-n}(CN)_n]^-$, $n = 1-3$, have been synthesized. From the three possible isomers for $n = 1$, one fluxional and two rigid complex ions have been found, while for $n = 2$ only one rigid species has been observed. For $n = 3$, the *mer* isomer has been clearly identified as the only existing species. Similarly, the 3-fold mixed compounds, $[PRCl_{5-n}(CN)_n]$, R = C_2H_5, C_6F_5, and CCl_3, have been examined by ^{31}P NMR with respect to their structure, stability, and reaction paths.[220] For several special cases, namely the series, $[PCl_n(N_3)_{6-n}]^-$, $n = 0-4$;[221] $[PCl_n(CN)_{6-n}]^-$, $n = 2-6$;[222] and $[PCl_n(NCS)_{6-n}]^-$, $n = 0-6$, special reaction pathways have been proposed.[222] For the stereoisomers of the chloroazido series the usual *cis* ($n = 4$)−*fac* ($n = 3$)−*cis* ($n = 2$) substitution pattern has been discussed, such as that found in $[PF_nCl_{6-n}]^-$ [216] and $[SbCl_nBr_{6-n}]^-$,[226] while for the chlorothiocyanato series the alternative sequence *trans* ($n = 4$)−*mer* ($n = 3$)−*cis* ($n = 2$) has been proposed. With exception of *cis*-$[PCl_2(CN)_4]^-$, all chlorocyano species have been identified. For all cases, the observed shifts are fitted very well by the pairwise additivity method. A great number of additional ^{31}P data is to be found in ref 223. From As and Sb, the series, $[AsF_nCl_{6-n}]^-$, $[SbF_nCl_{6-n}]^-$, and $[SbCl_nBr_{6-n}]^-$, $n = 0-6$, are known. The mixed fluoro systems of As[224] and Sb[225] have been studied by ^{19}F NMR and reinvestigated by ^{19}F, ^{75}As, and ^{121}Sb NMR.[226] The assignments of the more recent, and more dependable, multinuclear study [226] can be summarized as follows:

(i) The ^{19}F resonances obey the Dean−Evans relation (see Figure 27).

(ii) The chemical shifts of the central atoms in the mixed-fluoro complexes depend nonlinearly on the number of F ligands. Plots of the ^{75}As and the ^{121}Sb shift, respectively, versus n give U-shaped curves with highfield maxima for $n = 5$ and $n = 3$, respectively (see Figures 28 and 29).

(iii) Apart from trace amounts of *mer*-$[AsF_3Cl_3]^-$ the *cis*/*fac* isomers are present exclusively in all three series. This is concluded unambiguously from the multiplicities of the ^{75}As and ^{121}Sb signals, as well as from the quadrupole quartets in the ^{19}F spectra due to ^{75}As ($I = 3/2$, 100%) and the partially overlapping quadrupole sextets due to ^{121}Sb ($I = 5/2$, 57.25%)

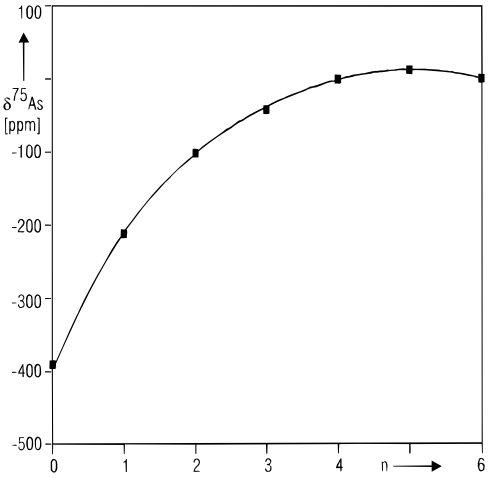

Figure 28. Plot of $\delta(^{75}As)$ vs n in the series $[AsF_nCl_{6-n}]^-$, $n = 0-6$.

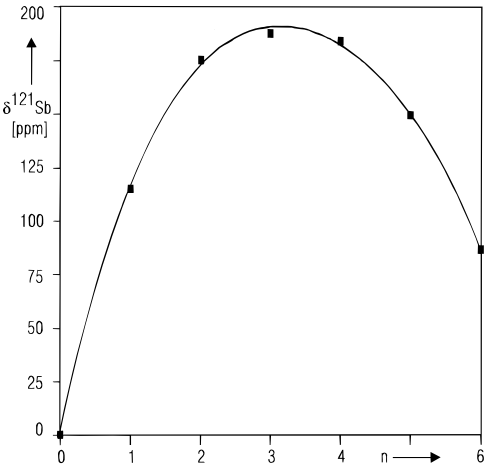

Figure 29. Plot of $\delta(^{121}Sb)$ vs n in the series $[SbF_nCl_{6-n}]^-$, $n = 0-6$.

Table 17. Quadrupolar Line Broadening Factor qb in Dependence of the Symmetry Due to Invariants of the Electric Field Gradient Tensor, g_q^2, in 2-fold Mixed Octahedral Complexes, qb = $g_q^2/(e_2/r_2^3 - e_1/r_1^3)^2$

point group	O_h	C_{4v}	D_{4h}	C_{2v} (*cis*)	C_{2v} (*mer*)	C_{3v} (*fac*)
qb	0	9	36	16	27	0

and the quadrupole octects due to ^{123}Sb ($I = 7/2$, 42.75%).

The half-widths of the ^{75}As and ^{121}Sb signals increase as the number of Cl ligands increase and is attributable to more efficient relaxation by two quadrupolar effects: first, by the influence of the electric field gradient on the relaxation of the quadrupole central atoms on deviation from cubic environment (see Table 17); and second, by coupling to the quadrupole nuclei, ^{35}Cl and ^{37}Cl. The quadrupolar coupling to the Cl isotopes may be the reason that the *fac*-F_3 complexes, with a broadening factor qb = 0 (see Table 17), exhibit lines no narrower than those found for the other mixed species.[226]

The ^{121}Sb resonances of the series, $[SbCl_nBr_{6-n}]^-$, span a wide range, from 0 ppm for $[SbCl_6]^-$, which serves as reference, to −2430 ppm for $[SbBr_6]^-$ at highest field, thus showing NHD. Seven systematically succeeding resonances have been found with statistical intensities according to the molar ratios of Br/Cl (see Figure 30). Due to the high quadrupole

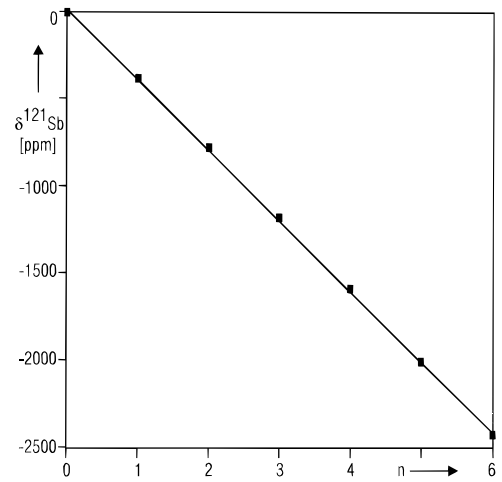

Figure 30. Plot of $\delta(^{121}Sb)$ vs n in the series $[SbCl_nBr_{6-n}]^-$, $n = 0-6$.

moment of the ^{121}Sb nucleus, the signals are very broad. The narrowest lines possess half-widths of 350 Hz and are present for the homoleptic terminal members, but in environments of lower than cubic symmetry considerable broadening occurs. By the pairwise additivity method, the *cis/fac* isomers have been postulated as the exclusively formed stereoisomers.[227] It should be mentioned, however, that at the low measuring frequency of 14.37 MHz, the calculated shift differences of 11 ppm between two corresponding stereoisomers result in a value of only 158 Hz. Therefore, overlapping signals of stereoisomeric pairs cannot be ruled out (cf. the $[NbCl_nBr_{6-n}]^-$ series in the following section).

Except for some *cis/trans* isomers of the sulfur compounds, $[SF_4ClR]$, with organic ligands, R, which have been characterized by ^{19}F NMR,[228] in group 16 there are only a few octahedral mixed series of Te like $[TeF_n(OH)_{6-n}]$, $n = 0-6$, and $[TeF_nCl_{6-n}]$, $n = 1-6$. The reaction of $[Te(OH)_6]$ with HF[229] and the hydrolysis of $[TeF_6]$ and $[TeF_5Cl]$[230,231] were studied by ^{19}F NMR. For the hydrolysis *cis* stereospecificity was observed. Also, by combining ^{19}F and ^{125}Te NMR spectroscopy and by deliberate synthesis of some single species of the series, the order of thermodynamic stability of the pairs of stereoisomers was found to be *trans*-F_4 > *cis*-F_4, *cis*-F_2 > *trans*-F_2 and *fac*-F_3 > *mer*-F_3. The ^{19}F resonances of $[TeF_6]$, at 73 ppm, are shifted upfield for $[TeF_5(OH)]$ and are found at higher field for F−Te−F axes than for F−Te−OH axes. Couplings of remarkable magnitude are observed: with $^2J(^{19}F,^{19}F)$ coupling constants of 132−190 Hz, and $^1J(^{19}F,^{125}Te)$ coupling constants of 3715 Hz for $[TeF_6]$ to 2754 Hz for the asymmetric axis in $[TeF_5(OH)]$. Thus the coupling constants of the F−Te−F axes are greater by 35% than those of the F−Te−OH axes. With $Te(CH_3)_2$ as a reference, the highest ^{125}Te signal is found at 544 ppm for $[TeF_6]$, while the lowest is found for $[Te(OH)_6]$ at 707 ppm, thus showing IED. Also, by ^{19}F and ^{125}Te NMR the 3-fold mixed series, $[TeF_{5-n}(OH)_nCl]$, $n = 1-3$, has been characterized.[231]

3. Transition Metals

In group 3, ^{45}Sc NMR data for several octahedral complexes have been reported showing IHD with $[ScCl_6]^{3-}$ at 249 ppm and $[ScBr_6]^{3-}$ at 288 ppm. Consequently, IED is presented by the series, $[ScCl_n(H_2O)_{6-n}]^{(3-n)+}$, $n = 0-6$, with $[Sc(H_2O)_6]^{3+}$ at 0 ppm, and inverse behavior has been proposed to be generally valid for d^0 systems.[232,233] In the series, $[ScCl_{6-x-y}(NCS)_x(CH_3CN)_y]^{(3-y)-}$, 10 different species have been characterized.[234] From the actinides, a few series of U(VI), like $[UF_n(OTeF_5)_{6-n}]$, $n = 0-6$;[235] $[UF_n(OCH_3)_{6-n}]$;[236] and $[UF_nCl_{6-n}]$, $n = 1-5$,[237] have been investigated by ^{19}F NMR spectroscopy with regard to their potential for uranium enrichment. The Dean−Evans relation is valid for the oxofluoro tellurate and the methoxy mixed series, but it fails for $[UF_nCl_{6-n}]$. Plots of $\delta(^{19}F)$ vs the total number of F atoms or the substituents in *cis* position to the resonating F result in U-shaped curves.[235−237]

In group 4, some single species of the type, $[TiF_5(OR)]^{2-}$, R = alkyl, aryl, *cis*- and *trans*-$[TiF_4(LL)]^{2-}$, LL = oxalate, malonate, have been characterized by ^{19}F NMR spectroscopy. The equilibrium constants and changes of the free energy ΔG have been calculated and compared to corresponding complexes of Si, Ge, and Sn.[207] In liquid SO_2 at 213 K, for the series, $[TiF_n(NCX)_{6-n}]^{2-}$, X = S, O; $n = 1-6$, all species including the stereoisomers except *trans*-$[TiF_2(NCS)_4]^{2-}$ have been obtained by distribution studies of $[TiF_6]^{2-}$ with $[Ti(NCX)_6]^{2-}$, and the dimeric species, $[Ti_2F_{11}]^{3-}$, $[Ti_2F_{10}]^{2-}$, and $[Ti_2F_9]^-$, have been found as byproducts.[238] From the validity of the Dean−Evans relation, it has been concluded that the constant T (eqs 3 and 4) is a measure of the p-donor ability of the substituents, and that the ^{19}F shift is largely determined by the degree of the p_F-d_{Ti} backdonation in the remarkable order F > NCS > NCO. The Dean−Evans constants, C and T (eqs 3 and 4), for complexes with the central atoms, P, Ge, Sn, and Ti, have been compared and critically discussed.[209]

From the transition metals of group 5, the series $[MF_nX_{6-n}]$, M = Nb, Ta, X = Cl, Br, have been characterized by ^{19}F NMR.[239−241] Only the fluorochlorotantalate(V) series is complete. Calculations of the complex stabilities revealed *trans/mer* isomers more stable than *cis/fac* isomers. Furthermore, stability decreases with increasing number of Cl ligands and to an even greater extent of Br ligands. The following stability series have been obtained for $[TaF_nCl_{6-n}]^-$ and for $[TaF_nBr_{6-n}]^-$: *trans*-F_4 > *trans*-F_2 > F_5 > *mer*-F_3 > *cis*-F_4 > *cis*-F_2 > *fac*-F_3; and *trans*-F_2 > *trans*-F_4 > F_5 > *mer*-F_3 > *cis*-F_4 > *cis*-F_2 > *fac*-F_3. Furthermore 19 3-fold mixed species of the type, $[TaF_xCl_yBr_z]^-$, $x + y + z = 6$, and 16 species out of the system, $[TaF_xR_yR'_z]$, $x + y + z = 6$, R = OC_2H_5, R′ = C_2H_5OH, CH_3CN, have been identified by ^{19}F NMR and assigned by means of the Dean−Evans relation.[242] The properties of ^{93}Nb ($I = 9/2$, 100%, $Q = 0.32$ barn) as the fourth most sensitive nucleus after ^3H, ^1H, and ^{19}F [194] has attracted the attention of coordination chemists despite its high quadrupole moment, Q, and the resulting broad lines. The inverse halogen dependence (IHD) has been discovered on the ^{93}Nb shifts of $[NbCl_6]^-$ and $[NbBr_6]^-$.[243] Later on this phenomenon has been found to be common for elements with s^1, d^3, d^4, d^5, ($d^{10}s^1$) valence electron configurations. The common feature of these configurations are less than half- or

half-filled shells and negative spin−orbit coupling constants.[244] Despite line width on the order of 5−7 kHz in the case of mixed species with noncubic symmetry, the shift ranges defined by the respective terminal members, $F_6 = -1550$ ppm, $(NCS)_6 = -1342$ ppm, $(SCN)_6 = -780$ ppm, $Cl_6 = 0$ ppm, and $Br_6 = +725$ ppm ($\Delta\nu_{1/2} < 30$ Hz for all homoleptic complexes), are sufficient for *in situ* measurements and the distinction of species with different running numbers n, although the resolution of stereoisomers is difficult. By reaction of $(NbCl_5)_2$ and $(NbBr_5)_2$ with HF in CH_3CN, the two series, $[NbF_nCl_{6-n}]^-$ and $[NbF_nBr_{6-n}]^-$, $n = 0-6$, have been obtained.[241,245] Also, by reaction with KSCN and KOCN in CH_3CN, the series $[NbX_n(NCS)_{6-n}]^-$, X = Cl, Br, $n = 0-6$; and $[NbX_n(NCO)_{6-n}]^-$, X = Cl, Br, $n = 1-6$, have been prepared. The stereoisomers of the mixed-fluoro species, which have been clearly identified by ^{19}F spectra, could not be resolved by ^{93}Nb spectroscopy. In the cases of mixed-pseudohalogeno/Cl or Br complexes, all three pairs of stereoisomers have been definitively characterized for the mixed-thiocyanato species, while for the cyanato series *cis*-$[NbCl_2(NCO)_4]^-$ has yet to be identified. As byproducts, solvate complexes with CH_3CN have been found, and the formation of $[Nb(NCS)_7]^{2-}$ has been suggested.[245] In a reinvestigation of these reactions, it was not possible to synthesize $[Nb(NCS)_7]^{2-}$ using very pure $(NbCl_5)_2$ with KSCN in rigorously dried CH_3CN under an N_2 inert atmosphere.[246] Furthermore, considerable deviations in the assignments in the $[Nb(NCS)_nCl_{6-n}]^-$ series became apparent, which have been attributed to the different preparation techniques.[190b] As the most essential result, thiocyanate has been found to behave as an ambidentate ligand in this series. This was expressed by the formulation of the series, $[Nb(NCS)_n(SCN)_mCl_{6-(n+m)}]^-$. From the 65 possible individual species, 16 have been identified and assigned by the pairwise additivity method, with interaction terms optimized by linear regression analysis. As a further result of prime importance, the existence of the series, $[Nb(NCS)_n(SCN)_{6-n}]^-$, $n = 0, 2, 4, 5$, has been demonstrated stringently[246] (see section III.C).

The octahedral series, $[NbCl_nBr_{6-n}]^-$ and $[NbCl_nBr_{5-n}(CH_3CN)]$, have been studied by ^{93}Nb CW NMR spectroscopy at 1.4 T, and the pairwise additivity model has been applied for the first time to octahedral complexes.[247] Seven, nearly equidistant, ^{93}Nb resonances have been found, and the intensity patterns behave according to the statistical distribution of the starting molar ratios of Cl/Br. With respect to the stereoisomers, a decision favoring the *cis*/*fac* isomers has been made. However, a reinvestigation, with the pulse Fourier transform technique at 2.35 T, revealed the existence of the three pairs of stereoisomers in nearly statistical ratios and calculated shifts that were clearly overestimated by the pairwise additivity method.[198] It was possible to assign all species by the combination of the axis method and a sophisticated line-shape analysis based on T_2 and T_1 relaxation time determinations. Additionally, the dependence of the quadrupolar broadening factors (qb) on the symmetry has been calculated. By the point charges of two ligands, e_2 and e_1, with distances, r_2 and r_1, from the resonating nucleus, the invariants of the tensor of the electric field gradient, g_q^2, have been calculated and are given in Table 17 for the respective point groups.[198,248]

Perhaps one of the most impressive examples of the benefits of combining theoretical and experimental NMR is the *ab initio* calculation of ^{93}Nb shifts for the series, $[NbCl_nF_{6-n}]^-$ and $[NbBr_nCl_{6-n}]^-$, $n = 0-6$, for which the calculated and observed values fit extremely well.[195] The unusual feature of nonlinear, more or less U-shaped correlations between observed shifts and the degree of substitution in the case of the fluoro mixed series, which has been mentioned several times previously, can be attributed to the calculated net Nb charge and the 4d population, which also show nonlinear dependence on n in the fluoro series. As has been shown in detail, the paramagnetic term, σ^{para}, contributes primarily to the ^{93}Nb shift and is determined by the nonlinear 4d population. Correspondingly, σ^{para} changes nonlinearly by −1748 ppm from $[NbF_6]^-$ to $[NbCl_6]^-$. The diamagnetic term, σ^{dia}, depends solely on structural parameters and changes linearly by only +150 ppm. However, it is not yet possible to generalize these results. Therefore similar calculations should be performed on series, for which experimental data are already available from previous NMR studies.

In group 6, there are only a few, but very good, examples of mixed halogeno complexes like the W(VI) series, $[WF_nCl_{6-n}]$, $n = 1-6$,[249] and $[WF_n(OCH_3)_{6-n}]$, $n = 1-5$,[250,251] which have been studied by ^{19}F NMR, and shown to fit well according to the Dean−Evans relation. Additionally, combined ^1H and ^{19}F NMR spectroscopy has been used to determine the stereochemical paths in the system, $[WF_n(OCH_3)_{6-n}]$,[252] and the INDOR technique has been used to determine the ^{183}W shifts.[250] In this context the pulse Fourier transform approach to indirect observation of spin $^1/_2$ nuclei with low gyromagnetic ratio γ like ^{57}Fe, ^{103}Rh, ^{183}W, and ^{187}Os should be mentioned, which is known as inverse or reverse INEPT. This two-dimensional polarization transfer experiment is exceedingly apt for complexes of such nuclei with ligands that are or contain spin $^1/_2$ nuclei of high abundance and sensitivity like ^1H, ^{19}F, and ^{31}P.[192]

In group 8, there are numerous examples of mixed hexahalogeno complexes, such as the following mixed fluoro series: $[OsF_nCl_{6-n}]^{2-}$,[253,254] $[RhF_nCl_{6-n}]^{3-}$,[255−257] and $[PtF_nX_{6-n}]^{2-}$, X = Cl, Br.[258,259] These series have been investigated by ^{19}F NMR spectroscopy, and the latter two have also been studied with regard to their hydrolysis products. The paramagnetic Os(IV) complexes are of special interest, because the line widths of the ^{19}F resonances remain sufficiently narrow to observe the ^{187}Os satellites with $^1J(^{19}F,^{187}Os)$ coupling constants of about 240 Hz.[253,254]

Because of its low gyromagnetic ratio, ^{103}Rh ($I = ^1/_2$, 100%) is very difficult to observe by direct measurement. Nevertheless, many ^{103}Rh NMR investigations have been carried out, especially due to great interest in the catalytic properties of the metal and its coordination compounds.[260] Therefore, the hydrolysis of $RhCl_3$ to octahedral aquachlororhodates(III) has been studied by ^{103}Rh and ^{17}O NMR

Table 18. Chemical Shifts $\delta(^{103}Rh)$ (ppm) in the Series $[RhCl_nBr_{6-n}]^{2-}$, $n = 0-6$ Observed and Calculated by the Pairwise Additivity Method

		$\delta(^{103}Rh)$	
n^a	pairs[b]	calcd	obsd
6	12u	7836	7836
5	8u + 4v	7700	7704
4b	4u + 8v	7564	7563
4a	5u + 6v + w	7556	7559
3b	2u + 8v + 2w	7412	7411
3a	3u + 6v + 3w	7404	7407
2b	8v + 4w	7260	7257
2a	u + 6v + 5w	7252	7252
1	4v + 8w	7092	7091
0	12w	6924	6924

[a] a corresponds to *cis/fac*; b corresponds to *trans/mer*. [b] $u = 653$; $v = 619$; $w = 577$ ppm.

spectroscopy.[256] The deliberate hydrolysis of $[RhX_6]^{3-}$, X = Cl, Br, results in the complete series, $[RhX_n(H_2O)_{6-n}]^{3-n}$, $n = 0-6$, which have been analyzed by ^{103}Rh NMR. Some species exhibit split signals according to the ^{35}Cl, ^{37}Cl isotopomers.[257,261-263] Because nitro complexes are used during the separation of rhodium from the other platinum metals a systematic multinuclear study on the hydrolysis of $[Rh(NO_2)_6]^{3-}$ by ^{14}N, ^{15}N, ^{17}O, ^{35}Cl, and ^{103}Rh NMR spectroscopy should be mentioned.[264,265] The complete series, $[RhCl_nBr_{6-n}]^{3-}$, including the three pairs of stereoisomers, has been characterized by ^{103}Rh NMR, and reveals NHD.[266] Also, a quantitative investigation with respect to the stepwise complex equilibria and stability constants has been performed.[35] A good agreement of the observed and the calculated shifts by the pairwise additivity method is found and presented in Table 18. The interaction terms, u, v and w, have been used for the Cl−Cl, Cl−Br, and Br−Br pairs, respectively.

In this context, attention should be brought to a similar utilization of chemical shift increments, which is based on different interactions of terminal and bridging ligands in dinuclear complexes.[267,268] This has allowed the assignment of all 64 ^{103}Rh resonances, which are attributed to the 40 possible individual species of the system, μ_3-$[Rh_2Cl_nBr_{9-n}]^{3-}$, $n = 0-9$.[267] As a reference for ^{103}Rh, the calculated absolute frequency, $\Xi(^{103}Rh) = 3.16$ MHz, has been generally accepted.[191]

The properties of the ^{195}Pt nucleus ($I = 1/2$, 33.8%) and its very large shift range of nearly 14 000 ppm make platinum complexes ideal for NMR studies. A generally accepted reference now is the absolute frequency of $\Xi(^{195}Pt) = 21.4$ MHz. The mixed chlorobromoplatinates(IV), $[PtCl_nBr_{6-n}]^{2-}$, have been studied by ^{195}Pt NMR as isolated compounds[269] and *in situ* in mixtures.[270,271] The ^{195}Pt shift depends strongly on the temperature, the nature of solvent, the ionic strength, the kind of counterions, the concentration of Pt itself, and in aqueous solutions, on the pH.[259,272,190c] Series of the type, $[PtX_n(NO_2)_{6-n}]^{2-}$, $n = 1-5$,[273] and $[Pt(CN)_nX_{6-n}]^{2-}$, $n = 0-3$,[274] X = Cl, Br, including the pairs of stereoisomers, have been characterized by ^{195}Pt NMR. Hydrolysis of $[PtCl_6]^{2-}$ produces the series, $[PtCl_n(OH)_{6-n}]^{2-}$, $n = 0-6$, which has been studied with respect to the pH influence.[275] By dissolving the products of the heterogenous reaction of $K_2[PtBr_6]$ with BrF_3, besides hydrolyzed complexes, $[PtF_5Br]^{2-}$ and *cis*-$[PtF_4Br_2]^{2-}$ have been identified by ^{19}F and ^{195}Pt NMR.[258] These compounds are of special interest with regard to the stability and the *trans* influence in comparison with the complete series, $[PtF_nCl_{6-n}]^{2-}$, $n = 0-6$, which has been analyzed by a combined $^{19}F-^{195}Pt$ study.[272] The individual species of this family, separated on DEAE cellulose[55] and isolated as bis(triphenylphosphiniminium) (PPN) salts, have been measured in CD_2Cl_2 at 9.4 T in equimolar solutions, while maintaining temperature and field homogeneity as constant as possible. The ^{195}Pt signals cover the range from 11 816 ppm for $[PtF_6]^{2-}$ to 4731 ppm for $[PtCl_6]^{2-}$ with the *cis/fac* resonances at higher field than those of the respective *trans/mer* isomers (see Figure 31).

Due to the coupling of ^{195}Pt and ^{19}F, all fluorochloro complexes exhibit ^{195}Pt multiplets. Depending on the point symmetry, two kinds of chemically different and magnetically inequivalent F ligands are present, namely those on symmetric F−Pt−F axes and those which have a mutual trans interaction with Cl on asymmetric F•−Pt−Cl′ axes. According to the sets of inequivalent F atoms, the nature of the individual species is indicated directly by the multiplicity of their ^{195}Pt resonances with the exception of $n = 2$, for which a triplet is observed for both the *cis* as well as the *trans* isomer. However, these are easily distinguished by their characteristic $^1J(^{19}F,^{195}Pt)$ coupling constants, which are in the order of 1890 Hz for F−Pt−F axes and 1300 Hz for F•−Pt−Cl′ axes. On average of all species of this series, the coupling constants for asymmetric axes are diminished by 33% due to the *trans* influence of Cl. The half-widths, $\Delta\nu_{1/2}$, of the Pt signals reflect the different contributions of the chemical shift anisotropy to the relaxation of the ^{195}Pt nucleus in complexes of different point symmetries (Table 19).

As has been exemplified by a comparative ^{195}Pt study on $[PtCl_6]^{2-}$ at different field strengths, the ^{35}Cl,^{37}Cl isotopomers are clearly resolved at 9.4 T.[276] This has been confirmed by the spectra of the isotopically pure species, $[Pt^{35}Cl_6]^{2-}$ and $[Pt^{37}Cl_6]^{2-}$, which are shown together with $[Pt^{n.a.}Cl_6]^{2-}$ in Figure 32. The intensities are in accordance with the statistical distribution of $^{n.a.}Cl$. On average, a high field shift of 0.18 ppm per ^{37}Cl is observed.[272]

The ^{19}F resonances are typical satellite spectra and appear as *pseudo* triplets (intensity ratio = 1:4:1). They are formed by a central singlet of F nuclei, which are attached to the 66.2% NMR-inactive Pt isotopes and are flanked by a doublet, which arises from coupling to ^{195}Pt with 33.8% natural abundance. Because the species with $n = 1$, 2, 3 (*fac*), 4 (*trans*), and 6 contain only one set each of chemically and magnetically equivalent ^{19}F nuclei, only one signal group is observed. In the case of $n = 3$ (*mer*), 4 (*cis*), and 5, with two sets of inequivalent F atoms each, two signal groups result, and the resonances of the F−Pt−F axes are always found at higher fields than the respective F•−Pt−Cl′ axes (Figure 33, Table 18). At high resolution, splittings due to $^2J(^{19}F,^{19}F)$ couplings in the order of 40 Hz are observable. For $[PtF_5Cl]^{2-}$, the *pseudo* triplet of F• is split by coupling

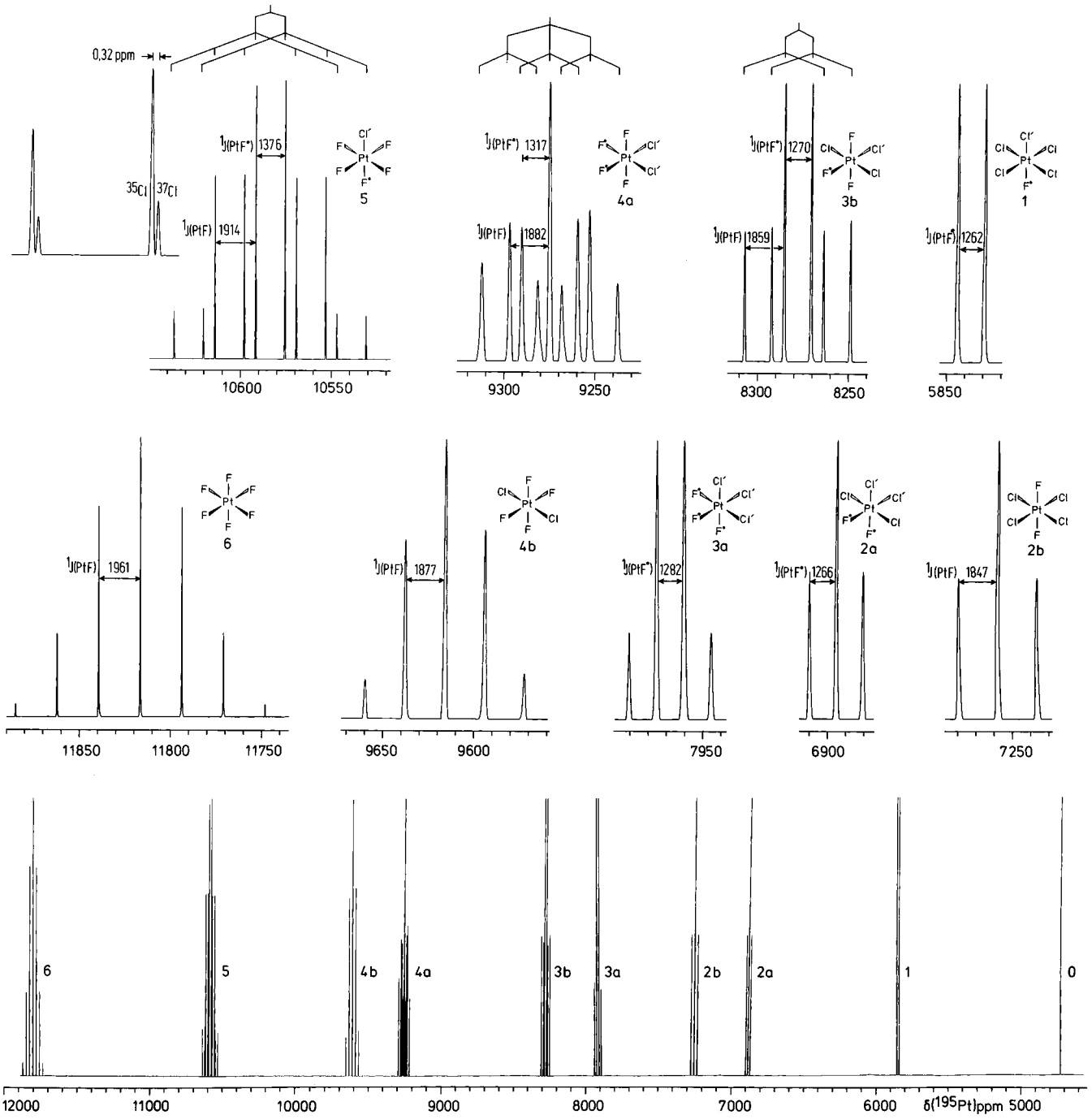

Figure 31. ^{195}Pt NMR spectra of the series $(PPN)_2[PtF_nCl_{6-n}]$, $n = 0-6$: overview (bottom), highly resolved multiplets (top).

Table 19. Chemical Shifts $\delta(^{195}Pt)$ of the Series $(PPN)_2[PtF_nCl_{6-n}]$, $n = 0-6$, at 283 ± 0.3 K vs $\Xi(^{195}Pt) = 21.4$ MHz and $\delta(^{19}F)$, $\delta(^{19}F^{\bullet})$ at 297 ± 0.3 K vs $\delta(^{19}F)(CF^{35}Cl_2{}^{37}Cl) = 0$ (ppm)[a]

species	$\delta(^{195}Pt)$	m[b]	$^1J_{PtF}$	$^1J_{PtF^{\bullet}}$	$\delta(^{19}F)$	signal group	$\delta(^{19}F^{\bullet})$	signal group	$^1J_{FPt}$	$^1J_{F^{\bullet}Pt}$	$^2J_{FF^{\bullet}}$	$\Delta\nu_{1/2}$
$[PtF_6]^{2-}$	11816	s	1961	–	−357	pst	–	–	1961	–	–	9
$[PtF_5Cl]^{2-}$	10582	d of qi	1914	1376	−360	pst of d	−268	pst of qi	1916	1377	36	9
trans-$[PtF_4Cl_2]^{2-}$	9616	qi	1877	–	−367	pst	–	–	1877	–	–	44
cis-$[PtF_4Cl_2]^{2-}$	9276	t of t	1882	1317	−364	pst of t	−267	pst of t	1885	1320	39	74
mer-$[PtF_3Cl_3]^{2-}$	8278	d of t	1859	1270	−372	pst of d	−273	pst of t	1860	1285	44	49
fac-$[PtF_3Cl_3]^{2-}$	7918	q	–	1282	–	pst	−266	–	–	1293	–	82
trans-$[PtF_2Cl_4]^{2-}$	7258	t	1847	–	−382	pst	–	–	1850	–	–	54
cis-$[PtF_2Cl_4]^{2-}$	6895	t	–	1266	–	pst	−276	–	–	1280	–	69
$[PtFCl_5]^{2-}$	5837	d	–	1262	–	pst	−287	–	–	1271	–	62
$[PtCl_6]^{2-}$	4731	–	–	–	–	–	–	–	–	–	–	11
averaged values			1890	1296					1892	1304	40	

[a] Coupling constants $^1J_{PtF}$, $^1J_{PtF^{\bullet}}$, $^1J_{FPt}$, $^1J_{F^{\bullet}Pt}$, $^2J_{FF^{\bullet}}$ (Hz); multiplicities, m; and half-widths, $\Delta\nu_{1/2}$, of ^{195}Pt signals (Hz) 35 mmol in CD_2Cl_2. ($^{\bullet}$) denotes F in F$^{\bullet}$–Pt–Cl axes. [b] d, doublet; t, triplet; q, quartet; qi, quintet; s, septet; pst, pseudotriplet.

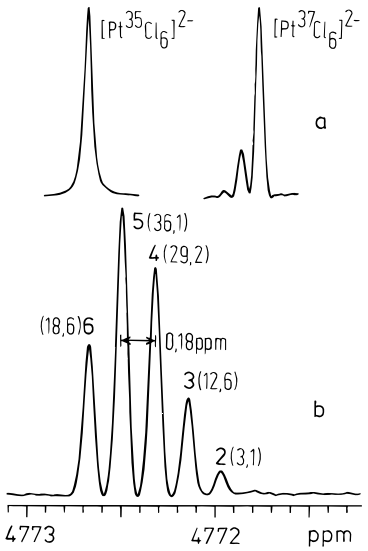

Figure 32. ^{195}Pt NMR spectra of $(TBA)_2[Pt^{35}Cl_6]$ (99.6% ^{35}Cl) and $(TBA)_2[Pt^{37}Cl_6]$ (95.7% ^{37}Cl) (a) and of the isotopomers, $(TBA)_2[Pt^{35}Cl_n{}^{37}Cl_{6-n}]$, $n = 2-6$, for $^{n.a.}$Cl.

to the four equatorial F atoms into quintets, which exhibit at highest resolution the theoretical 3:1pattern according to the ^{35}Cl:^{37}Cl ratio of $^{n.a.}$Cl (Figure 33, inset). Interestingly, the signal due to the ^{35}Cl isotopomer is found 0.007 ppm at higher field than that of the ^{37}Cl isotopomer. Thus, this isotopic effect, which operates across two bonds of the octahedron, is of the same magnitude as observed for tetrahedral $CFCl_3$, but the shielding of the ^{19}F nucleus is opposite. In comparison to the effect across one octahedral bond, which has been found as a downfield shift of 0.18 ppm per ^{35}Cl, it is 1 order of magnitude lower and also opposite in shielding in the ^{195}Pt spectrum of $[PtCl_6]^{2-}$.

Although there is a systematic trend in the ^{195}Pt shifts, they cannot be calculated with sufficient certainty, neither by the pairwise additivity method nor by the axis method. Also, the ^{19}F resonances do not obey the Dean−Evans relation to an acceptable extent (Figure 34). An exponential dependence on the total number of F atoms in the individual species has been found for the ^{19}F shifts of F•−Pt−Cl′ axes, while a logarithmic dependence is found for the F−Pt−F axes. Similar U-shaped curves have already been mentioned for the fluoro complexes of Sn, As, Sb, Te, U, W, and Nb. Also, the correlation of the $^1J(^{19}F,^{195}Pt)$ coupling constants with the respective number of F atoms in Figures 35 and 36 is nonlinear.

III. Linkage Isomers

A. Fundamental Considerations

In this section mixed complexes will be discussed, which are formed exclusively by an ambidentate ligand. Complexes of this type are known with the thiocyanate ligand as $[M(NCS)_n(SCN)_{6-n}]^{z-}$ [74,246,277−286] and with the selenocyanate ligand as found in the unique series $[Os(NCSe)_n(SeCN)_{6-n}]$.[287]

By definition, linkage isomerism requires the existence of at least two coordination compounds of the same composition with ambidentate ligands, which

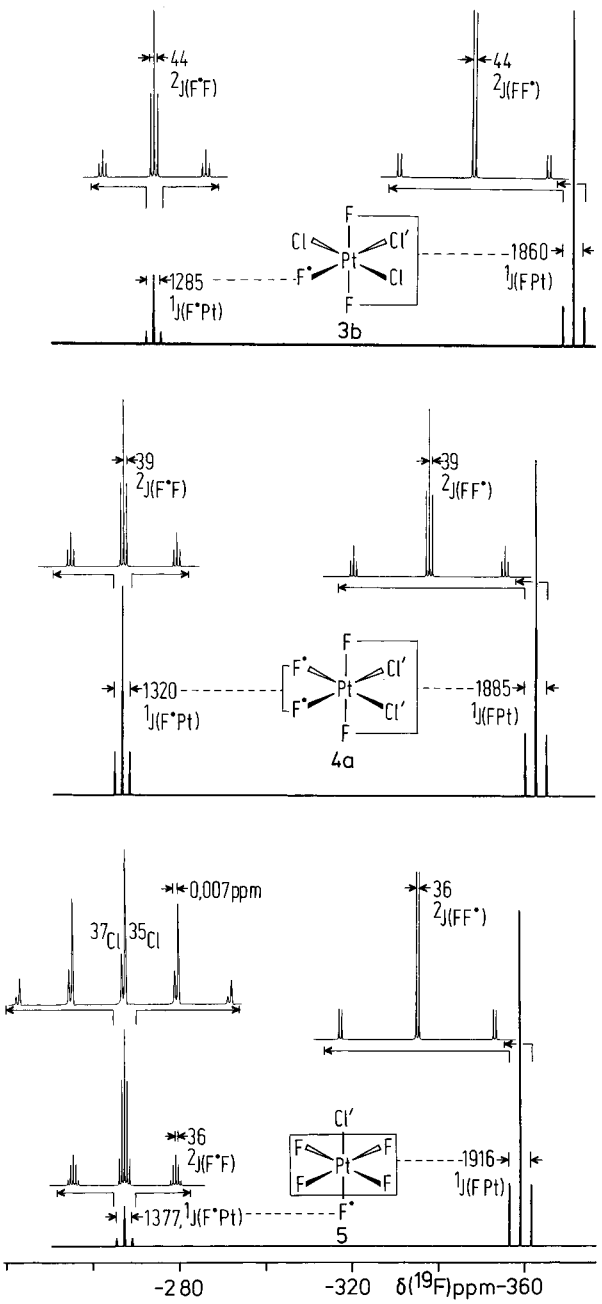

Figure 33. ^{19}F NMR spectra of *mer*-$(PPN)_2[PtF_3Cl_3]$, *cis*-$(PPN)_2[PtF_4Cl_2]$, and $(PPN)_2[PtF_5Cl]$ with highly resolved multiplets due to ^1J(FPt) and ^2J(F•F) couplings.

are attached to the central atom by two different donor atoms or even by two chemically inequivalent atoms of the same kind.[288] This isomerism was discovered by S. M. Jørgensen on the nitro/nitrito pair, $[Co(NH_3)_5(NO_2)]SO_4$ and $[Co(NH_3)_5(ONO)]SO_4$, at the end of the last century,[289] and long remained the only example of its kind. Then, in 1964, $[Pd(AsPh_3)_2(SCN)_2]$ and [Pd(bipy)$(SCN)_2$] were isolated in addition to the already known N-bonded species, $[Pd(AsPh_3)_2(NCS)_2]$ and [Pd(bipy)$(NCS)_2$].[290,291] With these two more pairs of linkage isomers a renewed sense of enthusiasm was brought into this area of research. The results have been summarized in several reviews with many examples of further ambidentate ligands.[288,292−295]

The thiocyanate ion is the most common and most comprehensively investigated ambidentate ligand,

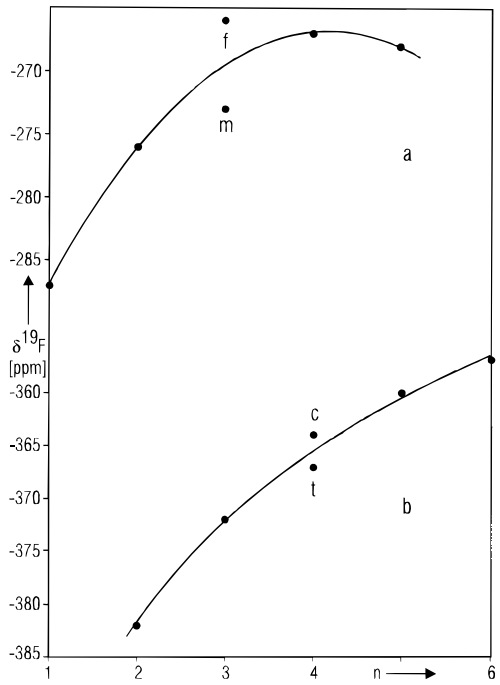

Figure 34. Plot of $\delta(^{19}F)$ vs n in the series $(PPN)_2[PtF_nCl_{6-n}]$, $n = 1-6$, with the resonances of F•−Pt−Cl′ axes (a) and of F−Pt−F axes (b).

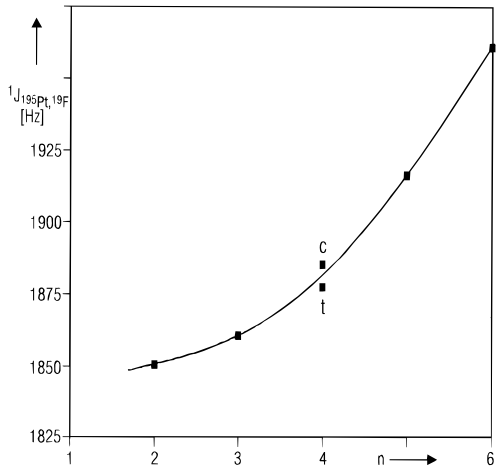

Figure 35. Plot of the $^1J(^{195}Pt,^{19}F)$ coupling constants of F−Pt−F axes vs n in the series $(PPN)_2[PtF_nCl_{6-n}]$.

because it is easily available, stable, and exhibits an especially decided ambidentate behavior. Referring to Ahrland, Chatt, and Davies,[296] or according to Pearson's concept of hard and soft acids and bases (HSAB),[297] the ambidentate thiocyanate ion should coordinate to hard Lewis acids with its N atom as a hard Lewis base and to soft Lewis acids with its S atom as a soft Lewis base. In this manner, it may serve as a probe for the classification of the Lewis acid character of the central atoms, especially if no other ligands participate in the coordination sphere, since these may influence the bonding of the thiocyanate by electronic effects like the symbiotic[298] or antisymbiotic[299] effect or by steric effects.[300]

The electronic structure of thiocyanate, with extensive delocalization of the 16 outer electrons, is exemplified by the following three resonance forms. The percentages indicate the states of the free ion

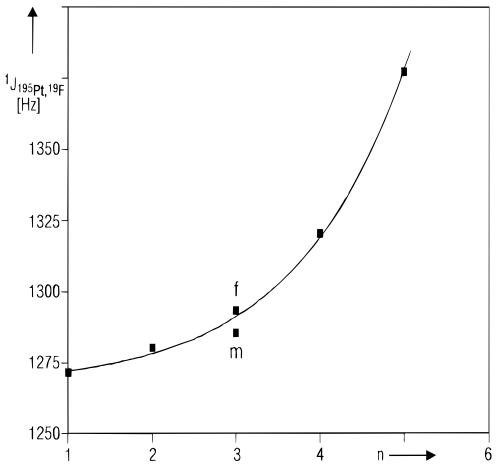

Figure 36. Plot of the $^1J(^{195}Pt,^{19}F)$ coupling constants of F•−Pt−Cl′ axes vs n in the series $(PPN)_2[PtF_nCl_{6-n}]$.

that are primarily involved:

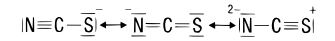

I	II	III
76%	5%	19%[301]
71%	12%	17%[302]

For the thiocyanate complexes, it has generally been found by X-ray structure determinations[141,295,303,304] that linear or almost linear M−N−C−S arrangements are typical for N coordination, while bent M−S−C−N arrangements, with a M−S−C angle around 105°, are common with S coordination. The three thiocyanate atoms form angles between 160° and 180°, and in most cases are very near to 180°. It is generally agreed that S coordination occurs via σ and π donation, while opinions vary for the mode of N bonding from pure σ donation[305] to a combination of σ donation along with π acceptance.[306,307] For a visualization of the bonding relations in metal complexes we refer to resonance structures,[306] which are given for S coordination mainly by

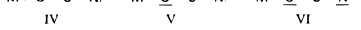

IV V VI

Preferentially, forms IV and V are the predominant mesomers. Thus, in vibrational spectroscopy, a shift to higher wavenumbers for the CN stretching vibration and a shift to lower wavenumbers for the CS stretching vibration, in comparison to the free thiocyanate ion, are expected and observed indeed.[85,306]

In case of N coordination, the following resonance structures must be considered:

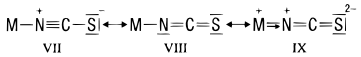

VII VIII IX

The predominance of the forms VIII and IX is responsible for a decrease in wavenumbers of the CN and an increase of the CS stretching vibration with respect to the free ion. As indicated by the above resonance structures, in particular by forms IV and IX, electron density is distributed to the central atom in the case of S coordination and to the complex periphery in the case of N coordination. These properties manifest themselves and can be observed

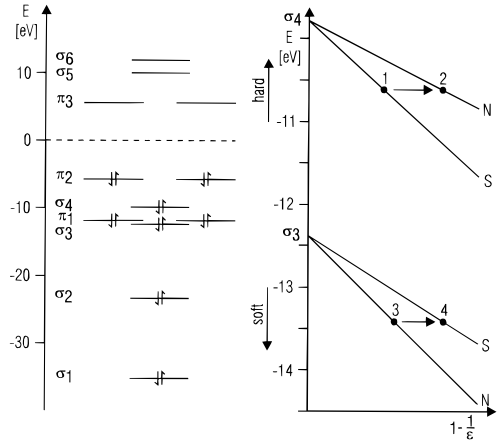

Figure 37. Molecular orbital diagram for the SCN^- ion (left) and the hardness and softness of the orbitals σ^3 and σ^4 on the N and the S atom of the SCN^- ion in dependence of the dielectricity constant ϵ of the solvent.

by the separability of the different species by means of ionophoresis or ion exchange chromatography and by significant ^{15}N NMR shifts. A more sophisticated description of the electronic ground state of the thiocyanate ion has been given by a SCF-LCAO calculation,[308] (see Figure 37), and an interesting approach to the chemical reactivity of the thiocyanate, depending on the dielectric constant of the solvent,[294,309] has been made on the basis of a many-electron perturbation calculation.[310] As a result, the view of the thiocyanate ion as a hard base with its N atom and as a soft base with its S atom is too simplified. Actually, the N atom is the hardest as well as the softest donor, while the S atom is intermediate in terms of hardness and softness (see Figure 37).

B. Preparation and Separation

An inspection of the empirical material shows that four groups of determining factors are responsible for the appearance of linkage isomers: (i) the electronic properties of the ambidentate ligand; (ii) the properties of the central atom; (iii) the steric demands and electronic properties of other ligands;[311,312] (iv) secondary effects caused by the phase, solid or liquid, in solution or melts,[312,313] by the properties of the solvent,[294,314−320] by counterions,[321−323] and by the environmental conditions, such as temperature[321,322] and pressure.[324]

The separation of these factors is by no means trivial, and in many cases it is impossible. In particular, the secondary effects are decisive for isomerization reactions if the primary effects (i−iii) are balanced in such a manner that a stable complex with a distinct coordination sphere and a defined bonding mode of the ambidentate ligand is fixed.

Generally, thiocyanato complexes are prepared from metal halides, mostly chlorides, or halogeno complexes by reaction with SCN^- ions in solution or melts. Besides mere substitution processes, in some cases the central atom is reduced by SCN^-. This reduction can be the initial step or occur at the same time as substitution proceeds, resulting in mixed-halogenothiocyanato complexes, which may be linkage isomers.[282] Usually the SCN^- ion is utilized as a salt with Na^+, K^+ or $(NH_4)^+$ or as HSCN in aqueous solution. Oxidative ligand exchange of I or Br by $(SCN)_2$ in organic solvents, preferably dichloromethane, have been performed on mixed-hexahalogeno metalates in the case of Os(IV)[170,171,325] and Re(IV)[326−328], resulting in mixed-halogenothiocyanato linkage isomers. The addition of SCN^- to Pt(II) during electrochemical oxidation[329] and oxidative addition by $(SCN)_2$ to bis(malonato)platinate(II), $[Pt(mal)_2]^{2-}$,[330] exclusively forms S-bonded octahedral mixed-thiocyanate species.

At the borderline of the hard and soft acids, the preparation of pure individual species is only marginally feasible. Normally, mixtures of linkage isomers of the type, $[M(NCS)_n(SCN)_{6-n}]^{z-}$, $n = 0-6$, are obtained. As an example of this, high-voltage paper ionophoresis proved at a very early date that the postulated $[Os(NCS)_6]^{3-}$ [293,331] and $[Ru(NCS)_6]^{3-}$ [293,331,332] are actually mixtures of linkage isomers. In the case of Ru, linkage isomerism has been supposed on the basis of ^{14}C tracer experiments and vibrational spectroscopy. However, the reported pure *trans*-$[Ru(NCS)_4(SCN)_2]^{3-}$ [333,334] actually has been a mixture of linkage isomers.[293,331,332] Because reactions in solution did not yield complete series of the type, $[M(NCS)_n(SCN)_{6-n}]^{z-}$, $n = 0-6$, isomerization reactions in the solid state have been investigated. On tempering of TBA or PPN salts of pure compounds as well as of mixtures of those systems, stepwise rearrangements occur, which result in an increasing amount of complexes with increased numbers of N-bonded thiocyanate ligands. Thus, the respective terminal members of the series are accessible; namely, for Ru $n = 5$ (TBA salt), $n = 6$ (PPN salt); Rh $n = 4$; Os $n = 6$; and for Ir $n = 5$.[278−284] Clearly, it is important to temper below the melting point, not only to limit decomposition, which can occur at elevated temperatures, but also because mixtures of $[M(NCS)_n(SCN)_{6-n}]^{3-}$ with lower values of n are rearranged or thiocyanate bridged dinuclear complexes are formed during melting.[335]

Very efficient methods are required for separation of the extremely similar linkage isomers, and even more for their stereoisomers. Suitable techniques for ionic species are ionophoresis as a basic analytical tool[277,278] and DEAE ion exchange column chromatography for larger scale preparations of pure compounds. Through this, the series, $[M(NCS)_n(SCN)_{6-n}]^{3-}$, M = Ru, $n = 1-5$;[74,277,280,283] Rh, $n = 0-4$;[281,286] Os, $n = 0-6$;[277−279,284,285] Ir, $n = 0-5$,[282] have been separated into the individual linkage isomers, or in some cases, into highly enriched stereoisomers.[278,279,284,285]

The reciprocal behavior of the mixed $[M(NCS)_n(SCN)_{6-n}]^{3-}$ complexes during separation by high-voltage paper ionophoresis and by ion exchange chromatography,[278] as well as the extreme differences between the migration velocities[277,278] and retention times[74,278−285] of the individual species, are attributable to the different electron densities according to the resonance structures IV−IX (see Table 20). Therefore, linkage isomers with increasing number of N-bonded ligands and high electron density at the complex periphery must migrate faster in the electric field during ionophoresis and interact more strongly

Table 20. Characteristics of the System $[Os(NCS)_n(SCN)_{6-n}]^{3-}$ [a]

n	color	mb	DEAE[b]	EF[c]
0	raspberry-red	220−225	83	decomp.
1	red	200−205	53	29.5
2	red-orange	175−180	28	33.0
3	orange	155−160	12	35.0
4	yellow-orange	160−165	4.6	36.0
5	yellow	175−177	1.7	37.0
6	bright yellow	185(sharp)	0.5	37.2

[a] Colors and melting behavior (mb) (°C) of TBA salts, migration distance on DEAE anion exchanger (cm), and in an electric field (EF) during high voltage paper ionophoresis (cm). [b] At −3 °C and a flow rate of 100 mL/h 1.5 N aqueous KSCN. [c] At 0 °C, special paper impregnated with 0.2 M KH_2HPO_4 and electric field of 50 V/cm.

Table 21. Half-Wave Potentials $E_{1/2}$ (mV), Anodic−Cathodic Peak Potential Difference ΔE (mV), and Peak Current Ratio of Oxidation and Reduction Step i_{ox}/i_{red} for the Linkage Isomers $[Os(NCS)_n(SCN)_{6-n}]^{m-}$, $n = 0-6$, $m = 2, 3, 4$, and Colors of $(TBA)_2[Os(NCS)_n(SCN)_{6-n}]$

	Os^{II}/Os^{III}			Os^{III}/Os^{IV}			
n[a]	$E_{1/2}$[b]	ΔE	i_{ox}/i_{red}[c]	$E_{1/2}$[b]	ΔE	i_{ox}/i_{red}	Os^{IV} color
0	−1144	162	≪1	+ 378	80	≈1	turquoise
1	−1072	144	↓	+ 380	72	≈1	deep blue
2a	−1022	119	↓	+ 399	60	≈1	violet-blue
2b	−1038	129	↓	+ 343	75	≈1	blue-violet
3a	−972	147	↓	+ 422	60	≈1	blue-violet
3b	−981	127	↓	+ 379	59	≈1	blue-violet
4a	−921	120	↓	+ 415	59	≈1	blue-violet
4b	−925	119	↓	+ 395	65	≈1	blue-violet
5	−869	109	↓	+ 432	71	≈1	blue-violet
6	−817	94	1	+ 450	71	≈1	blue-violet

[a] a corresponds to *cis/fac*; b corresponds to *trans/mer*. [b] At 293 K, Pt-bead working electrode, Pt-rod auxiliary electrode, Ag/AgCl/$LiCl_{sat}$ in EtOH reference electrode (E^0 = 143 mV), dU/dt = 100 mV/s, electrolyte 0.1 N (TBA)ClO_4 in CH_2Cl_2. Under the same conditions the ferrocene/ferrocenium couple has $E_{1/2}$ = 515 mV. [c] i_{ox}/i_{red} increases from ≪1 to 1.

with the stationary phase during ion exchange, and thus are eluted slower. In addition to the effect of charge dislocation, different degrees of protonation and/or hydration should be considered.

This migration behavior is quite different from that of the mixed-hexahalogeno complexes described in section II.A.5, which migrate in a similar manner during ionophoresis and ion exchange chromatography.[11,67,336,337] Further support for the discussed charge dislocation is given from the characteristic redox behavior of the individual species and the extreme differences within the pairs of stereoisomers (see Table 21). This can easily be explained by optimal synergetic enforcement of S σ and π donation and mutual N π acceptance in the asymmetric SCN−M−SCN arrangement compared to the symmetric axes, SCN−M−NCS or NCS−M−SCN (see resonance structures VI and IX).

C. Characterization

Although, common methods of characterization have been applied to linkage isomers, further discussion is required because of the special properties of these compounds in comparison with the simple mixed-halogeno metalates. Most frequently, single-crystal X-ray structure determination, UV−vis, IR, Raman, and NMR spectroscopy are used. However, due to the great similarities between these compounds, all of the other techniques, except NMR spectroscopy, require pure substances. These similarities result in electronic and vibrational spectra which are so closely related for the members of a series that these techniques must lead to invalid conclusions, if they are applied to mixtures. This is true with regard to both the bonding mode of the ambidentate ligand, as well as any systematic trends pertaining to the number n in $[M(NCS)_n(SCN)_{6-n}]^{z-}$ systems. Nevertheless, if separation into pure individual species is accomplished, as in the case of the series, $[M(NCS)_n(SCN)_{6-n}]^{3-}$, M = Ru, n = 1−5;[74,277,280,283] Rh, n = 0−4;[281,286] Os, n = 0−6;[277−279,284,285] and Ir, n = 0−5,[282] a definitive and consistent characterization by vibrational (IR and Raman) and electronic spectroscopy is possible. For the two series, $[Os(NCS)_n(SCN)_{6-n}]^{3-/2-}$, n = 0−6, the electrochemical reversibility of all 20 different individual complex ions has been studied by cyclic voltammetry.[285] Furthermore, the correct assignment in the system, $[Os(NCS)_n(SCN)_{6-n}]^{3-}$, has been verified by an extended X-ray absorption fine structure (EXAFS) investigation on samples of the pure linkage isomers.[338] Although single-crystal X-ray structure analysis is considered to provide the ultimate characterization, special considerations must be given to the fact that the crystal selected from a mixture may not be representative of the species being examined. Furthermore, the bonding mode may be influenced by the solid phase, and if the species is isolated as a salt, by the kind of counterions used. Finally the bonding mode may not only be different in solution, but also solvent dependent.

The final conclusion for these systems is that no single analytical method can provide confirmation of a species, identity and structure. For example, a high-voltage paper ionopherogram of the reaction products of $K_3[RhCl_6]$ with aqueous KSCN, obtained in 1 h, may be more informative than the X-ray structure of $K_3[Rh(SCN)_6]$, since the single crystal measured may be the primary component of the precipitate only because it forms crystals more easily than other species. Another astonishing example of this type of confusion can be found on the X-ray photoelectron spectroscopy of $[Os(SCN)_6]^{3-}$, in which a 6-fold S-coordinated complex is postulated,[339] although the cited reaction of $K_2[OsCl_6]$ with aqueous KSCN does not yield this species, not even in trace amounts.[284,285]

As already mentioned, NMR spectroscopy on solutions and on solids[340] is very efficient for the elucidation of mixtures of diamagnetic and, with restrictions, of weakly paramagnetic complexes.[341] Suitable nuclei are NMR active metals like ^{59}Co, ^{93}Nb, ^{103}Rh and ^{195}Pt and ligand atoms like ^{15}N, ^{77}Se, and ^{13}C.[342,343] However, incomplete or ambiguous results are obtained, if NMR spectroscopy on less sensitive nuclei like ^{103}Rh or ^{13}C is performed with insufficient number of scans or pulse repetition times.

Well-established evidence of mixed complexes, $[Nb(NCS)_n(SCN)_{6-n}]^-$, n = 0, 2, 4, 5, 6, including the *cis/trans* isomers for n = 2 and the *trans* isomer for n = 4, has been given by ^{93}Nb NMR spectroscopy in

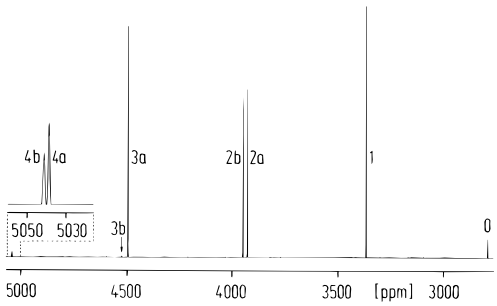

Figure 38. ^{103}Rh NMR spectrum of a mixture of the linkage isomers $(TBA)_3[Rh(NCS)_n(SCN)_{6-n}]$, $n = 0-4$ (a corresponds to *cis*/*fac*; b corresponds to *trans*/*mer*) in CD_2Cl_2 at 243 K.

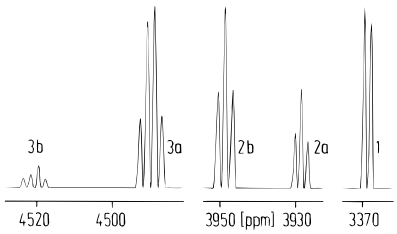

Figure 39. ^{103}Rh NMR spectra of the ^{15}N-labeled separated species, $(TBA)_3[Rh(^{15}NCS)_n(SC^{15}N)_{6-n}]$, $n = 1-3$ (a corresponds to *cis*/*fac*; b corresponds to *trans*/*mer*) in CD_2Cl_2 at 243 K.

combination with the pairwise additivity method.[246] An exemplary case of improper substance characterization is the history of the long-known $[Rh(SCN)_6]^{3-}$,[293,294,331,344,345] which has been considered until recently[260] as a purely S-bonded species. The X-ray structure determination on its K salt[346] has been quoted as proof of this assumption. And, although the 6-fold S-bonded species is the main product of the reaction of $RhCl_3$ or $K_3[RhCl_6]$ with SCN^- in aqueous solution under moderate temperature conditions (60 °C) and short reaction times, it is not possible to carry out the reaction in such a manner that only $[Rh(SCN)_6]^{3-}$ is formed. In every case, mixed $[Rh(NCS)_n(SCN)_{6-n}]^{3-}$ or $[RhCl_n(SCN)_{6-n}]^{3-}$ are present as byproducts.[281,286] A very impressive example for the efficiency of a meaningful combination of several methods is given for the system $[Rh(NCS)_n(SCN)_{6-n}]^{3-}$, which is known for $n = 0-4$, including the three pairs of stereoisomers. Additionally, this series has been prepared in the ^{15}N-labeled form. After separation by DEAE ion exchange chromatography, all species have been characterized unequivocally by ^{103}Rh (Figures 38 and 39) and ^{15}N (Figure 40) NMR spectroscopy utilizing characteristic shifts and couplings (Table 22). Furthermore, a single-crystal structure reinvestigation of $[Rh(SCN)_6]^{3-}$ in form of its tetraphenylphosphonium salt has been performed.[347]

Special attention should be drawn to the unsurpassed sensivity of ^{15}N NMR spectroscopy to the slightest changes in the electronic environment of this nucleus. In Figure 40 this can be seen in the clear separation of resonance ranges from −134 to −141 ppm for S-bonded thiocyanate, from −261 to −271 ppm for N-bonded thiocyanate in S−Rh−N arrangements, and from −292 to −297 ppm for N-bonded thiocyanate in N−Rh−N arrangements.

Table 22. Chemical Shifts $\delta(^{103}Rh)$ at 243 ± 1 K vs $\Xi(^{103}Rh) = 3.16$ MHz and $\delta(^{15}N)$ at 297 ± 1 K vs $\delta(^{15}N)$ (CH_3NO_2 neat) = 0 (ppm), Coupling Constants $^1J(^{103}Rh,^{15}N)$, $^1J(^{15}N,^{103}Rh)$, and $^3J(^{15}N,^{103}Rh)$ (Hz) of the Series $(TBA)_3[Rh(NCS)_n(SCN)_{6-n}]$, $n = 0-4$, in CD_2Cl_2

species	$\delta(^{103}Rh)$	$\Delta\delta(^{103}Rh)$	$^1J_{RhN}$	$\delta(^{15}N)(S)$ (**S**−Rh−**S**)	$\delta(^{15}N)(S)$ (**S**−Rh−N)	$\delta(^{15}N)(N)$ (**S**−Rh−**N**)	$\delta(^{15}N)(N)$ (**N**−Rh−**N**)	$^1J_{NRh}$ (**S**−Rh−**N**)	$^1J_{NRh}$ (**N**−Rh−**N**)	$^3J_{NRh}$ (**S**−Rh−**S**)	$^3J_{NRh}$ (**S**−Rh−N)
$[Rh(SCN)_6]^{3-}$	2791			−139.987						0.77	
				−140.006							
		538									
$[Rh(NCS)(SCN)_5]^{3-}$	3374		22.9	−138.712	−139.745	−270.248		21.9			
						−270.787					
		559									
cis-$[Rh(NCS)_2(SCN)_4]^{3-}$	3933		21.7	−137.453	−138.262	−269.901		21.6		0.72	0.79
				−137.471	−138.281	−270.433					
		21									
trans-$[Rh(NCS)_2(SCN)_4]^{3-}$	3954		25.1	−137.413			−293.017		24.8		
							−293.622				
		542									
fac-$[Rh(NCS)_3(SCN)_3]^{3-}$	4496		22.9		−136.265	−269.665		20.8			0.55
					−136.277	−270.177					
		30									
mer-$[Rh(NCS)_3(SCN)_3]^{3-}$	4526			−136.667	−136.843	−269.754	−293.840	20.9	24.2	0.63	0.82
				−136.683	−136.863	−270.270	−294.438				
		512									
cis-$[Rh(NCS)_4(SCN)_2]^{3-}$	5038				−135.037	−270.038	−295.441	20.0	23.9		
						−270.531	−296.031				
		4									
trans-$[Rh(NCS)_4(SCN)_2]^{3-}$	5042			−134.789			−295.044		23.8		
							−295.631				

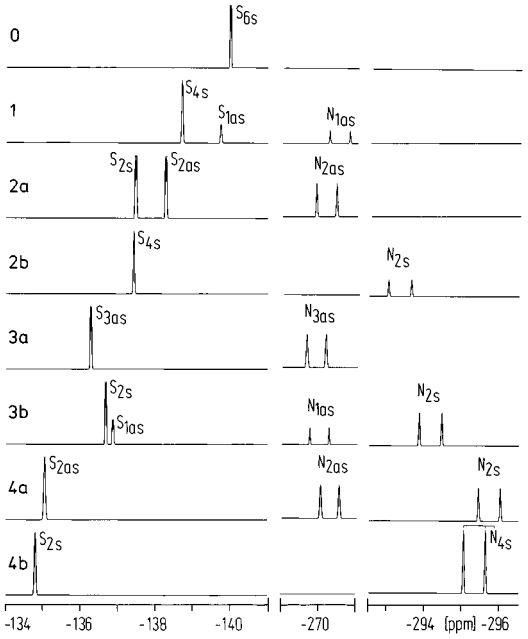

Figure 40. ^{15}N NMR spectra of the series $(TBA)_3[Rh(^{15}NCS)_n(SC^{15}N)_{6-n}]$, $n = 0-4$ (a corresponds to *cis*/*fac*; b corresponds to *trans*/*mer*) in CD_2Cl_2 at 297 K referenced to $\delta(^{15}N)$ (CH_3NO_2) neat = 0 ppm. N_i and S_i denote Rh−N respectively Rh−S bonds in symmetric (s) or asymmetric (as) axes.

From the available mixed systems, $[M(SCN)_n(NCS)_{6-n}]^{z-}$, the following series of increasing hardness in the borderline range of hard and soft acids is derived: $Rh^{3+} < Ir^{3+} \ll Ru^{3+} < Nb^{5+} \approx Os^{3+} < Os^{4+}$. The influence of the nephelauxetic ratio of the ligands on the metal shift by explicit incorporation of this parameter into the Ramsey equation[348] explains the increased shielding of a central nucleus with decreasing electronegativity and increasing polarizability of the ligands according to the series, F > Cl > NCS > Br > SCN > I, and thereby NHD, NED, and NPD. The optical electronegativities of NCS ≈ 2.8 and SCN ≈ 2.6 have been approximated from electronic spectra of mixed linkage isomers of halogenothiocyanatoosmates(IV).[170,171] On this basis, a not unexpected, but interesting result arises from a comparison of the metal shifts in the two series, $[M(NCS)_n(SCN)_{6-n}]^{z-}$, with M = ^{93}Nb and ^{103}Rh. In full confidence of the correct assignment in the Nb system, a ^{93}Nb high-field shift from $[Nb(SCN)_6]^-$ at −780 ppm to $[Nb(NCS)_6]^-$ at −1342 ppm is observed,[246] while ^{103}-Rh of $[Rh(SCN)_6]^{3-}$ resonates at highest field with a downfield shift as the number of N-bonded ligands increases.[286] With respect to electronegativity and polarizability, ^{93}Nb exhibits inverse behavior in agreement with its already discussed IHD, while ^{103}-Rh exhibits NED and NPD in agreement with its already discussed NHD (compare with section II.D.3).

IV. Mixed Octahedral Clusters

A. General Comments

Originally, clusters were defined as compounds "containing a finite group of metal atoms that are held together entirely, mainly, or at least to a significant extent, by bonds between the metal atoms, even though some non-metal atoms may be associated intimately with the cluster".[349] Generally, however, the term cluster can be applied to compounds where other atoms like nonmetals as boron or phosphorus are held together by direct bonds. Similar to the classic Wernerian one-center coordination compounds, the chemistry of these multicenter, non-Wernerian coordination compounds[350] has grown and become another area of extensive research.

For example, the chemistry of molybdenum dihalides started as early as 1826, when MoI_2 was mentioned,[351] followed by investigations on $MoCl_2$ and $MoBr_2$.[352,353] Further progress with respect to analytical and structural aspects was made until the early 1900s,[354−360] and then by establishing wet-chemistry techniques for these compounds[361−364] and an extension to the tantalum congeners.[365−367] Pioneering X-ray investigations[368−371] revealed as a common structural feature octahedral groups of metal atoms with short metal−metal distances—even shorter than in the metals themselves. The two building principles of an octahedral metal core surrounded by an inner ligand sphere X^i and an outer ligand sphere Y^a, as in $[(M_6X^i_{12})Y^a_6]^{4-}$ for M = Nb, Ta, and in $[(M_6X^i_8)Y^a_6]^{2-}$, X = halide, Y = or ≠ X, and M = Mo, W, are presented by Figure 1c,d.

The family of compounds derived by chemical modification of these species led to numerous publications in this field[372−394] and the discovery of other cluster compounds composed of other cluster building elements with ligands other than the halides.[395−401] An important inspiration for this was the discovery of strong metal−metal bonds by Cotton in the early 1960s,[350] especially with respect to bonding theory and numerical calculations of the electronic structures.[402−416] Not only because of the aesthetic nature of these structures and the interesting chemistry of these compounds, but also due to their importance in the field of photochemistry,[417−422] and even more so, their strong potential in catalysis,[423−426] this area is of high actuality. Because a plethora of these compounds is known, the ensuing discussion will be limited to spectroscopic investigations of octahedral clusters with mixed-halide coordination spheres or mixed-metal cages.

B. Preparation and Separation

The metal halide clusters are almost always prepared at high temperatures in heterogeneous solid-state reactions or in melts, so that there is little doubt that the products are thermodynamically favored and stable phases. Starting materials are the metal pentahalides or hexahalides, which are reacted with the respective metals or are reduced by other metals, e.g. Al in salt melts. By these synthetic techniques, mixed-metal cages and mixed inner ligand spheres may be obtained from appropriate mixtures of the educts. The considerable stability of the inner ligand sphere is reflected by the inability to prepare pure $[(Mo_6Br^i_8)Br_4]$ by the reaction of $[(Mo_6Cl^i_8)Cl_4]$ with LiBr.[427] Although there has been no evidence for byproducts from analytical and vibrational spectroscopic data, ^{19}F NMR spectroscopy has clearly indicated the existence of mixed species, $[(Mo_6\{Br^i_nCl^i_{8-n}\})F^a_6]^{2-}$, at least with $n = 6$ and 7.[427, 428] The more labile outer ligand sphere, Y^a_6, may be

mixed by common ligand exchange reactions, or by ligand redistribution between two respective terminal members (see section IV.C).

The mixed *closo*-hexahalogenohexaborates, $[B_6X_nY_{6-n}]^{2-}$, $n = 0-6$, X ≠ Y = Cl, Br, I,[429] have been prepared by treatment of partially halogenated hydrohexaborates, $[B_6H_nX_{6-n}]^{2-}$,[430-432] with a second halogen, followed by separation of the obtained mixtures by means of anion exchange on DEAE cellulose, or more conveniently, by reaction of the respective *N*-halogenosuccinimides with individual halogenohydrohexaborates, $[B_6H_nX_{6-n}]^{2-}$, obtained by preceding DEAE anion exchange chromatography. The compounds have been characterized by ^{11}B NMR spectroscopy.[429]

Three additional examples for the separation of mixed-metal clusters have also been reported. The first one, composed of Ta and Mo, has used the different properties and possible oxidation states of the group 5 and group 6 metals, and is given by the three individual species, $(TEA)_3[(\{Ta_5Mo\}Cl^i_{12})Cl^a_6]$, $(TEA)_2[(\{Ta_4Mo_2\}Cl^i_{12})Cl^a_6]$, and $(TBA)_2[(\{Ta_5Mo\}Cl^i_{12})Cl^a_6]$, which fortunately are separable on the basis of their different formal charges by means of ion exchange of aqueous/ethanolic solutions on Dowex in H^+ form.[433] These compounds have been characterized by their Gauss deconvoluted far infrared and UV spectra, and by Faraday measurements of their magnetic susceptibilities. Their properties have been discussed in context with their archetypes, $[(Ta_6Cl^i_{12})Cl^a_6]^{4-}$ and $[(Ta_6Cl^i_{12})Cl^a_6]^{3-}$, respectively. Again, inspection of the complex spectra emphasizes that these methods are useful only in the case of pure individual species, and are useless for analysis of multicomponent mixtures. The second example, $[(\{Nb_nTa_{6-n}\}Cl^i_{12})F^a_6]^{4-}$, $n = 0-6$, exhibits the highest degree of enrichment for the seven individual complexes, with the exception of the stereoisomers. This has been achieved by repeated UV-monitored ion exchange chromatography on DEAE cellulose and final energy dispersive X-ray microanalysis.[434] The third approach utilizes counterflow distribution over 550 steps of a statistical mixture of **[(**$Mo_6\{Cl^i_nI^i_{8-n}\})Cl^a_4$], and yields the individual species with $n = 5-7$; although the geometric isomers for $n = 5$ and 6 have not been separable.[435]

C. Spectroscopic Characterization

Generally, preparations of clusters aiming at species with defined mixed building units are rather improbable, and separations are very difficult or impossible. Nevertheless, there are some examples of clusters with defined mixed outer ligand spheres, which have been characterized by single-crystal X-ray structure analyses like the tetraphenylarsonium salts of *trans*-$[(Mo_6Cl^i_8)Cl^a_4Br^a_2]^{2-}$,[392] *trans*-$[(Mo_6Cl^i_8)Cl^a_4(PR_3)^a_2]$, R = *n*-$C_3H_7$, *n*-$C_4H_9$, *n*-$C_5H_{11}$, including ^{31}P NMR data,[436] *trans*-$[(Mo_6Cl^i_8)Cl^a_4(OR)^a_2]^{2-}$ R = CH_3, $CH_2C_{14}H_9$[437] and *cis*-$[(Mo_6Cl^i_8)Cl^a_4\{P(C_2H_5)_3\}^a_2]$ including Raman data.[438] *Cis* phosphine ligation of the outer sphere seems to depend on the phosphorus substituents, R. This most likely accounts for the results of the investigation of the series, $[(Mo_6Cl^i_8)Cl^a_4(PR_3)^a_2]$. With R = *n*-$C_3H_7$ the *cis* form is obtained only as a 3% byproduct of the *trans* form,[436] while for R = $P(C_2H_5)_3$ the *cis* form has been obtained in 97% yield from the reaction of *trans*-$[(Mo_6Cl^i_8)Cl^a_4\{P(n\text{-}C_5H_{11})_3\}^a_2]$ with $P(C_2H_5)_3$ in tetrahydrofuran (THF).[438] Attempts to conclusively define the inner and outer sphere of mixed clusters like the series, $Pb[Mo_6Cl_nBr_{14-n}]$, $n = 0-14$, by X-ray diffraction and IR spectroscopy and to identify species like $Pb[(Mo_6\{Cl^i_3Br^i_5\})Cl^a_3Br^a_3]$[439,440] are less convincing in the light of the following ^{19}F NMR spectroscopic investigations on the $[(Mo_6\{Cl^i_nBr^i_{8-n}\})F^a_6]^{2-}$ series.[428] With the aforementioned difficulties of vibrational and electronic spectroscopy, and the problems of separation in mind, it is clear that there are only a few examples of UV-vis, IR, and Raman investigations on mixed clusters. High enrichment by DEAE anion exchange chromatography of the species, $[(\{Nb_nTa_{6-n}\}Cl^i_{12})F^a_6]^{4-}$, $n = 1-5$, without separation of the stereoisomers, and work on $[(\{Nb_nTa_{6-n}\}Cl^i_{12})Br^a_2]\cdot 8H_2O$,[434] has enabled an IR, Raman, and UV-vis spectroscopic study of these compounds in comparison to the terminal members of these series, $[(Nb_6Cl^i_{12})Br^a_2]\cdot 8H_2O$ and $[(Ta_6Cl^i_{12})Br^a_2]\cdot 8H_2O$.[441]

The series, $[B_6Cl_nBr_{6-n}]^{2-}$, $[B_6Cl_nI_{6-n}]^{2-}$ and $[B_6Br_nI_{6-n}]^{2-}$, $n = 0-6$, have also been separated by means of DEAE cellulose[429] and investigated by IR and Raman spectroscopy.[442] On the basis of the known spectra and force constants of the homoleptic compounds, $[B_6Cl_6]^{2-}$, $[B_6Br_6]^{2-}$, and $[B_6I_6]^{2-}$, [443] normal coordinate analyses reveal force constants between 1.3 and 1.5 mdyne/Å for the B-B bonds of the mixed species.[442] In this context, the *closo*-hexahydrohexaborates may be considered as a special case of a mixed cage as is done for $Cs_2[^{10}B_n{}^{11}B_{6-n}H_6]$.[443-445] By using the vibrational spectra and normal coordinate analysis data of isotopically pure $Cs_2[^{10}B_6H_6]$ and $Cs_2[^{11}B_6H_6]$, the observed spectra of $Cs_2[^{n.a.}B_6H_6]$ (Figure 41) have been accurately reproduced by a statistically weighted superposition of the calculated spectra of the ten isotopomers, $Cs_2[^{10}B_n{}^{11}B_{6-n}H_6]$, $n = 0-6$. The ^{10}B,^{11}B isotopic pattern according $^{n.a.}B$ with 80.22% ^{11}B and 19.78% ^{10}B has been verified by the IR and Raman spectra of $Cs_2[^{10}B_n{}^{11}B_{6-n}I_6]$, $n = 0-6$, analogously.[446]

As already demonstrated for mononuclear octahedral mixed-fluoro complexes, ^{19}F NMR spectroscopy is a very specific, sensitive, and high-resolution method for the elucidation of reactions, the structures of the reaction products and the distribution of the individual species within a series (see section II.D). Therefore the application of this technique to the more complicated mixed hexanuclear metal halide clusters was very obvious, because these systems could not be completely analyzed in previous studies.[393,394,435,447] The respective terminal members of possible series, $[(M_6X^i_{12})Y^a_4]$ or $[(M_6X^i_{12})Y^a_6]^{4-}$ and $[(M_6X^i_8)Y^a_4]$ or $[(M_6X^i_8)Y^a_6]^{2-}$, Y = X or Y ≠ X, have been studied extensively by X-ray structure analyses[372-379] and by electronic and vibrational spectroscopy.[448,449] Apart from the condition Y ≠ X, the three cluster units of $[(M_6X^i_8)Y^a_6]^{2-}$ are known from Mo and W (see Figure 1c) and present three opportunities for systematic variations. Firstly, the outer octahedral coordination sphere Y^a_6 can be a mix of two ligands, which results in 10 species, where, preferentially, one

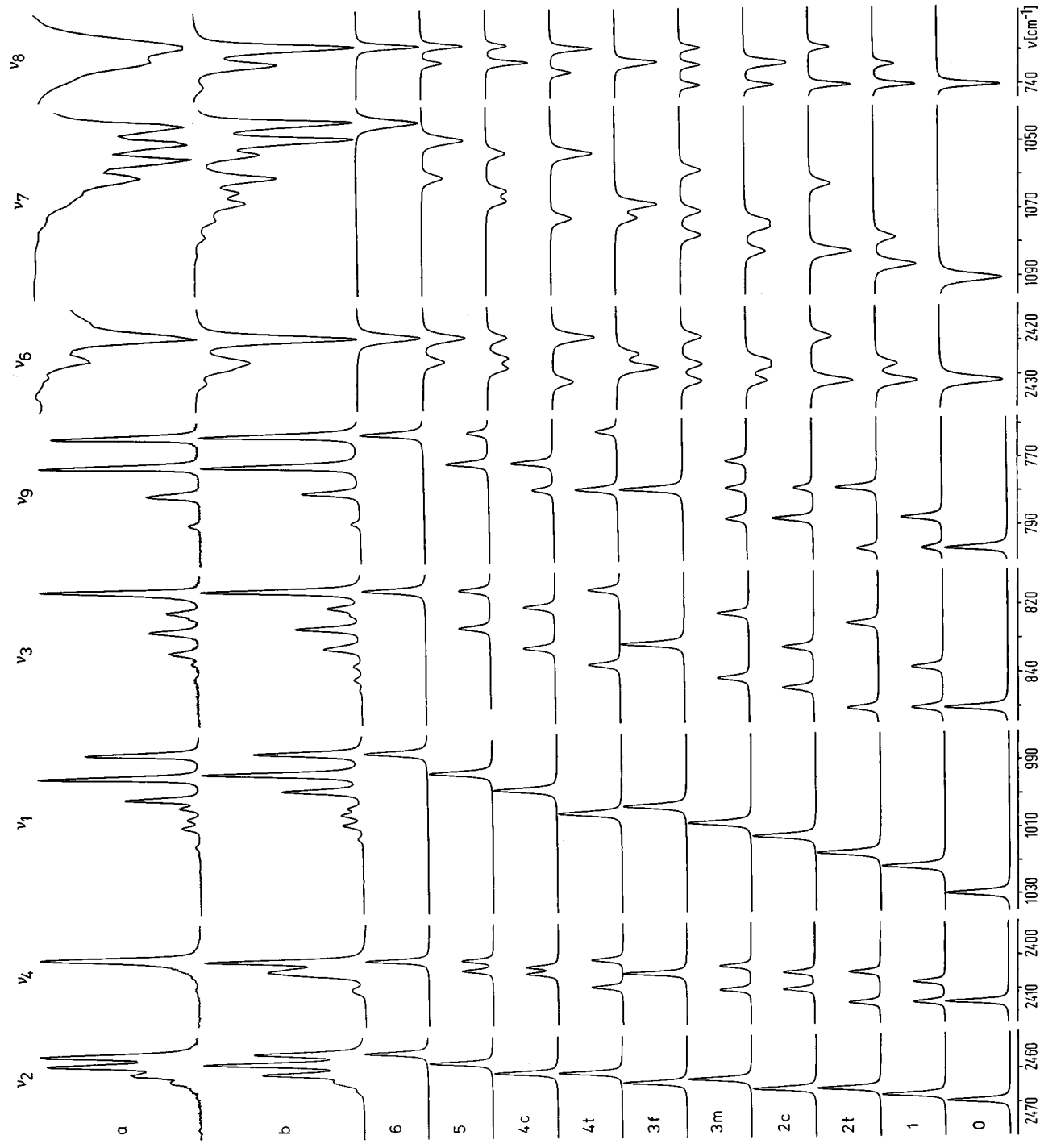

Figure 41. Comparison of the observed highly resolved Raman and IR spectra (10 K) of $Cs_2[^{n.a.}B_6H_6]$ (a) with the superposition (b) of the calculated spectra of the isotopomers $Cs_2[^{11}B_n{}^{10}B_{6-n}H_6]$, $n = 0-6$.

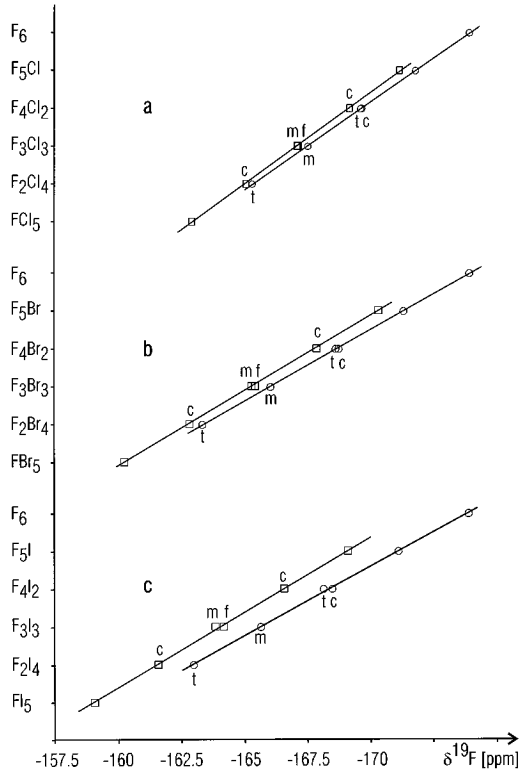

Figure 42. Plot of $\delta(^{19}F)$ vs the number of F atoms in the outer-sphere mixed cluster series $(TBA)_2[(Mo_6Cl^i_8)(F^a_nCl^a_{6-n})]$ (a), $(TBA)_2[(Mo_6Cl^i_8)(F^a_nBr^a_{6-n})]$ (b), and $(TBA)_2[(Mo_6Cl^i_8)F^a_nI^a_{6-n})]$ (c).

of the outer sphere ligands is F to allow for ^{19}F NMR spectroscopy. Secondly, the cube of the inner coordination sphere X^i_8 can be a mix of two halides, which results in 22 species and can be studied via ^{19}F NMR of the six F atoms in the outer sphere. Finally, the octahedral metal core M_6 may be a mix of two metals, which results in 10 species, and can also be studied by means of ^{19}F NMR if the outer sphere is F^a_6.

For the sake of clarity only one building unit has been varied at a time, while the two other remained unaltered; simultaneous mixing of all three building units in the manner, $[(\{Mo_nW_{6-n}\}\{X^i_mX'^i_{8-m}\})Y^a_pY'^a_{6-p}]^{2-}$, $n,p = 0-6$, $m = 0-8$, with the preparative feasible halides, X^i, X'^i = Cl, Br, I, and Y^a, Y'^a = F, Cl, Br, I, would result in 6570 individual cluster ions.

By intermolecular ligand exchange in solution between $(TBA)_2[(Mo_6Cl^i_8)F^a_6]$ and $(TBA)_2[(Mo_6Cl^i_8)Y^a_6]$, Y = Cl, Br, I, the complete three series, $(TBA)_2[(Mo_6Cl^i_8)F^a_nY^a_{6-n}]$, $n = 0-6$, including the three pairs of stereoisomers, have been obtained.[450] Besides the unequivocal characterization of the individual species, equilibration within the systems has been determined by time-dependent quantitative ^{19}F NMR spectroscopy. Interestingly, as in the case of one-center octahedrons, the Dean−Evans relation is valid for these octahedrons with a multicenter in the form of an octahedral metal core (see Figure 42).

Analogous to the *trans* influence, an influence of opposite ligands in the outer octahedron has been found and introduced as the *antipodal* influence in accordance with Hermanek's formulation of an *antipodal* effect on boron clusters.[451] Because this influence acts across the cage instead of along octahedral axes, it is considerably weaker. Starting from the N-bonded thiocyanato derivative, $(TBA)_2[(Mo_6Cl^i_8)(NCS)^a_6]$, which has also been synthesized ^{15}N enriched, the four series, $(TBA)_2[(Mo_6Cl^i_8)(^{15}NCS)^a_nY^a_{6-n}]$, $n = 0-6$, Y^a = F, Cl, Br, I, comprised of 37 individual cluster anions, have been obtained by reaction with $(TBA)_2[(Mo_6Cl^i_8)Y^a_6]$, Y = F, Cl, Br, I, in acetonitrile solution and characterized by ^{15}N as well as by time-dependent ^{19}F NMR spectroscopy. The ^{19}F spectra have been evaluated quantitatively with regard to equilibration, and all spectra have been interpreted with respect to the *antipodal* influence, as well as to the dependence on *n* of the mutual interactions of the outer-sphere ligands.[452] Toward different aims, the compound, $(MeS_4TTF^{\bullet})_2[(Mo_6Cl^i_8)(NCS)^a_6]$, has been isolated with the cation radical methyltetrathiafulvalen. It has been structurally characterized by single-crystal X-ray analysis and, with regard to zero field splitting and mobile Frenkel excitation, investigated by electron spin resonance (ESR) spectroscopy.[453] The following three single clusters are mentioned because of their synthetic utility as starting materials for new derivatives. $(TBA)_2[(Mo_6Cl^i_8)(CF_3COO)^a_6]$ dissolved in CD_2Cl_2 was characterized by its very sharp ^{19}F resonance at −73.38 ppm ($\Delta\nu_{1/2} < 1$ Hz), while $(TBA)CF_3COO$ resonates under the same conditions at −74.46 ppm vs $CFCl_3$.[454] With six labile outer-sphere $(CF_3SO_3)^-$ ligands, $(TBA)_2[(Mo_6Cl^i_8)(CF_3SO_3)^a_6]$ and $(TBA)_2[(Ta_6Cl^i_{12})(CF_3SO_3)^a_6]$ have been fully characterized by X-ray structure, fast-atom bombardment (FAB) mass spectrometry, and UV−vis and IR spectroscopy.[455,456]

The inner-sphere mixed system, $[(Mo_6\{Br^i_nCl^i_{8-n}\})Cl^a_6]^{2-}$, has been prepared by ligand exchange reaction in the solid state and transformed into $(TBA)_2[(Mo_6\{Br^i_nCl^i_{8-n}\})F^a_6]$, $n = 0-8$.[428] The complete series consists of 22 species with 55 ^{19}F resonances theoretically expected, which have been observed in the high resolution 1D-^{19}F NMR spectrum with characteristic homonuclear couplings. By utilization of incremental systematics of the chemical shift, the relative intensities of signals which belong together, and multiplicity analysis, all resonances have been assigned unequivocally and definitively confirmed by the required correlations in the 2D-^{19}F-^{19}F-COSY spectrum. The quantitative evaluation indicates statistical formation of the individual species.[428] In the same manner, the system, $(TBA)_2[(Mo_6\{Cl^i_nI^i_{8-n}\})F^a_6]$, $n = 1-8$, containing 21 individual cluster ions with 54 ^{19}F resonances, has been analyzed by means of 1D- and 2D-^{19}F NMR spectroscopy. The quantitative evaluation reveals significant deviation from statistical distribution with clear preference of I neighbors on the edges of the inner-sphere cube if compared with diagonals across the cube faces. The terminal member of the series, $(TBA)_2[(Mo_6I^i_8)F^a_6]$, has been synthesized separately, and fits in the system as expected with respect to its properties and its ^{19}F shift.[457]

The mixed-metal cage system, $[(\{Mo_nW_{6-n}\}Cl^i_8)Y^a_6]^{2-}$, $n = 0-6$, has been investigated independently in the forms, $[(\{Mo_nW_{6-n}\}Cl^i_8)Cl^a_6]^{2-}$, by LSIMS (liquid secondary ion mass spectroscopy),[458] and $[(\{Mo_nW_{6-n}\}Cl^i_8)F^a_6]^{2-}$, by 1D- and 2D-$^{19}F$-NMR spectroscopy.[459] The series, $[(\{Mo_nW_{6-n}\}Cl^i_8)Cl^a_6]^{2-}$, has

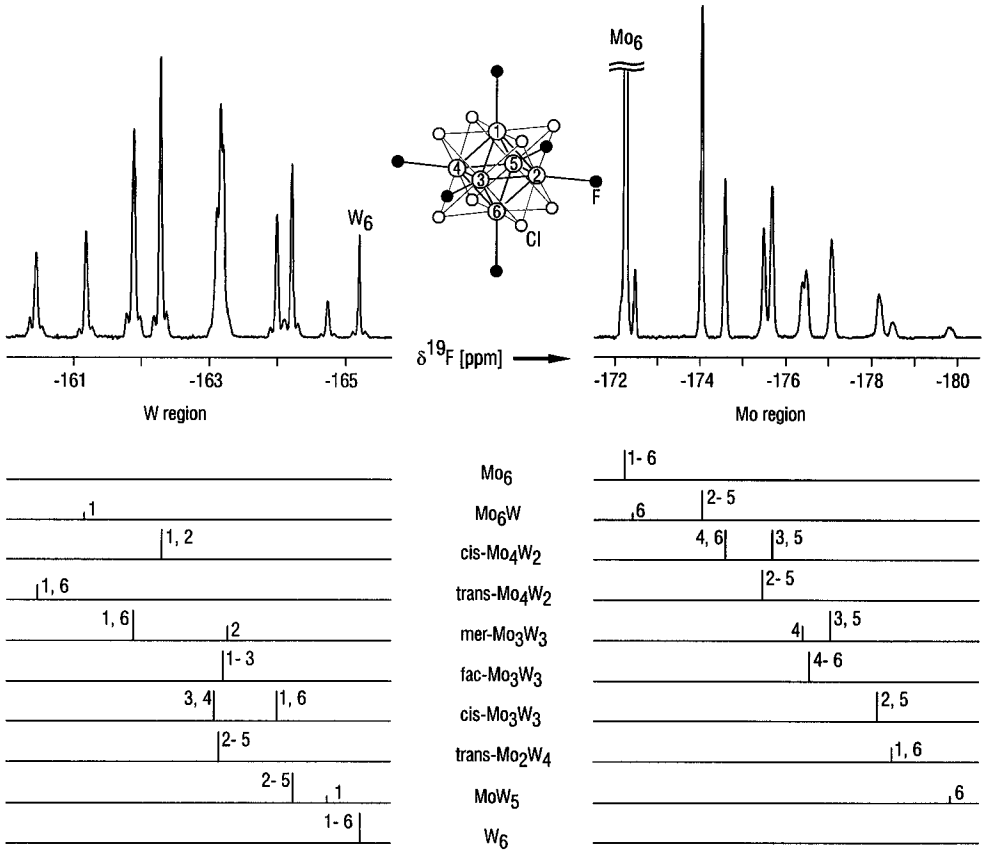

Figure 43. ^{19}F NMR spectra of the series $(TBA)_2[(\{Mo_nW_{6-n}\}Cl^i_8)F^a_6]$, $n = 0-6$, in acetone-d_6 at 297 K referred to $\delta(^{19}F)$ $(CF^{35}Cl_2{}^{37}Cl) = 0$ ppm: observed (top), expected (bottom).

been obtained by reaction of $MoCl_5$ and WCl_6 with Al in an $AlCl_3$/NaCl melt. The well-resolved mass spectra reveal the seven species for $n = 0-6$, naturally without the stereoisomers, which are not resolvable by this method. Each species evidenced two signals corresponding to $[(\{Mo_nW_{6-n}\}Cl^i_8)Cl^a_6]^{2-}$ and $[(\{Mo_nW_{6-n}\}Cl^i_8)Cl^a_5]^-$ and showed markedly decreasing intensity with an increasing number of W atoms. This is in qualitative agreement with the more robust nature of $[(Mo_6Cl^i_8)Cl^a_6]^{2-}$ in comparison with $[(W_6Cl^i_8)Cl^a_6]^{2-}$, but in contrast to the relative metal−metal bond energies in Mo and W metal.[458] This observation deviates significantly from the distributions obtained from the following NMR study, but may be due to the different synthetic routes. From the reaction of Mo powder and WCl_6 at 600 °C, the complete metal mixed-cluster system, $[(\{Mo_nW_{6-n}\}Cl^i_8)Cl_6a]^{2-}$, has been prepared and transformed into $(TBA)_2[(\{Mo_nW_{6-n}\}Cl^i_8)F^a_6]$. All 10 individual cluster ions have been identified by 1D- und 2D-^{19}F NMR spectroscopy (see Figures 43 and 44).

The expected 24 signals are observed in two clearly separated ranges with twelve signals each. The low-field range is attributed to those F atoms coordinated to the more electronegative W (Pauling electronegativity, EN = 2.36) and shows ^{19}F signals with characteristic satellites of ^{183}W ($I = {}^1/_2$, 14.28%). Consequently, the resonances in the high-field range are attributed to F atoms attached to the more electropositive Mo (EN = 2.16) without observable couplings to the two quadrupolar nuclei, ^{95}Mo and ^{97}Mo (see Figures 43 and 44). As an inspection of the W range of the 1D spectrum shows, resolution is insufficient for an unambiguous assignment of the stereoisomeric pairs of *cis*- and *trans*-Mo_2W_4 as well as of *fac*- and *mer*-Mo_3W_3. However, the resonances have been assigned unequivocally by the 2D-^{19}F spectrum via correlations to the respective resonances in the Mo range. From the integrated intensities, a nonstatistical distribution of the 10 cluster ions has been proven. Species containing symmetrical *trans* positioned Mo−Mo and W−W arrangements are favored to those with an asymmetrical Mo−W arrangement; the Mo_6 and W_6 species are found to a considerably higher degree than statistically expected. A thorough analysis of the ^{19}F shifts and shift differences has brought to light two significant effects. First, F atoms attached to W of W−Mo arrangements resonate at higher fields than those of W−W arrangements. This increased shielding, due to Mo, has been termed the positive *antipodal* influence of molybdenum. Exactly the reverse is observed for F atoms coordinated to Mo, namely a downfield shift of their respective resonances for Mo−W arrangements in comparison to Mo−Mo arrangements, thus corresponding to the negative *antipodal* influence of tungsten. Second, the *antipodal* influences and the resulting shifts are different for the individual species, but the difference of the *antipodal* influences of two successive substitution products has been found to be a characteristic constant of the series and has been called the *antipodal shift constant* (ASC).[459] This phenomenon has also proven valid for other cluster systems.[429,459] (see Tables 23 and 24). Interestingly, the relation, $ASC_{Mo}/ASC_W = EN_W/EN_{Mo}$, is valid. Furthermore, it seems worthwhile to mention that the ^{19}F shifts are to be calculated by a Dean−Evans relation

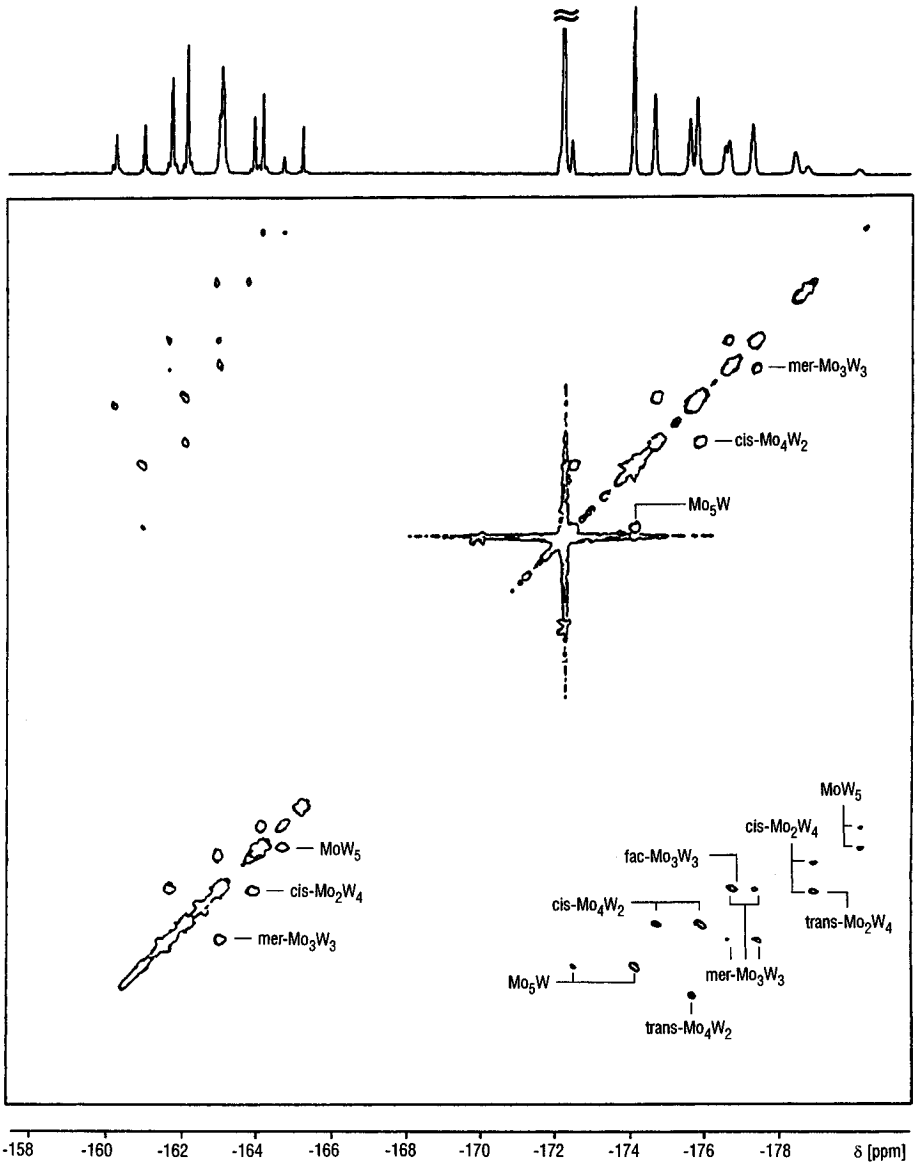

Figure 44. Two-dimensional $^{19}F,^{19}F$-COSY 45 spectrum of the series $(TBA)_2[(\{Mo_nW_{6-n}\}Cl^i_8)F^a_6]$, $n = 0-6$; conditions see Figure 43.

Table 23. Chemical Shifts $\delta(^{19}F)$ (ppm) of $[(\{Mo_nW_{6-n}\}Cl^i_8)F^a_6]^{2-}$ Fitted by Linear Regression from Observed Values for F Atoms Coordinated to Mo and W in Symmetric F−Mo−Mo−F and F−W−W−F Arrangements and Asymmetric F−Mo−W−F Arrangements [The Differences Reveal the Antipodal Influences (*A*) and the Antipodal Shift Constants (ASC)]

	$\delta(^{19}F)$ (ppm)			
	symmetric	asymmetric	*A* (ppm)	ASC (ppm)
		Mo		
Mo_5W	−173.887	−172.549	+1.338	−0.290
Mo_4W_2	−175.490	−174.442	+1.048	−0.287
Mo_3W_3	−177.094	−176.333	+0.761	−0.289
Mo_2W_4	−178.697	−178.225	+0.472	
		W		
MoW_5	−164.178	−164.869	−0.691	−0.311
Mo_2W_4	−162.957	−163.959	−1.002	−0.313
Mo_3W_3	−161.735	−163.050	−1.315	−0.312
Mo_4W_2	−160.513	−162.140	−1.627	

modified by implementation of the ASC.[459,460]

As already stated with emphasis on mononuclear octahedral mixed-ligand complexes, it is absolutely impossible to prepare defined mixed species by simple adjustment of distinct molar ratios of the educts (see section II.A.1). This statement is also valid for clusters, as has been demonstrated unambiguously by the NMR results of the substitution of the three cluster building units. Therefore, the postulated possibility of preparing defined mixed clusters[435,447] is ruled out; at best enrichments may be achieved.

For molybdenum, the three series, $[(Mo_6Cl^i_8)Y^a_6]^{2-}$, $[(Mo_6Br^i_8)Y^a_6]^{2-}$, and $[(Mo_6I^i_8)Y^a_6]^{2-}$, Y = F, Cl, Br, I, have been characterized by means of ^{95}Mo NMR spectroscopy, with the shifts referred to 2 M $NaMoO_4$ in D_2O and compiled in Table 25.[372,450,460]

The correlation of the ^{95}Mo shifts with the Pauling electronegativities $EN(Y^a)$ of the outer sphere ligands results in the following three linear functions:

$$[(Mo_6Cl^i_8)Y^a_6]^{2-}: \quad \delta(^{95}Mo) = 618 \times EN(Y^a) + 988$$

$$[(Mo_6Br^i_8)Y^a_6]^{2-}: \quad \delta(^{95}Mo) = 720 \times EN(Y^a) + 1066$$

$$[(Mo_6I^i_8)Y^a_6]^{2-}: \quad \delta(^{95}Mo) = 822 \times EN(Y^a) + 1116$$

Table 24. Chemical Shifts $\delta(^{11}B)$ (ppm) of *closo*-$[B_6X_nY_{6-n}]^{2-}$, X ≠ Y = Cl, Br, I, Fitted by Linear Regression of the Observed Values for Symmetric X−B−B−X and Asymmetric X−B−B−Y Arrangements [The Differences Result in the Antipodal Influences (*A*) and Antipodal Shift Constants (ASC).]

	$\delta(^{11}B)$ (ppm)			
	symmetric	asymmetric	*A* (ppm)	ASC (ppm)
Cl_5Br	−17.00	−17.18	−0.18	
Cl_4Br_2	−16.54	−16.38	+0.16	+0.34
Cl_3Br_3	−16.08	−15.58	+0.50	+0.34
Cl_2Br_4	−15.62	−14.78	+0.84	+0.34
$ClBr_5$	−19.31	−19.42	−0.11	
Cl_2Br_4	−19.95	−20.04	−0.08	+0.03
Cl_3Br_3	−20.61	−20.66	−0.05	+0.03
Cl_4Br_2	−21.26	−21.28	−0.02	+0.03
Cl_5I	−15.97	−13.82	+2.15	
Cl_4I_2	−14.50	−11.99	+2.51	+0.36
Cl_3I_3	−13.03	−10.16	+2.87	+0.36
Cl_2I_4	−11.57	−8.33	+3.24	+0.36
ClI_5	−26.57	−27.28	−0.71	
Cl_2I_4	−28.58	−29.31	−0.73	−0.02
Cl_3I_3	−30.59	−31.34	−0.75	−0.02
Cl_4I_2	−32.60	−33.37	−0.77	−0.02
Br_5I	−17.50	−16.78	+0.72	
Br_4I_2	−16.57	−16.38	+0.19	−0.53
Br_3I_3	−15.65	−15.98	−0.33	−0.52
Br_2I_4	−14.72	−15.58	−0.86	−0.53
BrI_5	−26.00	−25.86	+0.14	
Br_2I_4	−27.26	−27.34	−0.08	−0.22
Br_3I_3	−28.52	−28.82	−0.30	−0.22
Br_4I_2	−29.78	−30.30	−0.52	−0.22

Table 25. Electronegativity Dependence of $\delta(^{95}Mo)$ (ppm) in $[(Mo_6X^i_8)Y^a_6]^{2-}$, X^i = Cl, Br, I, Y^a = F, Cl, Br, I

X^i/Y^a	F	Cl	Br	I
Cl	3450	2933	2812	2639
Br	3926	3353	3202	2970
I	4368	3757	3569	3262
EN(Y^a)	3.98	3.16	2.96	2.66

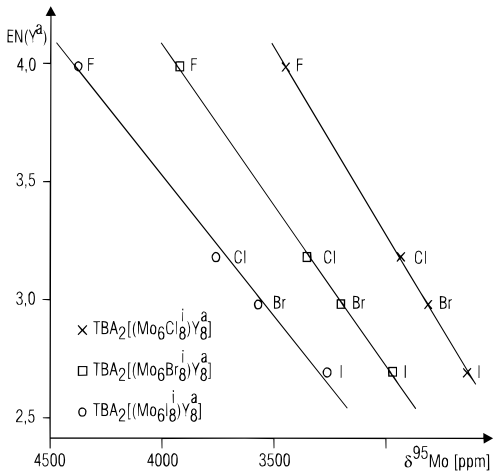

Figure 45. Plots of $\delta(^{95}Mo)$ vs the Pauling electronegativity EN of the outer-sphere ligands Y^a in the series $(TBA)_2[(Mo_6X^i_8)Y^a_6]$, X^i = Cl, Br, I, Y^a = F, Cl, Br, I.

Thus, NHD is observed for ^{95}Mo with respect to the outer ligand sphere, present in these clusters according to a high-field shift trend, $F^a < Cl^a < Br^a < I^a$ (see Figure 45 and rows in Table 25). A comparison of the ^{95}Mo shifts with an identical outer coordination sphere but with the three different inner spheres,

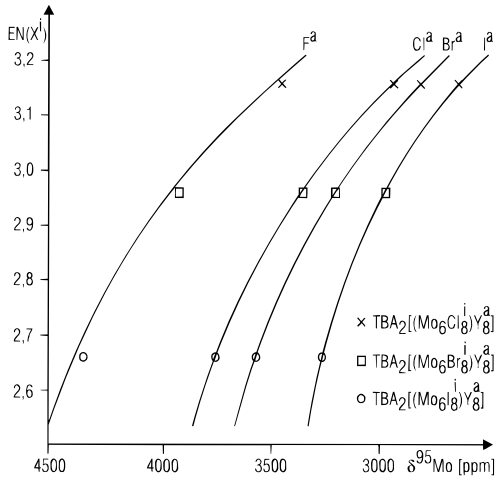

Figure 46. Plots of $\delta(^{95}Mo)$ vs the Pauling electronegativity EN of the inner-sphere ligands X^i in the series $(TBA)_2[(Mo_6X^i_8)Y^a_6]$, X^i = Cl, Br, I, Y^a = F, Cl, Br, I.

Cl^i_8, Br^i_8, and I^i_8, (see columns in Table 25) reveals in all four cases a highfield shift of ^{95}Mo according to the series, $Cl^i > Br^i > I^i$, thus exhibiting IHD with respect to the inner coordination sphere (see Figures 45 and 46).

V. Concluding Remarks

This paper has not only reviewed various aspects of mixed octahedral complexes and clusters, but has demonstrated the advantages and the special insight that can be provided by studying complete series of these compounds. The evolution of ideas and fundamental concepts with regard to the preparation, characterization, and basic theory of these series offers classic examples of some of the most important aspects of coordination chemistry and may serve as paradigms of high educational clarity.

For instance, the application of the *trans* effect, as a kinetic phenomenon, has been extensively utilized in stereospecific ligand exchange reactions. Also, the use of ion exchange chromatography on DEAE cellulose has been shown to be an extremely useful tool in the separation of pure mixed-ligand complexes. The combination of these and other synthetic approaches mentioned in the text have made it possible to isolate the ten individual members of many $[MX_nY_{6-n}]$, $n = 0-6$, series, including their three pairs of stereoisomers. Of these compounds with finely graduated properties, the relations between molecular structure, molecular symmetry, and spectroscopic properties have been investigated. The resulting systematics of stepwise substitution and descent in symmetry have been demonstrated by the group theoretically demanded splittings of degenerate terms in the electronic and vibrational spectra. Additionally, these systematics have enabled the assured assignment of electronic transitions and molecular vibrations and the reasonable application of normal coordinate analysis. By the experimental data of high reliability, progress has been made in a more detailed insight and the quantitative description of a phenomenon known as *trans* influence. This thermodynamic phenomenon of mutual interactions of two different ligands, which constitute asymmetric

axes in the mixed octahedral coordination sphere, is responsible for the special ground-state properties observed for these compounds and reveals distinct effects of different magnitudes on observable parameters. For example, in the fluorochloroplatinate(IV) series, the bond distances vary by 1−2%, the vibrational frequencies by 10%, the force constants calculated by normal coordinate analysis by up to 20%, and the $^1J(^{19}F, ^{195}Pt)$ NMR coupling constants by about 35%.

With regard to NMR spectroscopy, the study of complete series has enabled the calculation of chemical shifts of central and ligand nuclei by means of incremental empirical relations, revealing distinct dependences of the chemical shift and of the coupling constants on the degree and type of substitution. Because of the greater number of electronic states in the clusters in comparison with the mononuclear complexes, the effects of electron redistribution due to chemical variation and mutual influences are considerably more difficult to identify. However, if a sufficiently sensitive probe is used, such as the fluorine nucleus in ^{19}F NMR spectroscopy, it is possible to unequivocally and consistently identify mixed-metal and mixed-halogeno clusters. From such experiments, the *antipodal* influence, which is analogous to the *trans* influence, has been found, resulting in the formulation of an *antipodal* shift constant.

Historically, the evolution of this work, which has been outlined from the beginning of coordination chemistry and the discovery of clusters with strong metal−metal bonds to the use of modern instrumental techniques together with better and better theoretical models, has depended first on the skill of synthetic chemists. Clearly, the study of these mixed compounds presents in and of itself a historical backdrop of how synthetic and analytical techniques have worked together to provide crucial insight into the workings of such fundamental aspects like the structure, bond conditions, symmetry, and spectroscopic properties in dependence of systematically varied ligand spheres or cluster units. Thus, the future of the work in this field rests in the skilled hands of synthetic and analytic chemists, who will undoubtedly continue to provide new substances and to advance our understanding of the fundamental principles controlling coordination chemistry.

VI. References

(1) (1) Chernyaev, I. I. *Ann. Inst. Platine Autres Met Precieux (Leningrad) USSR* **1926**, *4*, 261; **1927**, *5*, 109.
(2) Pidcock, A.; Richards, R. E.; Venanzi, L. M. *J. Chem. Soc. (A)* **1966**, 1707.
(3) Appleton, T. G.; Clark, H. C.; Manzer, L. E. *Coord. Chem. Rev.* **1973**, *10*, 335.
(4) Hartley, F. R. *Chem. Soc. Rev.* **1973**, *2*, 163.
(5) Yatsimirskii, K. B. *Pure Appl. Chem.* **1974**, *38*, 341.
(6) Shustorovich, E. M.; Porai-Koshits, A.; Buslaev, Y. A. *Coord. Chem. Rev.* **1975**, *17*, 1.
(7) Palkin, V. A.; Kuzina, T. A. *Russ. J. Coord. Chem.* **1995**, *21*, 172.
(8) Basolo, F.; Pearson, R. G. *Mechanisms of Inorganic Reactions*; John Wiley & Sons, Inc.: New York, 1967.
(9) Werner, A. *Neuere Anschauungen auf dem Gebiet der anorganischen Chemie* (*Novel Aspects in the Field of Inorganic Chemistry*); F. Vieweg & Sohn: Braunschweig, 1905.
(10) Fremy, E. *Liebigs Ann. Chem.* **1852**, *83*, 227.
(11) Blasius, E.; Preetz, W. *Z. Anorg. Allg. Chem.* **1965**, *335*, 16.
(12) Dé, A. K. Ph.D. Thesis, Universität Karlsruhe, 1972.
(13) Keller, H.-L.; Homborg, H. *Z. Anorg. Allg. Chem.* **1976**, *422*, 261.
(14) Preetz, W.; Nadler, J. P. *Z. Anorg. Allg. Chem.* **1974**, *410*, 48.
(15) Preetz, W.; Irmer, K. *Z. Naturforsch.* **1990**, *45b*, 283.
(16) Clark, R. J. H.; Maresca, L.; Puddephatt, R. J. *Inorg. Chem.* **1968**, *7*, 1603.
(17) Sillen, L. G. *J. Inorg. Nucl. Chem.* **1958**, *8*, 176.
(18) Schläfer, H. L. *Komplexbildung in Lösung* (*Complex Formation in Solution*); Springer: Berlin, 1961; p 11.
(19) Preetz, W.; Kühl, H. *Z. Anorg. Allg. Chem.* **1976**, *425*, 97.
(20) Pitkin, L. *J. Am. Chem. Soc.* **1879**, *1*, 472.
(21) Pitkin, L. *J. Am. Chem. Soc.* **1880**, *2*, 196.
(22) Klement, R. *Z. Anorg. Allg. Chem.* **1927**, *164*, 195.
(23) Kraus, F.; Wilken, D. *Z. Anorg. Allg. Chem.* **1924**, *137*, 362.
(24) Fenn, E.; Nyholm, R. S.; Owston, P. G.; Turco, A. *J. Inorg. Nucl. Chem.* **1961**, *17*, 387.
(25) Dubinskii, V. I.; Astakhova, I. S. *Russ. J. Inorg. Chem.* **1987**, *32*, 874.
(26) Herber, R. H.; Cheng, H. S. *Inorg. Chem.* **1969**, *8*, 2145.
(27) Ozin, G. A.; Fowles, G. W. A.; Tidmarsh, D. J.; Walton, R. A. *J. Chem. Soc. (A)* **1969**, 642.
(28) Kolditz, L.; Calov, U. *Z. Anorg. Allg. Chem.* **1970**, *376*, 1.
(29) Kolditz, L.; Malzahn, R. *Z. Anorg. Allg. Chem.* **1970**, *379*, 279.
(30) Swartz, W. E.; Watts, P. H.; Lippincott, E. R.; Watts, J. C.; Huheey, J. E. *Inorg. Chem.* **1972**, *11*, 2632.
(31) Bjerrum, J. *Metal Ammine Formation in Aqueous Solution*; P. Haase & Sohn: Kopenhagen, 1941.
(32) Bjerrum, J. *Chem. Rev.* **1950**, *46*, 381.
(33) Preetz, W.; Bührens, K.-G. *Z. Anorg. Allg. Chem.* **1976**, *426*, 131.
(34) Cotton, F. A.; Wilkinson, G. *Advanced Inorganic Chemistry*, 5th ed.; John Wiley & Sons: New York, 1988; p 44.
(35) Kuhr, W.; Peters, G.; Preetz, W. *Z. Naturforsch.* **1989**, *44b*, 1402.
(36) Preetz, W.; Walter, H. J. *Z. Anorg. Allg. Chem.* **1973**, *402*, 169.
(37) Preetz, W.; Walter, H. J.; Fries, E. W. *Z. Anorg. Allg. Chem.* **1973**, *402*, 180.
(38) Preetz, W.; Zerbe, H.-D. *Z. Anorg. Allg. Chem.* **1981**, *479*, 7.
(39) Zerbe, H.-D.; Preetz, W. *Z. Anorg. Allg. Chem.* **1981**, *479*, 17.
(40) Preetz, W.; Homborg, H. *Z. Anorg. Allg. Chem.* **1974**, *407*, 1.
(41) Zerbe, H.-D.; Preetz, W. *Z. Anorg. Allg. Chem.* **1982**, *484*, 33.
(42) Preetz, W.; Shukla, A. K. *Z. Anorg. Allg. Chem.* **1977**, *433*, 140.
(43) Shukla, A. K.; Preetz, W. *Angew. Chem.* **1979**, *91*, 160.
(44) Shukla, A. K.; Preetz, W. *J. Inorg. Nucl. Chem.* **1979**, *41*, 1295.
(45) Shukla, A. K.; Preetz, W. *Inorg. Chem.* **1980**, *19*, 2272.
(46) Müller, H.; et al. *J. Inorg. Nucl. Chem.* **1966**, *28*, 2081; *Radiochim. Acta* **1973**, *19*, 176; **1983**, *34*, 173; **1991**, *55*, 199; **1992**, *56*, 73; *J. Chem. Phys.* **1981**, *85*, 3514; **1986**, *90*, 3414; **1994**, *98*, 193; *Z. Anorg. Allg. Chem.* **1983**, *503*, 15.
(47) Preetz, W.; Nadler, J. P. *Z. Anorg. Allg. Chem.* **1974**, *410*, 48.
(48) Preetz, W.; Nadler, J. P. *Z. Anorg. Allg. Chem.* **1974**, *410*, 59.
(49) Preetz, W.; Nadler, J. P. *Z. Anorg. Allg. Chem.* **1974**, *410*, 121.
(50) Preetz, W.; Hasenpusch, W. *Z. Anorg. Allg. Chem.* **1976**, *420*, 97.
(51) Hasenpusch, W.; Preetz, W. *Z. Anorg. Allg. Chem.* **1977**, *432*, 101, 107.
(52) Preetz, W.; Scheffler, A.; Homborg, H. *Z. Anorg. Allg. Chem.* **1974**, *406*, 92.
(53) Brown, D. H.; Dixan, K. R.; Sharp, B. W. A. *J. Chem. Soc. London (A)* **1966**, 1244.
(54) Preetz, W.; Petros, Y. *Z. Anorg. Allg. Chem.* **1975**, *415*, 15.
(55) Preetz, W.; Erlhöfer, P. *Z. Naturforsch.* **1989**, *44b*, 412.
(56) Preetz, W.; Ruf, D.; Tensfeld, D. *Z. Naturforsch.* **1984**, *39b*, 1100.
(57) Preetz, W.; Groth, T. *Z. Naturforsch.* **1986**, *41b*, 885.
(58) Tensfeld, D.; Preetz, W. *Z. Naturforsch.* **1984**, *39b*, 1185.
(59) Preetz, W.; Tensfeld, D. *Z. Anorg. Allg. Chem.* **1985**, *522*, 7.
(60) Groth, T.; Preetz, W. *Z. Anorg. Allg. Chem.* **1987**, *548*, 76.
(61) Preetz, W.; Thilmann, L. *Z. Anorg. Allg. Chem.* **1993**, *619*, 403.
(62) Preetz, W.; Rimkus, G. *Z. Naturfosch.* **1983**, *38b*, 442.
(63) Rimkus, G.; Preetz, W. *Z. Anorg. Allg. Chem.* **1985**, *502*, 73.
(64) Preetz, W.; Grabowski, A. *Z. Anorg. Allg. Chem.* **1984**, *518*, 129.
(65) Skoog, D. A.; West, D. M. *Analytical Chemistry*, 4th ed.; Saunders College Publishing: Philadelphia, 1986.
(66) Christian, G. D., O'Reilly, J. E., Eds. *Instrumental Analysis*, 2nd ed.; Allyn and Bacon: Boston, 1986.
(67) Preetz, W. *Fortschr. Chem. Forsch.* **1969**, *11*, 375.
(68) Müller, H. *Naturwissenschaften* **1962**, *49*, 182.
(69) Blasius, W.; Preetz, W. *Z. Anorg. Allg. Chem.* **1965**, *335*, 16.
(70) Preetz, W. *Talanta* **1966**, *13*, 1649.
(71) Preetz, W.; Pfeifer, H.-L. *Talanta* **1967**, *14*, 143; **1969**, *16*, 1444.
(72) Preetz, W.; Pfeifer, H.-L. *Anal. Chim. Acta* **1967**, *38*, 255.
(73) Barka, G.; Preetz, W. *Z. Anorg. Allg. Chem.* **1977**, *433*, 147.
(74) Preetz, W.; Fricke, H.-H. *Z. Anal. Chem.* **1981**, *306*, 115.
(75) Kaufman, G. B.; Cump, B. H.; Anderson, G. L.; Stedjec, B. J. *J. Chromatogr.* **1976**, *117*, 455.
(76) Müller, H.; Bekk, P. *Z. Anal. Chem.* **1983**, *314*, 758.
(77) Obergfell, P.; Müller, H. *Z. Anal. Chem.* **1987**, *328*, 242.
(78) Preetz, W.; Bütje, K. *Z. Anorg. Allg. Chem.* **1988**, *557*, 112.
(79) Rossiter, B. W.; Hamilton, J. R. Determination of Chemical Composition and Molecular Structure. *Physical Methods of Chemistry*; John Wiley & Sons: New York, 1987; Vol. IIIA, Part A.

(80) Ebsworth, E. A. V.; Rankin, D. W. H.; Cradock, S. *Structural Methods in Inorganic Chemistry*; Blackwell Scientific Publications: Oxford, 1987.
(81) Griffiths, P. R.; de Haseth, J. A. *Fourier-Transform Infrared Spectroscopy*; John Wiley & Sons: New York, 1986.
(82) Mac Dowell, R. S. High Resolution Infrared Spectroscopy with Tunable Lasers. In *Adv. Infrared Raman Spectrosc.* **1978**, *5*, 1.
(83) Long, D. A. *Raman Spectroscopy*; McGraw Hill: New York, 1977.
(84) Hendra, P.; Jones, C.; Warnes, G. *Fourier Transform Raman Spectroscopy*; Ellis Horwood: New York, 1991.
(85) Nakamoto, K. *Infrared and Raman Spectra of Inorganic and Coordination Compounds*, 4th ed.; John Wiley & Sons: New York, 1991.
(86) Harris, D. C.; Bertolucci, M. D. *Symmetry and Spectroscopy*; Oxford University Press: Oxford, 1978.
(87) Herzberg, G. *Infrared and Raman Spectra*; Van Nostrand Reinhold Company: New York, 1945.
(88) Cotton, F. A. *Chemical Applications of Group Theory*, 3rd ed.; John Wiley & Sons: New York, 1990.
(89) Wilson, E. B.; Decius, J. C.; Cross, P. C. *Molecular Vibrations*; Dover Publication: New York, 1980.
(90) Shimanouchi, T. *Computer Programs for Normal Coordinate Treatment of Polyatomic Molecules*; University of Tokyo: Tokyo, 1968.
(91) Gwinn, W. D. *J. Chem. Phys.* **1971**, *55*, 477.
(92) Snyder, R. G.; Schachtschneider, J. H. *Spectrochim. Acta* **1963**, *19*, 117.
(93) Sundius, T. *J. Mol. Spectrosc.* **1980**, *82*, 138.
(94) Homborg, H.; Preetz, W. *Spectrochim. Acta* **1976**, *32A*, 709.
(95) Homborg, H. *Z. Anorg. Allg. Chem.* **1980**, *460*, 17.
(96) Homborg, H. *Z. Anorg. Allg. Chem.* **1982**, *493*, 104.
(97) Preetz, W.; Parzich, E. *Z. Naturforsch.* **1993**, *48b*, 1737.
(98) Erlhöfer, P.; Preetz, W. *Z. Naturforsch.* **1989**, *44b*, 619.
(99) Erlhöfer, P.; Preetz, W. *Z. Naturforsch.* **1989**, *44b*, 1214.
(100) Hepworth, M. A.; Robinson, P. L.; Westland, G. J. *J. Chem. Soc.* **1958**, 611.
(101) Lane, A. P.; Sharp, D. W. A. *J. Chem. Soc. (A)* **1969**, 2942.
(102) Papadimitriou, C.; Tsangaris, J. M.; Papdimitriou, A. *J. Less-Common Met.* **1985**, *108*, 217.
(103) Bruhn, C.; Drews, H.-H.; Meynhardt, B.; Preetz, W. *Z. Anorg. Allg. Chem.* **1995**, *621*, 373.
(104) Preetz, W.; Wendt, A. *Z. Naturforsch.* **1991**, *46b*, 1496.
(105) Preetz, W.; v. Allwörden, H. N. *Z. Naturforsch.* **1987**, *42b*, 381.
(106) Preetz, W.; Kuhr, W. *Z. Naturforsch.* **1989**, *44b*, 1221.
(107) Schmidtke, H. H.; Grzonka, C.; Schoenherr, T. *Spectrochim. Acta* **1989**, *45A*, 129.
(108) Preetz, W.; Steinebach, H.-J. *Z. Naturforsch.* **1985**, *40b*, 745.
(109) Preetz, W.; Rimkus, G. *Z. Naturforsch.* **1982**, *37b*, 579.
(110) Lipnitzkii, I. V.; Ksenofontova, N. M.; Prima, A. M.; Umreiko, D. S. *Dokl. Akad. Nauk Beloruss. SSR* **1973**, *17*, 898.
(111) Adams, D. M.; Morris, D. M. *J. Chem. Soc.(A)* **1967**, 1666.
(112) Prillwitz, P.; Preetz, W. *Z. Naturforsch.* **1994**, *49b*, 753.
(113) Preetz, W.; Manthey, M. *Z. Naturforsch.* **1992**, *47b*, 1667.
(114) Preetz, W.; Walter, H. J. *J. Inorg. Nucl. Chem.* **1971**, *33*, 3179.
(115) Manthey, M.; Preetz, W. *Z. Naturforsch.* **1993**, *48b*, 747.
(116) Adams, D. M.; Fraser, G. W.; Mooris, D. M.; Peacock, R. D. *J. Chem. Soc. (A)* **1968**, 1131.
(117) Fraser, G. W.; Mercer, M.; Peacock, R. D. *J. Chem. Soc. (A)* **1967**, 1091.
(118) Murrell, J. N. *J. Chem. Soc. (A)* **1969**, 297.
(119) Legon, A. C. *Trans. Faraday Soc.* **1969**, *65*, 2595; **1973**, *69*, 29.
(120) Atvars, T. D. Z.; Zaniquelli, M. E. D.; Lin, C. T. *Acta Sud Am. Quim.* **1983**, *3*, 37.
(121) Müller, U.; Dehnicke, K.; Vorres, K. S. *J. Inorg. Nucl. Chem.* **1968**, *30*, 1719.
(122) So, S. P.; Li, K. K.; Hung, L. K. *Bull. Soc. Chim. Belg.* **1978**, *87*, 411.
(123) Christe, K. O.; et. al. *Inorg. Chem.* **1972**, *11*, 583; *J. Am. Chem. Soc.* **1994**, *116*, 7123; *Inorg. Chem.* **1973**, *12*, 620; *Spectrochem. Acta* **1973**, *33A*, 69.
(124) Christen, D.; Mack, H.-G.; Oberhammer, H. *J. Chem. Phys.* **1987**, *87*, 2001.
(125) Griffiths, J. E. *Spectrochim. Acta* **1967**, *23A*, 2145.
(126) Cross, L. H.; Roberts, H. L.; Goggin, P.; Woodward, L. A. *Trans. Faraday Soc.* **1960**, *56*, 945.
(127) Schack, C. J.; Wilson, R. D.; Hon, J. F. *Inorg. Chem.* **1972**, *11*, 208.
(128) Abriel, W.; Ehrhardt, H. *Z. Naturforsch.* **1988**, *43b*, 557.
(129) Ozin, G. A.; van der Voet, A. *J. Mol. Struct.* **1972**, *13*, 435.
(130) Brooks, W. V. F.; Eshaque, M.; Lau, C.; Passmore, J. *Can. J. Chem.* **1976**, *54*, 817.
(131) Böhling, H.; Geiseler, G. In Molecular Vibrations and Force Constants. *Nova Acta Leopoldina* **1988**, *13*.
(132) Labonville, P.; Ferraro, J. R.; Wall, M. C.; S. M. C.; Basile, L. J. *Coord. Chem. Rev.* **1972**, *7*, 257.
(133) Krynauw, G. N. *Spectrochim. Acta* **1990**, *46A*, 741.
(134) McDowell, R. S.; Sherman, L. B.; Arsrey, L. B.; Kennedy, R. C. *J. Chem. Phys.* **1975**, *62*, 3974.
(135) Irmer, K.; Preetz, W. *Z. Naturforsch.* **1991**, *46b*, 1200.
(136) Ravikumar, K. G.; Gunasekaran, S.; Mohan, S. *Bull. Soc. Chim. Belg.* **1984**, *93*, 847.
(137) Creighton, J. A.; Timmins, K. J. *Proc. 5th Int. Conf. Raman Spectrosc.*; Schmid, E. D., Brandmueller, J., Kiefer, W., Eds.; Hans Ferdinand Schulz Verlag: Freiburg/Br., Germany, 1976; p 122.
(138) Mohan, S. *Bull. Soc. Chim. Belg.* **1977**, *86*, 531.
(139) Kale, A. J.; Sathianandan, K. *Spectrochim. Acta* **1970**, *26A*, 1337.
(140) Bruhn, C.; Preetz, W. *Acta Crystallogr.* **1994**, *50C*, 1555, 1687; **1995**, *51C*, 865, 1112; **1996**, *52C*, 321.
(141) Preetz, W.; Semrau, M. *Z. Anorg. Allg. Chem.* **1995**, *621*, 725; **1996**, in press.
(142) Thesing, J.; Preetz, W. *Z. Anorg. Allg. Chem.* **1993**, *619*, 1331.
(143) Lever, A. B. P. *Inorganic Electronic Spectroscopy*, 2nd ed.; Elsevier: Amsterdam, 1984.
(144) Orgel, L. E. *An Introduction to Transition-Metal Chemistry, Ligand-Field Theory*; Methuen & Co Ltd.: London, 1961.
(145) Ballhausen, C. J. *Introduction to Ligand-Field Theory*; McGraw-Hill: New York, 1962.
(146) Schläfer, H. L.; Gliemann, G. *Einführung in die Ligandenfeld-theorie* (*Introduction to Ligand-Field Theory*); Akad. Verlagsges.: Frankfurt a. M., 1967.
(147) Jørgensen, C. K. *Modern Aspects of Ligand Field Theory*; North-Holland Publ. Company: Amsterdam, 1971.
(148) Preetz, W.; Rudzik, L. *Z. Anorg. Allg. Chem.* **1977**, *437*, 87.
(149) Preetz, W.; Homborg, H. *Z. Anorg. Allg. Chem.* **1975**, *415*, 8.
(150) Piepho, S. B.; Schatz, P. N. *Group Theory in Spectroscopy*; John Wiley & Sons: New York, 1983.
(151) Preetz, W.; Ruf, D. *Z. Naturforsch.* **1986**, *41a*, 871.
(152) Jørgensen, C. K.; Preetz, W. *Z. Naturforsch.* **1967**, *22a*, 945.
(153) Groth, Th.; Preetz, W. *Z. Naturforsch.* **1986**, *41a*, 1222.
(154) Preetz, W.; Tensfeld, D. *Z. Naturforsch.* **1984**, *38a*, 966.
(155) Schmidtke, H. H.; Schönherr, T. *Chem. Phys. Lett.* **1990**, *168*, 101.
(156) Schenk, H. J.; Schwochau, K. *Z. Naturforsch.* **1973**, *28a*, 89.
(157) Rudzik, L.; Preetz, W. *Z. Anorg. Allg. Chem.* **1978**, *443*, 118.
(158) Preetz, W. *Z. Anorg. Allg. Chem.* **1966**, *348*, 151.
(159) Jørgensen, C. K.; Preetz, W.; Homborg, H. *Inorg. Chim. Acta* **1971**, *5*, 223.
(160) v. Allwörden, H. H.; Preetz, W. *Z. Naturforsch.* **1987**, *42a*, 597.
(161) Piepho, S. B.; Inskeep, W. H.; Schatz, P. N.; Preetz, W.; Homborg, H. *Mol. Phys.* **1975**, *30*, 1569.
(162) Earnshaw, A.; Figgis, B. N.; Lewis, J.; Peacock, R. D. *J. Chem. Soc.* **1961**, 3132.
(163) Johannesen, R. B.; Candela, C. A. *Inorg. Chem.* **1963**, *2*, 67.
(164) Kozikowski, B. A.; Keiderling, T. A. *J. Phys. Chem.* **1983**, *87*, 4630.
(165) Homborg, H. *Z. Anorg. Allg. Chem.* **1982**, *493*, 121.
(166) Piepho, S. B.; Dickinson, J. R.; Spencer, J. A.; Schatz, P. N. *Mol. Phys.* **1972**, *24*, 609.
(167) Homborg, H.; Preetz, W.; Barka, G.; Schätzel, G. *Z. Naturforsch.* **1980**, *35b*, 554.
(168) Preetz, W.; Schulz, H. *Z. Naturforsch.* **1981**, *36b*, 62.
(169) Schulz, H.; Preetz, W. *Z. Anorg. Allg. Chem.* **1982**, *490*, 55.
(170) Preetz, W.; Horns, U. *Z. Anorg. Allg. Chem.* **1984**, *516*, 159.
(171) Horns, U.; Preetz, W. *Z. Anorg. Allg. Chem.* **1986**, *535*, 195.
(172) Schmidtke, H. H. *Top. Curr. Chem.* **1994**, *171*, 69.
(173) Schmidtke, H. H. *Quantenchemie*; VCH-Verlagsgesellschaft: Weinheim, 1987.
(174) Sartori, C.; Preetz, W. *Z. Naturforsch.* **1988**, *43a*, 239.
(175) Allen, C. C.; Al-Mobarak, R.; El-Sharkawy, G. A. M.; Warren, K. D. *Inorg. Chem.* **1972**, *11*, 787.
(176) Irmer, K.; Preetz, W. *Z. Naturforsch.* **1991**, *46a*, 803.
(177) Flint, C. D.; Paulusz, G. *Mol. Phys.* **1980**, *41*, 907.
(178) Jørgensen, C. K.; Schwochau, K. *Z. Naturforsch.* **1965**, *20a*, 65.
(179) Flint, C. D.; Long, P. F. *J. Chem. Soc. Farday Trans. 2* **1986**, *82*, 465.
(180) Manthey, M.; Preetz, W. *Z. Naturforsch.* **1994**, *49a*, 767.
(181) Strand, D.; Linder, R.; Schmidtke, H. H. *Mol. Phys.* **1990**, *71*, 1075.
(182) Strand, D.; Linder, R.; Schmidtke, H. H. *Inorg. Chim Acta* **1991**, *182*, 205.
(183) Wendt, A.; Preetz, W. *Z. Naturforsch.* **1992**, *47a*, 882.
(184) Flint, C. D.; Lang, P. F. *J. Chem. Soc., Dalton Trans.* **1986**, 921.
(185) Flint, C. D.; Lang, P. F. *J. Chem. Soc., Dalton Trans.* **1987**, 1929.
(186) Muetterties, J. L. *J. Am. Chem. Soc.* **1960**, *82*, 1082.
(187) Rapdale, R. O.; Stewart, B. B. *Inorg. Chem.* **1965**, *4*, 740.
(188) Rapdale, R. O.; Stewart, B. B. *Proc. Chem. Soc.* **1964**, 194.
(189) (a) McFarlane, W. *Annu. Rep. NMR Spectrosc.* **1972**, *5a*, 353. (b) McFarlane, W. *Annu. Rep. NMR Spectrosc.* **1979**, *9*, 319. (c) McFarlane, W.; Rycroft, D. S. *Annu. Rep. NMR Spectrosc.* **1985**, *16*, 293.
(190) Mason, J., Ed. *Multinuclear NMR*; Plenum Press: New York, 1987; (a) p 52; (b) p 495; (c) p 547 ff.
(191) Harris, R. K., Mann, B. E., Eds. *NMR and the Periodic Table*; Academic Press: London, 1978.
(192) Pregosin, P. S., Ed. *Transition Metal Nuclear Magnetic Resonance*; Elsevier: Amsterdam, 1991; p 186.

(193) Lambert, J. B., Riddell, F. G., Eds. *The Multinuclear Approach to NMR Spectroscopy*; D. Reidel Publishing Company: Dordrecht, 1983.
(194) Brevard, C.; Granger, P. *Handbook of High Resolution Multinuclear NMR*; John Wiley & Sons: New York, 1981.
(195) Sugimoto, M.; Kanyama, M.; Nakatsuji, H. *J. Phys. Chem.* **1992**, *96*, 4375.
(196) Dean, P. A. W.; Evans, D. F. *J. Chem. Soc.* **1968**, 1164.
(197) Vladimiroff, T.; Malinowski, E. *J. Chem. Phys.* **1968**, *46*, 1830.
(198) Tarasov, V. P.; Privalov, V. I.; Buslaev, Y. A. *Mol. Phys.* **1978**, *35*, 1047.
(199) Dillon, K. B.; Marshall, A. J. *J. Chem. Soc., Dalton Trans.* **1984**, 1245.
(200) Colton, R.; Dakternieks, D.; Harvey, C.-A. *Inorg. Chim. Acta* **1982**, *61*, 1.
(201) Dillon, K. B.; Marshall, A. J. *J. Chem. Soc., Dalton Trans.* **1987**, 315.
(202) Good, M. L.; Clausen, C. A. *Proc. 3rd Symp. Coord. Chem.* **1970**, *1*, 445.
(203) Clausen, C. A.; Good, M. L. *Inorg. Chem.* **1970**, *9*, 817.
(204) Berger, S.; Braun, S.; Kalinowski, H. O. ^{19}F NMR Spektroskopie. *NMR Spektroskopie von Nichtmetallen* (*^{19}F NMR Spectroscopy. NMR Spectroscopy of Nonmetals*); Georg Thieme Verlag: Stuttgart, New York, 1994; Vol. 4.
(205) Marat, R. K.; Janzen, A. F. *J. Chem. Soc., Chem. Commun.* **1971**, 671.
(206) Gibson, I. A.; Ibott, D. G.; Janzen, A. F. *Can. J. Chem.* **1973**, *51*, 3203.
(207) Dean, P. A. W.; Evans, D. F. *J. Chem. Soc. (A)* **1970**, 2569.
(208) Adley, A. D.; Gibson, D. F. R.; Onyszchuk, M. *J. Chem. Soc., Chem. Commun.* **1968**, 813.
(209) Brownstein, S. *Can. J. Chem.* **1980**, *58*, 1407.
(210) Bohlen, R.; Francke, R.; Röschenthaler, G.-V. *Chem. Ztg.* **1988**, *112*, 343.
(211) Brown, S.; Clark, J. H. *J. Chem. Soc., Chem. Commun.* **1983**, 1256.
(212) Appel, R.; Ruppert, I.; Knoll, F. *Chem. Ber.* **1972**, *105*, 2492.
(213) Reddy, G. S.; Schmutzler, R. *Z. Naturforsch.* **1970**, *25b*, 1199.
(214) Rusmidah, A.; Dillon, K. B. *J. Chem. Soc., Dalton Trans.* **1990**, 1375.
(215) Buslaev, Y. A.; Ilyin, E. G.; Shcherbakova, M. N. *Dokl. Akad. Nauk SSSR* **1974**, *217*, 337; **1974**, *219*, 1154.
(216) Chevrier, P. J.; Brownstein, S. *J. Inorg. Nucl. Chem.* **1980**, *42*, 1397.
(217) Dillon, K. B.; Platt, A. W. G. *J. Chem. Soc., Dalton Trans.* **1983**, 1159.
(218) John, K.-P.; Schmutzler, R. *Z. Naturforsch.* **1974**, *29b*, 730.
(219) Dillon, K. B.; Platt, A. W. G. *J. Chem. Soc., Chem. Commun.* **1983**, 1089.
(220) Rusmidah, A.; Dillon, K. B. *J. Chem. Soc., Dalton Trans.* **1988**, 2077.
(221) Dillon, K. B.; Platt, A. W. G. *J. Chem. Soc., Chem. Commun.* **1979**, 889.
(222) Dillon, K. B.; Platt, A. W. G. *J. Chem. Soc., Dalton Trans.* **1982**, 1199.
(223) Berger, S.; Braun, S.; Kalinowski, H. O. ^{31}P NMR Spektroskopie. *NMR Spektroskopie von Nichtmetallen* (*^{31}P NMR Spectroscopy. NMR Spectroscopy of Nonmetals*); Georg Thieme Verlag: Stuttgart, 1994; Vol. 3.
(224) Ilyin, E. G.; Nazarov, A. P.; Buslaev, Y. A. *Sov. J. Coord. Chem. (Engl. Transl.)* **1979**, *248*, 431.
(225) Ilyin, E. G.; Kluynev, L. I.; Buslaev, Y. A. *Sov. J. Coord. Chem. (Engl. Transl.)* **1976**, *2*, 981.
(226) Dove, M. F. A.; Sanders, J. C. P.; Jones, E. L.; Parkin, M. J. *J. Chem. Soc., Chem. Commun.* **1984**, 1578.
(227) Kidd, R. G.; Spinney, H. G. *Can. J. Chem.* **1981**, *59*, 2940.
(228) O'Brien, B. A.; Des Marteau, D. D. *Inorg. Chem.* **1984**, *23*, 644.
(229) Elgad, U.; Selig, H. *Inorg. Chem.* **1975**, *14*, 140.
(230) Tötsch, W.; Sladky, F. *Z. Naturforsch.* **1983**, *38b*, 1025.
(231) Lawlor, L. J.; Martin, A.; Murchie, M. P.; Passmore, J.; Sanders, J. C. P. *Can. J. Chem.* **1989**, *67*, 1501.
(232) Haid, E.; Köhnlein, D.; Kössler, G.; Lutz, O.; Messner, W.; Mohn, K. R.; Nothaft, G.; van Rickelen, B.; Schick, W.; Steinhauser, N. *Z. Naturforsch.* **1983**, *38a*, 317.
(233) Kirakosyan, G. A.; Tarasov, V. P. *Koord. Khim.* **1982**, *8*, 261.
(234) Buslaev, Y. A.; Kirakosyan, G. A.; Tarasov, V. P. *Koord. Khim.* **1980**, *6*, 361.
(235) Seppelt, K. *Chem. Ber.* **1976**, *103*, 1046.
(236) Cuellar, E. A.; Marks, T. J. *Inorg. Chem.* **1981**, *20*, 2129.
(237) Downs, A. J.; Gardner, C. J. *J. Chem. Soc., Dalton Trans.* **1984**, 2127.
(238) Dean, P. A. W.; Ferguson, B. J. *Can. J. Chem.* **1974**, *52*, 667.
(239) Buslaev, Y. A.; Ilyin, E. G. *Dokl. Akad. Nauk. SSSR* **1971**, *196*, 374.
(240) Buslaev, Y. A.; Ilyin, E. G.; Krutkina, M. N. *Dokl. Akad. Nauk. SSSR* **1971**, *200*, 1345.
(241) Buslaev, Y. A.; Ilyin, E. G. *J. Fluorine Chem.* **19/4**, *4*, 271.
(242) Buslaev, Y. A.; Kokunov, Y. V.; Kopanev, V. D.; Gustyakova, M. P. *J. Inorg. Nucl. Chem.* **1974**, *36*, 1569.
(243) Buslaev, Y. A.; Kopanev, V. D.; Tarasov, V. P. *J. Chem. Soc., Chem. Commun.* **1971**, 1175.
(244) Kidd, R. G. *Annu. Rep. NMR Spectrosc.* **1980**, *10A*, 1.
(245) Ilyin, E. G.; Tarasov, V. P.; Ershova, M. M.; Ermakov, V. A.; Glushkova, M. A.; Buslaev, Y. A. *Sov. J. Coord. Chem. (Engl. Transl.)* **1978**, *4*, 1039.
(246) Kidd, R. G.; Spinney, H. G. *J. Am. Chem. Soc.* **1981**, *103*, 4759.
(247) Kidd, R. G.; Spinney, H. G. *Inorg. Chem.* **1973**, *12*, 1967.
(248) Valiev, K. A.; Zaripov, M. M. *J. Struct. Chem. (Engl. Transl.)* **1966**, *7*, 470.
(249) Fraser, G. W.; Gibbs, C. J. W.; Peacock, R. D. *J. Chem. Soc. (A)* **1970**, 1708.
(250) Noble, A. M.; Winfield, J. M. *J. Chem. Soc. (A)* **1970**, 948.
(251) Noble, A. M.; Winfield, J. M. *J. Chem. Soc. (A)* **1970**, 2574.
(252) Handy, L. B.; Sharp, K. G.; Brinckman, F. E. *Inorg. Chem.* **1972**, *11*, 523.
(253) Alyoubi, A. O.; Greenslade, D. J.; Forster, M. J.; Preetz, W. *J. Chem. Soc., Dalton Trans.* **1990**, 381.
(254) Bruhn, C.; Peters, G.; Preetz, W. *Z. Naturforsch.* **1996**, in press.
(255) Kirkosyan, G. A.; Tarasov, V. P. *Russ. J. Coord. Chem.* **1992**, *18*, 74.
(256) Belyaev, A. V.; Fedotov, M. A. *Sov. J. Coord. Chem.* **1983**, *9*, 715.
(257) Belyaev, A. V.; Fedotov, M. A. *Sov. J. Coord. Chem.* **1984**, *10*, 683.
(258) Shipachev, V. A.; Zemskov, S. V.; Tkachev, S. V.; Al't, L. Y. *Sov. J. Coord. Chem.* **1980**, *6*, 959.
(259) Evans, D. F.; Turner, G. K. *J. Chem. Soc., Dalton Trans.* **1975**, 1238.
(260) Read, M. C.; Glaser, J.; Persson, I.; Sandström, M. *J. Chem. Soc., Dalton Trans.* **1994**, 3243.
(261) Read, M. C.; Glaser, J.; Sandström, M. *J. Chem. Soc., Dalton Trans.* **1992**, 233.
(262) Mann, B. E.; Spencer, C. M. *Inorg. Chim. Acta* **1982**, *65*, L57.
(263) Carr, C.; Glaser, J.; Sandström, M. *Inorg. Chim. Acta* **1987**, *131*, 153.
(264) Belyaev, A. V.; Venediktov, A. B.; Fedotov, M. A.; Kranenkho, S. P. *Sov. J. Coord. Chem.* **1986**, *12*, 405.
(265) Kranenkho, S. P.; Fedotov, M. A.; Belyaev, A. V.; Venediktov, A. B. *Sov. J. Coord. Chem.* **1990**, *16*, 533.
(266) Mann, B. E.; Spencer, C. M. *Inorg. Chim. Acta* **1983**, *76*, L65.
(267) Vogt, J.-U.; Peters, G.; Preetz, W. *Z. Anorg. Allg. Chem.* **1995**, *621*, 186.
(268) Duvigneau, J.; Peters, G.; Preetz, W. Z. *Anorg. Allg. Chem.* **1993**, *619*, 2043.
(269) Pregosin, P. S.; Kretschmer, M.; Preetz, W.; Rimkus, G. *Z. Naturforsch.* **1982**, *37b*, 1422.
(270) Kerrison, S. J. S.; Sadler, P. J. *J. Magn. Reson.* **1978**, *31*, 321.
(271) von Zelewsky, A. *Helv. Chim. Acta* **1968**, *51*, 803.
(272) Parzich, E.; Peters, G.; Preetz, W. *Z. Naturforsch.* **1993**, *48b*, 1169.
(273) Kerrison, S. J. S.; Sadler, P. J. *J. Chem. Soc., Dalton Trans.* **1982**, 2368.
(274) Brown, C.; Heaton, B. T.; Sabounchei, J. *J. Organomet. Chem.* **1977**, *142*, 413.
(275) Carr, C.; Goggin, P. L.; Goodfellow, R. J. *Inorg. Chim. Acta* **1984**, *81*, L25.
(276) Ismail, I. M., Kerrison, S. J. S.; Sadler, P. J. *J. Chem. Soc., Chem. Commun.* **1980**, 1175.
(277) Schwerdtfeger, H. J.; Preetz, W. *Angew. Chem.* **1977**, *89*, 108.
(278) Preetz, W.; Peters, G. *Z. Naturforsch.* **1979**, *34b*, 1243.
(279) Peters, G.; Preetz, W. *Z. Naturforsch.* **1980**, *35b*, 994.
(280) Preetz, W.; Fricke, H.-H. *Z. Anorg. Allg. Chem.* **1982**, *486*, 49.
(281) Fricke, H.-H.; Preetz, W. *Z. Anorg. Allg. Chem.* **1983**, *507*, 12.
(282) Fricke, H.-H.; Preetz, W. *Z. Anorg. Allg. Chem.* **1983**, *507*, 23.
(283) Fricke, H.-H.; Preetz, W. *Z. Naturforsch.* **1983**, *38b*, 917.
(284) Bütje, K.; Preetz, W. *Z. Naturforsch.* **1988**, *43b*, 371.
(285) Bütje, K.; Preetz, W. *Z. Naturforsch.* **1988**, *43b*, 382.
(286) Preetz, W.; Peters, G.; Vogt, J.-U. *Z. Naturforsch.* **1993**, *48b*, 348.
(287) Bütje, K.; Preetz, W. *Z. Naturforsch.* **1988**, *43b*, 574.
(288) Burmeister, J. L. *Coord. Chem. Rev.* **1968**, *3*, 225.
(289) Jørgensen, S. M. *Z. Anorg. Allg. Chem.* **1893**, *5*, 169.
(290) Burmeister, J. L.; Basolo, F. *Inorg. Chem.* **1964**, *3*, 1687.
(291) Basolo, F.; Burmeister, J. L.; Poe, A. J. *J. Am. Chem. Soc.* **1963**, *85*, 1700.
(292) Balahura, J. L.; Lewis, N. A. *Coord. Chem. Rev.* **1976**, *20*, 109.
(293) Bailey, R. A.; Kozak, S. L.; Michelsen, T. W.; Mills, W. N. *Coord. Chem. Rev.* **1971**, *6*, 407.
(294) Norbury, A. H. *Adv. Inorg. Chem. Radiochem.* **1975**, *17*, 231.
(295) Burmeister, J. L. *Coord. Chem. Rev.* **1990**, *105*, 77.
(296) Ahrland, S.; Chatt, J.; Davies, N. R. *Q. Rev.* **1958**, *12*, 265.
(297) Pearson, R. G. *J. Am. Chem. Soc.* **1963**, *85*, 3533. *Hard and soft acids and bases*; Dowden, Hutchinson & Ross Inc.: Stroudsburg, PA, 1973.
(298) Jørgensen, C. K. *Inorg. Chem.* **1964**, *3*, 1201.
(299) Pearson, R. G. *Inorg. Chem.* **1973**, *12*, 712.
(300) Basolo, F.; Baddley, W. H.; Burmeister, J. L. *Inorg. Chem.* **1964**, *3*, 1202.
(301) Norbury, A. H.; Sinha, A. I. P. *J. Chem. Soc. (A)* **1968**, 1598.
(302) Jones, L. H. *J. Chem. Phys.* **1956**, *25*, 1069.

(303) Meek, D. W.; Nicpon, P. E.; Meek, V. I. *J. Am. Chem. Soc.* **1970**, *92*, 5351.
(304) Sotofte, I.; Rasmussen, S. E. *Acta Chem. Scand.* **1967**, *21*, 2028.
(305) Gutterman, D. F.; Gray, H. B. *J. Am. Chem. Soc.* **1971**, *93*, 3364.
(306) Siebert, H. *Anwendungen und Schwingungsspektroskopie in der Anorganischen Chemie* (*Applications of Vibrational Spectroscopy in Inorganic Chemistry*); Springer-Verlag: Berlin, 1966; pp 155 ff.
(307) Fujita, J.; Nakamoto, K.; Kobayashi, M. *J. Am. Chem. Soc.* **1956**, *78*, 3295.
(308) DiSipio, L.; Oleari, L.; De Michelis, G. *Coord. Chem. Rev.* **1966**, *1*, 7.
(309) Norbury, A. H. *J. Chem. Soc. (A)* **1971**, 1089.
(310) Klopman, G. *J. Am. Chem. Soc.* **1968**, *90*, 223.
(311) Basolo, F.; Baddley, W. H.; Weidenbaum, K. J. *J. Am. Chem. Soc.* **1966**, *88*, 1576.
(312) Sabatini, A.; Bertini, I. *Inorg. Chem.* **1965**, *4*, 1665.
(313) Farona, M. F., Wojcicki, A. *Inorg. Chem.* **1965**, *4*, 857.
(314) Harris, C. M.; Lockyear, T. M. *Aust. J. Chem.* **1970**, *23*, 1703.
(315) Hart, F. A.; Laming, F. P. *J. Inorg. Nucl. Chem.* **1964**, *25*, 579.
(316) Burmeister, J. L.; Hassel, R. L.; Phelan, R. J. *J. Chem. Soc., Chem. Commun.* **1970**, 679.
(317) Burmeister, J. L.; Hassel, R. L.; Phelan, R. J. *Inorg. Chem.* **1971**, *10*, 2032.
(318) Epps, L. A.; Marzilli, L. G. *J. Chem. Soc., Chem. Commun.* **1972**, 109.
(319) Norbury, A. H.; Shaw, P. E.; Sinha, A. I. P. *J. Chem. Soc., Chem. Commun.* **1970**, 2032.
(320) Norbury, A. H.; Shaw, P. E.; Sinha, A. I. P. *J. Chem. Soc., Dalton Trans.* **1975**, 742.
(321) Stotz, I.; Wilmarth, W. K.; Haim, K. *Inorg. Chem.* **1968**, *7*, 1250.
(322) Gutterman, D. F.; Gray, H. B. *J. Am. Chem. Soc.* **1969**, *91*, 3105.
(323) Burmeister, J. L.; Lim, J. C. *J. Chem. Soc., Chem. Commun.* **1968**, 1346.
(324) Drickamer, H. G.; Lewis, G. K.; Fung, S. C. *Science* **1969**, *163*, 885.
(325) Preetz, W.; Horns, U. *Z. Anorg. Allg. Chem.* **1984**, *516*, 159.
(326) Preetz, W.; Kelm, W. *Z. Anorg. Allg. Chem.* **1985**, *531*, 7.
(327) Kelm, W.; Preetz, W. *Z. Anorg. Allg. Chem.* **1988**, *565*, 7.
(328) Kelm, W.; Preetz, W. *Z. Anorg. Allg. Chem.* **1989**, *568*, 106.
(329) Grabowski, A.; Preetz, W. *Z. Anorg. Allg. Chem.* **1987**, *544*, 95.
(330) Grabowski, A.; Preetz, W. *Z. Anorg. Allg. Chem.* **1988**, *544*, 101.
(331) Schmidtke, H.-H.; Garthoff, D. *Helv. Chim. Acta* **1967**, *50*, 1631.
(332) Schmidtke, H.-H. *J. Inorg. Nucl. Chem.* **1966**, *28*, 1735.
(333) Wajda, S.; Rachlewicz, K. *Nukleonika* **1973**, *18*, 407.
(334) Wajda, S.; Rachlewicz, K. *Bull. Acad. Pol. Sci., Ser. Sci. Chim.* **1977**, *25*, 39.
(335) Peters, G.; Preetz, W. Unpublished results.
(336) Preetz, W.; Homborg, H. *J. Inorg. Nucl. Chem.* **1970**, *33*, 1979.
(337) Preetz, W.; Homborg, H. *J. Chromatogr.* **1972**, *54*, 115.
(338) Rabe, P.; Tolkiehn, G.; Werner, A.; Haensel, R. *Z. Naturforsch.* **1979**, *34A*, 1528.
(339) Jørgensen, C. K.; Berthou, H. *Kgl. Dan. Vidensk. Selsk., Mat.-Fys. Medd.* **1972**, *38*, 93.
(340) Zumbulyadis, N.; Gysling, H. J. *J. Am. Chem. Soc.* **1982**, *104*, 3246.
(341) Klopp, U.; Preetz, W. *Z. Anorg. Allg. Chem.* **1993**, *619*, 1336.
(342) Pan, W. H.; Fackler, J. P., Jr.; Kargol, J. A.; Burmeister, J. L. *Inorg. Chim. Acta Lett.* **1980**, *44*, L95.
(343) Kargol, J. A.; Crecely, R. W.; Burmeister, J. L. *Inorg. Chem.* **1979**, *18*, 2532.
(344) Barbieri, G. A. *Atti Accad. Naz. Lincei, Rend. Cl. Sci. Fis. Mat. Nat.* **1931**, *13*, 434.
(345) Schmidtke, H.-H. *Z. Phys. (Frankfurt/M.)* **1964**, *10*, 96.
(346) Zvonkova, Z. V. *Zh. Fiz. Khim.* **1953**, *27*, 100.
(347) Vogt, J.-U.; Haeckel, O.; Preetz, W. *Z. Anorg. Allg. Chem.* **1995**, *621*, 1033.
(348) Bramley, R.; Brorson, M.; Sargeson, A. M.; Schäffer, C. E. *J. Am. Chem. Soc.* **1985**, *107*, 2780.
(349) Cotton, F. A. *Q. Rev.* **1966**, *20*, 389.
(350) Cotton, F. A.; Walton, R. A. *Multiple Bonds Between Metal Atoms*, 1st ed.; John Wiley & Sons: New York, 1982; 2nd ed.; Oxford University Press: New York, 1993.
(351) Berzelius, J. J. *Poggend. Ann.* **1826**, *6*, 377.
(352) Svanberg, L.; Struve, H. *Philos. Mag.* **1848**, *33*, 524.
(353) Blomstrand, C. W. *J. Prakt. Chem.* **1859**, *77*, 88.
(354) Atterburg, M. A. *Bull. Soc. Chim. Fr.* **1872**, *18*, 21.
(355) Hampe, W. *Chem. Ztg.* **1888**, *12*, 5.
(356) Liechti, L. P.; Kempe, B. *Liebigs Ann.* **1873**, *169*, 354.
(357) Muthmann, W.; Nagel, N. *Ber. Dtsch. Chem. Ges.* **1898**, *31*, 2009.
(358) Rosenheim, A.; Kohn, F. *Z. Anorg. Allg. Chem.* **1910**, *66*, 1.
(359) Guichard, M. *Compt. Rend.* **1896**, *123*, 821.
(360) Guichard, M. *Ann. Chim. Phys.* **1901**, *23*, 565.
(361) Lindner, K.; Haller, E; Helwig, H. *Z. Anorg. Allg. Chem.* **1923**, *130*, 209.
(362) Lindner, K.; Helwig, H. *Z. Anorg. Allg. Chem.* **1925**, *142*, 182.
(363) Lindner, K. *Z. Anorg. Allg. Chem.* **1927**, *162*, 203.
(364) Biltz, W. *Z. Anorg. Allg. Chem.* **1928**, *172*, 389.
(365) Chabrie, M. C. *Compt. Rend. Acad. Sci.* **1907**, *144*, 804.
(366) Chapin, W. H. *J. Am. Chem. Soc.* **1910**, *32*, 327.
(367) Harned, S. *J. Am. Chem. Soc.* **1910**, *35*, 1078.
(368) Brosset, C. *Ark. Kemi, Mineral. Geol.* **1945**, *20A* (7), 1; **1946**, *22A* (11), 1; **1947**, *25A* (19), 1.
(369) Brosset, C. *Ark. Kemi* **1950**, *1*, 353.
(370) Vaughan, P. A. *Proc. Natl. Acad. Sci. U.S.A.* **1950**, *36*, 461.
(371) Vaughan, P. A.; Sturdivant, J. H.; Pauling, L. C. *J. Am. Chem. Soc.* **1950**, *72*, 5477.
(372) Preetz, W.; Bublitz, D.; von Schnering, H. G.; Sassmannshausen, J. *Z. Anorg. Allg. Chem.* **1994**, *620*, 234.
(373) Schäfer, H.; von Schnering, H. G. *Angew. Chem.* **1964**, *76*, 833.
(374) Schäfer, H.; von Schnering, H. G.; Thillack, J.; Kuhnen, F.; Wöhrle, H.; Baumann, H. *Z. Anorg. Allg. Chem.* **1967**, *353*, 281.
(375) Guggenberger, L. J.; Sleight, A. W. *Inorg. Chem.* **1969**, *8*, 2041.
(376) Preetz, W.; Harder, K.; von Schnering, H. G.; Kliche, G.; Peters, K. *J. Alloys Compd.* **1992**, *183*, 413.
(377) Lesaar, H.; Schäfer, H. *Z. Anorg. Allg. Chem.* **1971**, *385*, 65.
(378) Hogue, R. D.; McCarley, R. E. *Inorg. Chem.* **1970**, *9*, 1354.
(379) McCarley, R. E.; Brown, T. M. *Inorg. Chem.* **1964**, *3*, 1232.
(380) Böschen, S.; Keller, H.-L. *Z. Kristalogr.* **1992**, *200*, 305.
(381) Sheldon, J. C. *J. Chem. Soc.* **1960**, 1007; **1961**, 750; **1963**, 4183; **1964**, 1287; *Nature* **1959**, *184*, 1210.
(382) McCarley, R. E.; et al. *Inorg. Cem.* **1965**, *4*, 1482; 1491; 1496; **1967**, *6*, 1; **1970**, *9*, 1343; 1347; 1361; 1769; **1972**, *11*, 812; **1974**, *13*, 295; **1988**, *27*, 4532.
(383) McCarley, R. E.; et al. *J. Am. Chem. Soc.* **1966**, *88*, 1063; **1967**, *89*, 159.
(384) Schäfer, H.; et al. *Z. Anorg. Allg. Chem.* **1968**, *357*, 273; **1972**, *389*, 57; **1972**, *392*, 10; **1975**, *415*, 241; **1978**, *441*, 219; **1984**, *517*, 185; **1985**, *524*, 137; **1985**, *526*, 168; **1985**, *530*, 222; **1986**, *542*, 207.
(385) von Schnering, H. G.; et al. *Z. Anorg. Allg. Chem.* **1965**, *339*, 155; **1967**, *355*, 295; **1968**, *361*, 235; **1968**, *361*, 259; **1971**, *386*, 27; *J. Less-Common Met.* **1965**, *9*, 95.
(386) Harder, K.; Preetz, W. *Z. Anorg. Allg. Chem.* **1990**, *591*, 32.
(387) Gibson, J. F.; Meier, P. O. W. *J. Chem. Res. (S)* **1978**, 66.
(388) Siepmann, R.; von Schnering, H. G. *Z. Anorg. Allg. Chem.* **1968**, *357*, 289.
(389) Kepert, D. L.; Marshall, R. E.; Taylor, D. *J. Chem. Soc., Dalton Trans.* **1974**, 506.
(390) Lessmeister, P.; Schäfer, H. *Z. Anorg. Allg. Chem.* **1975**, *417*, 171.
(391) Holste, G.; Schäfer, H. *Z. Anorg. Allg. Chem.* **1972**, *391*, 263.
(392) Schäfer, H.; Brendel, C.; Henkel, G.; Krebs, B. *Z. Anorg. Allg. Chem.* **1982**, *491*, 275.
(393) Schäfer, H.; Spreckelmeyer, B. *J. Less-Common Met.* **1966**, *11*, 73.
(394) Juza, D.; Schäfer, H. *Z. Anorg. Allg. Chem.* **1970**, *379*, 122.
(395) Liebman, J. F., Greenberg, A., Williams, R. E., Eds. *Advances in Boron and the Boranes*; VCH Publishers, Inc.: New York, 1988.
(396) Shriver, D. F., Kaesz, H. D., Adams, R. D., Eds. *The Chemistry of Metal Cluster Complexes*; VCH Publishers, Inc.: New York, 1990.
(397) King, R. B. *Prog. Inorg. Chem.* **1972**, *15*, 287.
(398) Corbett, J. D. *Perspectives in Coordination Chemistry*; VCH Publishers Inc.: New York, 1992.
(399) Rogel, F.; Zhang, J.; Payne, M. W.; Corbett, J. D. *Adv. Chem. Ser.* **1990**, *226*, 369.
(400) Lee, S. C.; Holm, R. H. *Angew. Chem.* **1990**, 868.
(401) Johnson, B. F. G. *Transition Metal Clusters*; John Wiley & Sons: New York, 1980.
(402) Cotton, F. A.; Haas, T. E. *Inorg. Chem.* **1964**, *3*, 10.
(403) Ebihara, M.; Isobe, K.; Sasaki, Y.; Saito, K. *Inorg. Chem.* **1992**, *31*, 1644.
(404) Elian, M.; Hoffmann, R. *Inorg. Chem.* **1975**, *14*, 1058.
(405) Hall, M. B.; Fenske, R. F. *Inorg. Chem.* **1972**, *11*, 768.
(406) Johnson, K. H. *Annu. Rev. Phys. Chem.* **1975**, *26*, 39.
(407) Cotton, F. A.; Stanley, G. G. *Chem. Phys. Lett.* **1978**, *58*, 450.
(408) Bursten, B. E.; Cotton, F. A.; Stanley, G. G. *Israel. J. Chem.* **1980**, *19*, 132.
(409) Seifert, G.; Grossmann, G.; Müller, H. *J. Mol. Struct.* **1980**, *64*, 93.
(410) Woolley, R. G. *Inorg. Chem.* **1985**, *24*, 3519.
(411) Woolley, R. G. *Inorg. Chem.* **1985**, *24*, 3525.
(412) Mingos, D. M. P. *Chem. Soc. Rev.* **1986**, *15*, 31.
(413) Ceulemans, A.; Fowler, P. W. *Inorg. Chim. Acta* **1985**, *105*, 75.
(414) Stone, A. J. *Mol. Phys.* **1980**, *41*, 1339. Stone, A. J. *Inorg. Chem.* **1981**, *20*, 563.
(415) Perchenek, N.; Simon, A. *Z. Anorg. Allg. Chem.* **1993**, *619*, 103.
(416) Gillespie, R. J.; Hargittai, I. *The VSEPR-Model of Molecular Geometry*; Allyn Bacon: Boston, 1991.
(417) Zietlow, T. C.; Schaefer, W. P.; Sadhegi, B.; Hua, N.; Gray, H. B. *Inorg. Chem.* **1986**, *25*, 2195.
(418) Zietlow, T. C.; Schaefer, W. P.; Sadhegi, B.; Hua, N.; Gray, H. B. *Inorg. Chem.* **1986**, *25*, 2198.
(419) Maverick, A. W.; Najdzionek, J. S.; MacKenzie, D.; Nocera, D. G.; Gray, H. B. *J. Am. Chem. Soc.* **1983**, *105*, 1878.
(420) Nocera, D. G.; Gray, H. B. *J. Am. Chem. Soc.* **1984**, *106*, 824.
(421) Zietlow, T. C.; Hopkins, M. D.; Gray, H. B. *J. Sol. State Chem.* **1985**, *57*, 112.

(422) Zietlow, T. C.; Nocera, D. G.; Gray, H. B. *Inorg. Chem.* **1986**, *25*, 1351.
(423) Mussel, R. D.; Nocera, D. G. *Inorg. Chem.* **1990**, *29*, 3711.
(424) Kraut, B.; Ferraudi, G. *Inorg. Chim. Acta* **1989**, *156*, 7.
(425) Kraut, B.; Ferraudi, G. *Inorg. Chem.* **1989**, *28*, 4578.
(426) Jackson, J. A.; Turro, C.; Newsham, M. D.; Nocera, D. G. *J. Phys. Chem.* **1990**, *94*, 4500.
(427) Sheldon, J. C. *J. Chem. Soc.* **1962**, 410.
(428) Brückner, P.; Peters, G.; Preetz, W. *Z. Anorg. Allg. Chem.* **1993**, *619*, 551.
(429) Preetz, W.; Fritze, J. *Z. Naturforsch.* **1987**, *42b*, 282.
(430) Preetz, W.; Fritze, J. *Z. Naturforsch.* **1987**, *42b*, 287.
(431) Preetz, W.; Fritze, J. *Z. Naturforsch.* **1987**, *42b*, 293.
(432) Preetz, W.; Stallbaum, M. *Z. Naturforsch.* **1990**, *45b*, 1113.
(433) Meyer, J. L.; McCarley, R. E. *Inorg. Chem.* **1978**, *17*, 1867.
(434) Preetz, W.; Harder, K. *Z. Anorg. Allg. Chem.* **1991**, *597*, 163.
(435) Than, H.; Schäfer, H. *Z. Anorg. Allg. Chem.* **1984**, *519*, 10.
(436) Saito, T.; Masakazu, N.; Yamagata, T.; Yamagata, Y. *Inorg. Chem.* **1986**, *25*, 1111.
(437) Perchenek, N.; Simon, A. *Z. Anorg. Allg. Chem.* **1993**, *619*, 98.
(438) Ehrlich, G. E.; Deng, H.; Hill, L. I.; Steigerwald, M. L.; Squattrito, P. J.; DiSalvo, F. J. *Inorg. Chem.* **1995**, *34*, 2480.
(439) Zelverte, A.; Mancour, S.; Caillet, P. *Spectrochim. Acta* **1986**, *42A*, 837.
(440) Mancour, S.; Potel, M.; Caillet, P. *J. Mol. Struct.* **1987**, *162*, 1.
(441) Preetz, W.; Harder, K. *Z. Anorg. Allg. Chem.* **1991**, *591*, 32.
(442) Thesing, J.; Stallbaum, M.; Preetz, W. *Z. Naturforsch.* **1991**, *46b*, 602.
(443) Thesing, J. Ph.D. Thesis, Universität Kiel, 1991.
(444) Preetz, W.; Thesing, J. *Z. Naturforsch.* **1989**, *44b*, 121.
(445) Thesing, J.; Preetz, W. *Z. Naturforsch.* **1990**, *45b*, 641.
(446) Thesing, J.; Preetz, W.; Baurmeister, J. *Z. Naturforsch.* **1991**, *46b*, 19.
(447) Baumann, H.; Plautz, H.; Schäfer, H. *J. Less-Common Met.* **1971**, *24*, 301.
(448) Mattes, R. *Z. Anorg. Allg. Chem.* **1968**, *357*, 30.
(449) Hartley, D.; Ware, M. J. *J. Chem. Soc., Chem. Commun.* **1967**, 912.
(450) Harder, K.; Peters, G.; Preetz, W. *Z. Anorg. Allg. Chem.* **1991**, *598/599*, 139.
(451) Hermanek, S.; Plesek, J.; Stibr, B. *2nd International Meeting on Boron Compounds*. Abstr. No. 38, University of Leeds: Leeds, 1974.
(452) Preetz, W.; Braack, P.; Harder, K.; Peters, G. *Z. Anorg. Allg. Chem.* **1992**, *612*, 7.
(453) Girauden, A.; Johannsen, I.; Batail, P.; Coulon, C. *Inorg. Chem.* **1993**, *32*, 2446.
(454) Harder, K.; Preetz, W. *Z. Anorg. Allg. Chem.* **1992**, *612*, 97.
(455) Kennedy, V. O.; Stern, C. L.; Shriver, D. F. *Inorg. Chem.* **1994**, *33*, 5967.
(456) Johnston, D. H.; Garwick, D. C., Lonergan, M. C.; Stern, C. L.; Shriver, D. F. *Inorg. Chem.* **1992**, *31*, 1869.
(457) Brückner, P.; Peters, G.; Preetz, W. *Z. Anorg. Allg. Chem.* **1993**, *619*, 1920.
(458) Hodali, H. A.; Hung, H.; Shriver, D. F. *Inorg. Chim. Acta* **1992**, *198−200*, 245.
(459) Brückner, P.; Peters, G.; Preetz, W. *Z. Anorg. Allg. Chem.* **1993**, *620*, 1669.
(460) Brückner, P. Ph.D. Thesis, Universität zu Kiel, 1994.

CR940393I